ON-LINE ULTRASONIC MONITORING OF INJECTION MOLDING AND DIE CASTING PROCESSES

Bin Cao

Department of Electrical Engineering
McGill University
Montreal, Quebec, Canada

May 1996

A Thesis submitted to the Faculty of Graduate Studies and Research in partial fulfillment of the requirements of the Degree of Master of Engineering.

0-612-44084-2

Abstract

On-line ultrasonic monitoring of injection molding of polyethylene and die casting of aluminum is studied using pulse-echo techniques. The flow front of molten materials including the polymers and aluminum inside the mold has been probed by a multiple-channel probing system with a time resolution of about 1 ms. This information can be used to control the plunger movements. The gap development which is important for the understanding of the thermal contact between the mold and the part due to the shrinkage is also monitored. Gap formation time periods versus different packing pressure and at different part locations with different part thickness have been investigated. The ultrasonic velocity inside the part during the solidification has been also measured for the interpretation of the solidification process.

For monitoring the die casting of aluminum with a melt temperature above 690°C, novel high performance buffer rods together with cooling channels are integrated into the die thus the ultrasonic measurement such as flow front and gap formation can be carried out with high signal-to-noise ratio signals for the first time at such elevated temperature.

Résumé

La caractérisation en-ligne du moulage par injection de polyéthylène et du moulage sous pression d'aluminium a été étudiée grâce à des techniques ultrasonores de pulse-écho. Le front d'arrivée des matériaux fondus (polymère et aluminium) à l'intérieur du moule a été sondé avec une résolution de 1 ms grâce un système d'inspection à canaux multiples. Cette information peut être utilisée pour contrôler les mouvements du plongeur. Le développement d'un interstice, dû à la contraction de la pièce dans le moule, a également été observé. Cette information est importante pour la compréhension des phénomènes reliés au contact thermique entre le moule et la pièce. Le temps de formation de cet interstice a été évalué pour différentes pressions de remplissage et à différentes positions sur le moule où la pièce est caractérisée par différentes épaisseurs. Dans le but de pouvoir interpréter le processus de solidification des pièces, la vitesse des ondes ultrasonores se propageant à travers les matériaux moulés a également été mesurée tout au long du processus de solidification.

Pour inspecter le moulage sous pression de l'aluminium qui fond à des températures supérieures à 690°C, une nouvelle tige d'isolation (buffer rod) à hautes performances a été développée. Plusieurs de ces tiges, jumelées à des canaux de réfrigération, ont été intégrées dans le moule permettant, ainsi, des mesures ultrasonores avec d'excellents rapports signal-sur-bruit malgré les températures élevées.

Acknowledgments

I would like to thank my beloved wife Xiaoyi Chen, my dear parents and sister, for their love and support during the entire study.

Next, I wish to express my sincere gratitude to my thesis supervisor, Dr. C.K. Jen. Without his guidance, care and encouragement, this work is not possible. I know what I have learned from him is not only about the ultrasound techniques, but also about how to do the research and about the life.

Special appreciation is given to Industrial Material Institute, National Research Council Canada, where all the thesis research was carried out, and to Drs. J.F. Bussiére and C.A. Loong for their encouragement and enthusiasm of this research.

Many thanks go to my thesis co-supervisor Dr. Ky T. Nguyen, who taught me about the injection molding and die casting, and to Dr. Hao Wang, who guided me in the study of injection molding.

I also thank Dr. M. Viens for the initial implementation of data acquisition and signal processing and Dr. M. Prystay for providing the figures for infrared measurements. Thanks are also given to Y. Simard and G. Chouinard for the operation of injection molding and R. Lalonde for the operation of die casting.

Finally, the financial support from Natural Science and Engineering Research Council of Canada and National Research Council of Canada is gratefully acknowledged.

Dedication

To My parents

Table of Contents

List of Figures

List of Tables

Chapter 1:

Introduction

1.1 Background

Increasing requirements for high quality products and efficient production are pushing material process to undergo a fast evolution in the past decade [1-4]. Material processes are usually dynamic and difficult to attain a steady state, thus complex control strategies are needed to be applied to the process control [2-7]. For instance, intelligent control systems which are centered on sophisticated and integrated decision-making computer systems, base on mathematical models, may automatically select and adjust process variables during the process [1]. Often, to perform such a control task, instruments are required to provide precise feedback on process parameters and materials properties during production, thus development of cost effective sensors as well as on-line measurement technologies are important [2-,4,7,8]. At present, the lagged development of material processing sensors hampers the advancement of the material processing control [9]. Meanwhile, process modeling, analysis and operation parameter's optimization have been investigated intensively both from the theory and experiment [10-20]. Thus the improvement of the basic physical understanding of the process is essential and requires available sensors and measurement methods to perform such investigation. In addition, numerical models are frequently used for computer simulation to economize the design and optimize the process [11,18,20-30]. Even a virtual mold concept has been mentioned recently that the entire product process may be virtually simulated by computer without going through any real process [31]. However, computer simulation models often simplify the real but complicated situation in order to reduce e.g. computation time. The experimental verification and evaluation of the computer simulation software are thus becoming crucial [24,25,29,30,32] creating demands for the development of available measurement methods and advanced instrumentation.

Injection molding and die casting have been widely used in many industries as mass production methods. Improved quality control and efficient manufacturing are critical issues which enable the manufacturers to survive in a severely competitive market. Different advanced control strategies such as close loop, statistics, knowledge based expert system etc., are now integrated into the production [2-7]. Computer simulation is extensively used to optimize different production stages (filling, packing, etc.) [21-30]. Understanding the associated physical phenomena such as flow path, heat transfer, part solidification, packing pressure effects, part cooling, etc. are essential for the improvement of the process control parameters as well as the numerical simulation [33,34]. Many measurement sensors such as traditional thermocouples and pressure sensors that measure the parameters, i.e., temperature and pressure profiles have also been applied in the process [35-37]. It is understood that there are many limitations such as slow response, unsteady, nonrepeatability, etc., of these traditional sensors, thus they often do not fulfill many requirements of the fast processing control. Due to these shortcomings, new and advanced measurement sensors and methods are being continually applied to the process monitoring and control. Several monitoring techniques such as infrared [38-42], visible optics [43-46] and real time radioscopy [47] were reported.

The ability of the ultrasound to interrogate noninvasively, nondestructively and rapidly the surface and internal regions of material objects is clearly desirable for a modern process control. Such a control should not disturb constant process conditions and consistent product properties in a batch or continuous process and at the same time acquires the desired information fast enough to prevent the errors [48]. Although ultrasonic techniques have also been used for the improvement of material processes for a long time, recent advances in transducer materials, microprocessors and measurement techniques, allow one to obtain data rapidly, reliably and economically [48]. Thus high speed data acquisition systems and complex signal processing techniques make ultrasound an attractive tool for on-line production monitoring. For example, ultrasonic pulse-echo method was utilized to characterize polymers in both the solid and molten states [49-54]. The polymer melt temperature was measured during injection molding [34] and a simple plate mold was used to study the mold cavity conditions [55,56]. The interface in multi-layer polymer flows was monitored in [57]. In addition, closed loop control of injection molding hold time using ultrasonic sensor was reported in [55,58] and ultrasonic measurements of material properties during injection molding were demonstrated in [59]. Ultrasound is also a useful method to characterize the properties of metals, such as the temperature, cracks and flaws inside the metal part and even the grain size.

It is known that industrial processes are often performed at elevated temperatures which are, for instances, between 200 to 700°C for aluminum die casting, polymer injection molding, polymer extrusion, etc. Even with the cooling lines the temperature at the external surface of the mold or die may be between 100 to 300°C. Noncontact ultrasonic methods such as laser ultrasound [60-64] and electromagnetic acoustic transducers (EMAT) [9] are attractive approaches. Laser ultrasonic systems can provide advantages such as fast scanning and probing materials of complex shapes but is generally bulky and costly, and laser safety is also a concern. The signals produced by EMATs have much poorer qualities in frequency bandwidth and signal-to-noise ratio than those generated by piezoelectric ultrasonic transducers (UTs). Thus there is a strong need to find alternative ultrasonic methods to perform on-line ultrasonic monitoring measurements.

1.2 Injection molding and die casting process monitoring

The processes of injection molding and die casting are similar. Material is heated, melt and then fed into the cavity of a mold (or a die) which has a unique shape for a designed production part. Then the part is cooled and solidified inside the mold until it is ejected out at some stage and another run starts.

When the molten material is pushed by the hydraulic cylinder (piston or plunger) into the mold or die, the flow advances with certain paths inside the mold. Usually, a high pressure is applied and the molten material fills the cavity at a high speed with a strong force. When the cavity is filled, the filling pressure should be immediately switched to a much lower packing pressure for injection molding of polymer and much higher intensification pressure for die casting of metal alloys. With the monitoring of the advancement of the flow front a smooth transition from the filling stage to packing or intensification stage could be achieved. For injection molding this operation can reduce the part flashing and avoid the mold being impacted on with such a high force that may shorten the mold life. For die casting more materials are allowed to enter the cavity in order to compensate for the volumetric shrinkage. Moreover, flow front advancement measurements can be used to verify the computer simulation. The study of flow is also important for large single and multi-gated injection molding process in which a secondary flow phenomenon exists [65].

In some cases, the partial shots method was used to analyze the flow advancement qualitatively [65] and pressure sensor array was installed inside the die to monitor the flow quantitatively [15,30]. For die casting, the physical understanding of the molten metal is very difficult due to the lack of high performance sensors operated at high temperature and it has been reported that water is used for the study of the flow [17]. Although some useful information have been obtained but other methods are further needed to analyze the flow quantitatively and directly from the real process. Also many manufacturers studied the impact force control during the filling stage for the die casting machine. Their control methods were based on mechanical controlled devices and may not be precise and fast enough, thus more efficient and dynamic methods are desirable [68-68].

The ultrasonic pulse-echo method to be presented in this thesis can be used to monitor the change of the reflection coefficient at the mold (or die)-part interface since the flow front arrival changes the interface condition, hence the reflection coefficient [55]. Therefore the flow front advancement inside the cavity can be monitored.

After the filling stage, the part is subjected to a packing pressure for injection molding and an intensification pressure for die casting through the gate as it is cooled and solidified. Usually, for die casting, the gate is frozen soon after the filling and no more intensification pressure is applied during the part solidification. But for injection molding, since the gate is frozen at a much later time after the filling, the packing pressure keeps pushing the molten polymer into the cavity and the packing pressure forces the part to contact with interior walls of the mold. When the solidified material begins to shrink through its thickness, a gap is likely to be formed between the mold (or die) wall and the part [69-72]. Due to the formation of the gap, there might be a significant thermal contact resistance (TCR) between the part and the cavity wall, and it may reduce the heat transfer efficiency which affects the production cycle. Effects of the gap formation on injection molding of plastics have been mentioned by many researchers [70-72], but little effort has been devoted to its monitoring. At present, it seems that all cooling analysis software neglect the effect of the gap thermal resistance because of the little knowledge about the air gap development. It was suggested that the omission of the gap thermal resistance could be the main reason for the discrepancies between the experiments and the simulation [69,72]. Detection of the gap formation may provide more information about the heat transfer inside the parts and improve the physical understanding of thermal contact resistance of the gap. In addition, for injection molding after the gap is developed, and especially after the gate is frozen, the holding pressure will not further affect the part [11]. Thus keeping the holding pressure through the gate is not necessary. A dynamic control of the hold time of injection molding may be achieved by monitoring the gap development at the gate location resulting in energy savings.

Using pressure sensors which monitor the cavity pressure to detect the gap is one approach [58,69]. The onset of gap corresponds to the instant when the pressure drops to zero. However, a precise detection can hardly be achieved because the pressure sensors are made to measure the peak pressures and significant errors may occur, particularly in the low pressure range which corresponds to the critical period when the gap starts to be formed. Also, the approach requires direct contact of the sensor with the cavity hence material (i.e. polymer or aluminum), so locations of measurement can be limited since the mold needs to be permanently modified to accommodate such measurement.

By monitoring the reflection coefficient of the ultrasound signal from the mold-material interface, it is expected to detect the ultrasonic gap within 1 micron. From the detection of the ultrasonic gap, one may deduce some useful information about the thermal gap formation and contact resistance of the gap.

During the part solidification, it is desirable to use the properties of the solidifying material as input parameters to the process control system in order to achieve the quality control. Moreover, the basic understanding of the solidification is also highly needed. For instance, the temperature and the pressure during the packing or intensification stage are interesting in many ways as they determine the part quality characteristics such as part weight, density distribution, shrinkage and warpage [52-54,73]. How does the part undergo the solidification stage is essential to the mold and cooling line design, ejection time prediction, etc.

Because it is preferred that the monitoring does not perturb the process, non-destructive evaluation (NDE) methods such as ultrasound are attractive. Different ultrasonic wave velocities and attenuation inside material may relate to a range of the material properties such as density, temperature, grain size, residual stress and elastic constants, directly or indirectly [48]. The gap development itself is also part of the information about the solidification. Thus ultrasonic techniques indeed may characterize the material evolution from liquid to solid state [52,53]. For another example, the velocity of the ultrasonic wave inside the material is known to be strongly influenced by temperature of most materials. As one can measure the average velocity inside the material using ultrasound, the internal temperature distribution may be obtain based on certain reconstruction theory [9].

Overall, there are several essential tasks during the process such as (a) flow front monitoring during the filling stage, (b) monitoring of the gap development which is caused by the shrinkage of the part during the cooling and (c) monitoring of the material solidification which significantly affects the quality of the part. Performing all these monitoring can lead to an improved on-line quality control system and improve the basic understanding of the process.

Ultrasonic monitoring of polymer injection molding process [54-56,58,59] have been recently reported. In their studies ultrasonic pulse echo methods were used to monitor several aspects of the processing concerning mold filling, flash, and shrinkage in the mold and the ultrasonic velocity of the part during solidification was found to be sensitive to the temperature and pressure. The objective of this study is to improve the above monitoring tasks by using better ultrasonic measurement systems and techniques such as echo selection, two-channel acquisition system, advanced digital signal processing, etc., and performing additional tasks such as flow front advancement and gap development.

It appears that there has been no report concerning the ultrasonic monitoring of the die casting of aluminum because of the elevated temperatures. In this investigation, the flow front advancement of the molten aluminum and gap formation during aluminum solidification inside the cavity of a die will be monitored using a novel approach.

1.2 Thesis content

The ultrasonic pulse-echo method using longitudinal wave will be employed for the thesis study. The flow front and gap development monitoring will be mainly performed by observing the changes of the ultrasonic reflection or transmission coefficients at interface between the mold (or die) wall and processed part. The ultrasonic velocity measurement will be performed to continuously monitor the part under solidification. A two-channel PC based acquisition system will be developed in order to acquire the data at a high speed. All monitoring will be carried out on the industrial machine and a special design of buffer rod will be installed for aluminum die casting to perform the monitoring at the high temperatures. Intensive investigation will be performed on the polymer injection molding machine at different operation conditions for the monitoring of flow front, gap development and solidification. The investigation of the monitoring of flow and gap development of die casting of aluminum will also be implemented in this work.

In Chapter 2, the methodologies of the on-line ultrasonic monitoring of injection molding and die casting will be presented. First, reflection and transmission modes will be introduced and how the ultrasonic wave propagates at a boundary of two media will be studied theoretically. Then the reflection (or transmission) coefficient variation used to monitor the flow front advancement or gap development during the material process will be demonstrated experimentally. The theoretical calculation of the effects of the gap thickness on ultrasound reflection and transmission coefficients will also be presented in order to show the sensitivity of the technique. Finally, the results of the ultrasonic pulse-echo measurements operated in both transmission and reflection modes measuring the ultrasonic velocity of the processed part during solidification will be discussed.

Ultrasonic system designs and signal processing methods will be shown in Chapter 3. A PC based plug in two-channel data acquisition and data processing system will be developed for both the injection molding and die casting monitoring. High speed data acquisition will be implemented and evaluated to handle the fast signal acquisition especially for the die casting. Then, we will discuss several digital ultrasonic signal processing algorithms and processing routines used in our study. In the end, the acquisition system control and digital processing programs will be developed using Labview, a graphic programming software.

Investigations of on-line ultrasonic monitoring of the injection molding process will be presented in Chapter 4. The flow front advancement, gap development and solidification will be monitored by using longitudinal ultrasonic wave on a box shape mold. The installation of the ultrasonic sensors to the mold, choice of the couplant and injection molding operation conditions will be illustrated. In order to optimize the monitoring operation, several practical factors i.e., ultrasonic echo selections and temperature effects will be discussed. We will monitor the flow front at different locations using a two-channel acquisition system with different injection speed thus the flow front speed and the flow front advancement path inside the cavity can be deduced. Ultrasonic monitoring of gap development will be implemented and compared to the corresponding measurements carried out by the pressure sensor. Different packing pressures, melt temperatures and locations will be tried. In addition, the dependence of contact time on packing pressure and the gap effects on part cooling will be demonstrated by relating the contact time detected by ultrasound to the part temperature evaluated by infrared camera. Finally, the ultrasonic monitoring of solidification will be illustrated. For the solidification monitoring, we will measure the ultrasonic wave travel time inside the part first in transmission mode so that the velocity changes during the process can be obtained. The velocity measurement will also be performed in reflection mode in which the desired signal could be weak and signal enhancement processing will be introduced.

In Chapter 5, similar monitoring will be carried out on die casting of aluminum. The main differences of the implementation will be the considerations of the operation under high temperature and much faster casting speed. We will employ the latest buffer rod technology which can achieve the high temperature test and improve the ultrasonic SNR in our study. The design concept of such device and the integration with the die will be presented. The monitoring of the flow behavior during the filling stage will be performed using a high speed acquisition system with the time resolution of 1 ms. The gap development during the aluminum part solidification will also be investigated at different locations of different thickness. The gap development from the amplitude profile of the reflected signal at the die-part interface will be compared to the signal transit time shift during the process which may indicate the change of the die temperature thus the gap effects on the thermal contact resistance (TCR).

The summary and future plan will be presented in the final Chapter 6.

Chapter 2:

Ultrasonic Techniques

Ultrasonic techniques have been extensively applied to the industry for a long time. Because of the non-destructive nature, high accuracy, fast response and low cost, they play an important role in nondestructive testing, material evaluation and process control. Ultrasonic measurements are usually carried out by emitting an ultrasonic wave into the media and capturing the waves that propagate inside the material carrying the information corresponding to the properties, state or quality of the media. The results can be analyzed in terms of observations related to transit time or wave amplitude propagating inside the media. The measured ultrasonic velocity and attenuation coefficient can be correlated to material properties such as Young's and shear moduli, Poisson ratio, density, viscosity, grain size, temperature, pressure, etc., [48].

2.1 Reflection and transmission

As shown in Figure 2.1, when ultrasonic waves impinge on a boundary of two different media from the first medium, some of the energy will be transmitted through the boundary into the second medium and the rest of the energy will be reflected back.

It is understood that the reflection and transmission coefficients as R and T, respectively, can be given as

Reflection coefficient: $$R = \frac{Z_1 - Z_2}{Z_1 + Z_2} \tag{2.1}$$

Transmission coefficient: $$T = 2\frac{Z_2}{Z_1 + Z_2} = 1 - R \tag{2.2}$$

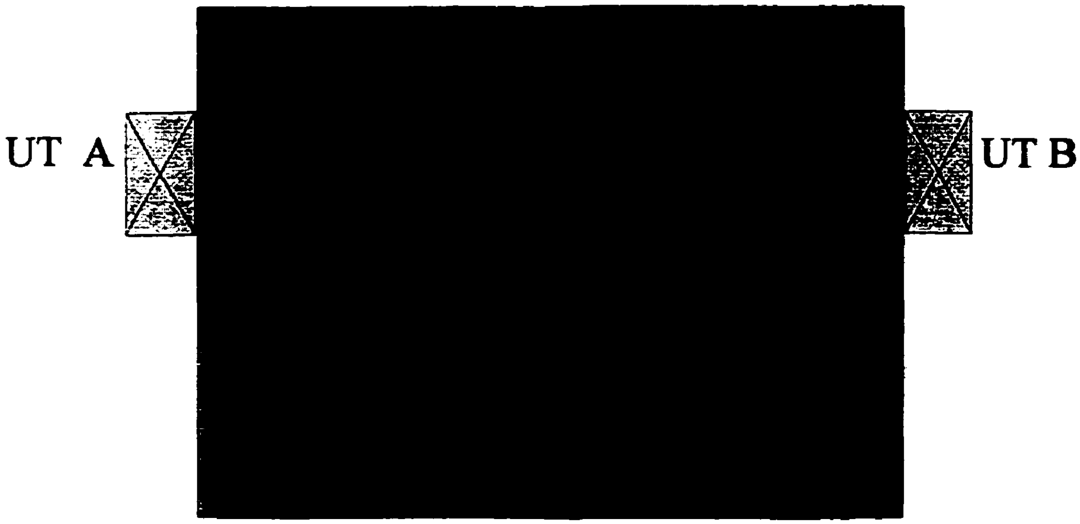

Fig.2.1: Reflection and transmission of ultrasonic waves at the interface of two media.

The reflected power P_R and transmitted power P_T over the incident power P_I depend on the acoustic impedance of the two media, Z_i,

$$P_R / P_I = [(Z_1 - Z_2)/(Z_1 + Z_2)]^2 \tag{2.3}$$

$$P_T / P_I = 4Z_1 Z_2 /(Z_1 + Z_2)^2 \tag{2.4}$$

Z_i is the product of the density ρ_i and wave velocity V_i of the materials, i.e., $Z_i = \rho_i V_i$, $(i = 1,2)$

Pulse-echo ultrasonic measurements can be operated in reflection and transmission modes. In the reflection mode, the signal is transmitted and received by the same ultrasonic transducer (UT) while in transmission mode, signal is transmitted by a UT and received by another one separately. For example, in figure 2.1, UT A emits an ultrasonic wave and the wave impinges on the interface between two media. Partial energy is reflected back and received by the UT A and other part of the energy goes through the interface and received by the UT B.

2.2 On-line ultrasonic monitoring

In-situ ultrasonic monitoring during the process has been reported [34,49-59]. The fast response and non destructive nature are the advantages over many other alternatives. Usually the operation principles are simple and electronics systems are required to perform the measurements.

The principle in probing the flow front and gap development is to monitor the mold (or die)-part interface condition through the ultrasonic wave reflection and transmission coefficients. Ultrasonic wave propagation velocity measurements can be related to the properties of the processed materials such as the solidification. All these measurements may be carried out by analyzing the reflection or transmission coefficients that can be obtained from the signal amplitudes or time delays between echoes.

2.2.1 Flow front monitoring

As shown in Figure 2.2, the UT is operated in reflection mode. Before the injection of molten materials into the mold or die, the cavity is empty. The UT that is mounted on the mold external surface emits the signal and the signal almost totally reflected back at the steel (mold or die)-air (cavity) interface due to the small acoustic impedance of the air comparing to that of steel, thereby the reflection coefficient is almost 1. During the filling, the flow front advances inside the cavity. As soon as the molten materials wet the mold inner surface where the ultrasonic waves impinge, a part of the ultrasonic wave energy will penetrate into the molten material thus the reflected ultrasonic wave energy decreases indicating the arrival of the flow front at that particular location. Comparing polymer injection molding with die casting of aluminum (Al), the reflection coefficient will decrease more for die casting as Al has a closer acoustic impedance value than polymers to that of the steel mold. Therefore more ultrasonic energy can go into the molten Al. Also the flow front speed is much faster for die casting case (total filling time is less than 30 ms in our case) thus a high speed acquisition system is needed to perform such measurements. Using an array of UTs at different locations, flow front advancement inside the cavity can be obtained.

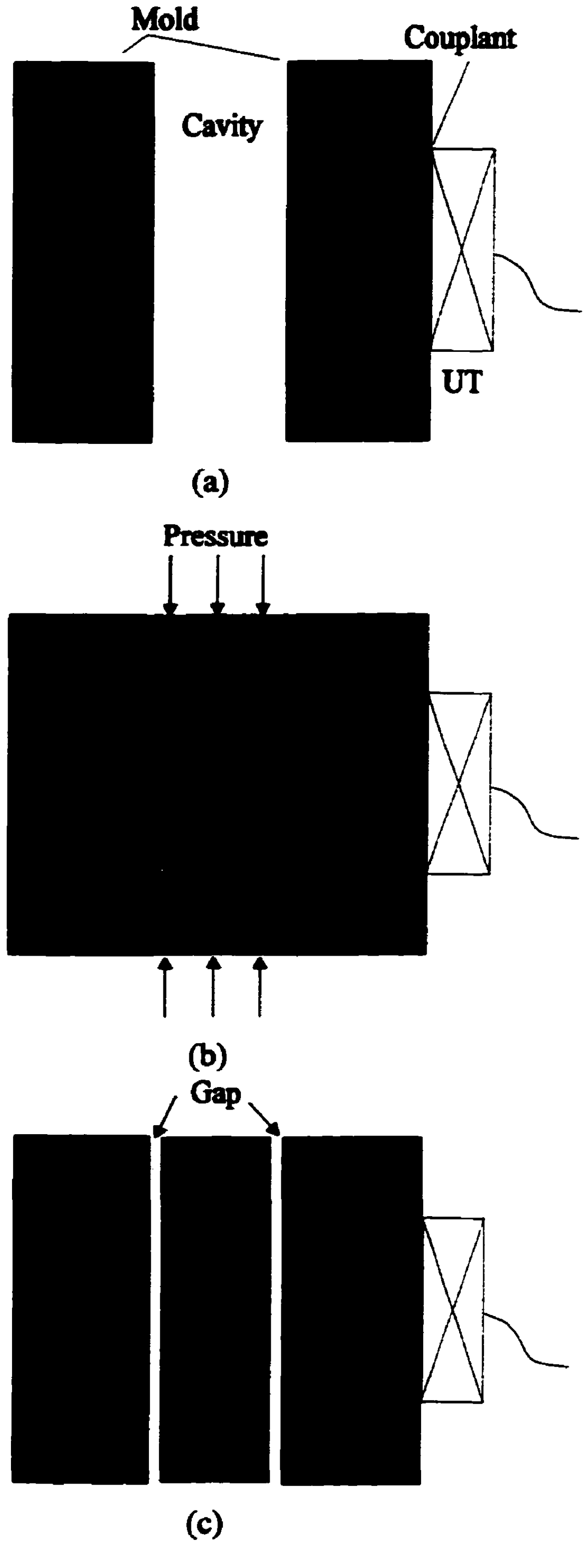

Fig.2.2: Ultrasonic monitoring of flow front and gap development in reflection mode. (a) Empty cavity before injection (b) Good contact after injection and (c) Loss of contact after gap formation.

2.2.2 Gap development monitoring

Figures 2.2(a)-(c) show the schematic to detect the gap development in reflection mode. As mentioned in 2.2.1 before the filling, the ultrasonic signal is totally reflected back at the steel-air interface (Fig.2.2 (a)). As soon as the flow front arrives (Fig.2.2(b)), the amplitude suddenly drops as the interface changes to steel-material interface. After the filling, the part cools down and then becomes solidified. In the beginning, the ultrasonic signal amplitude changes slightly due to minor change of the elastic properties of the part. As the solidification progresses, the part begins to shrink through its thickness and a gap is likely to be formed. After a sizable (>1μm thick) gap is developed, the interface return to the steel-air condition , therefore, the amplitude returns to the high level (Fig. 2.2 (C)).

Similar monitoring can be carried out in transmission mode in which another UT is installed on the other side of the cavity. In that case, the receiving UT can only receive the signal when the molten material contacts with both sides of the cavity and lose the signal when there is a gap formed on either side.

It is understood that the gap detected by ultrasound represents a physical gap that prevents the transfer of energy in terms of stress waves. It is of interest to examine the sensitivity of the technique for detecting the range of gaps that may present resistance to heat transfer because in injection molding and die casting processes the transfer of thermal energy is mainly in the form of conduction. In other words, the gap makes the cooling inefficient.

Next, we will explain how the thickness of the gap affects the reflection or transmission coefficient. Figure 2.3 presents a three-layer model in which they are infinite in other two dimensions. Z_1, Z_2 and Z_3 are the acoustic impedance values of steel, air gap and molten material, respectively. v is the velocity inside air gap, f is the ultrasonic operating frequency and d is the thickness of the gap.

$$Z_{in} = \frac{Z_3 - iZ_2 \tan(\frac{2\pi f}{v} d)}{Z_2 - iZ_3 \tan(\frac{2\pi f}{v} d)} Z_2 \qquad (2.5)$$

The reflection coefficient at the boundary between steel wall and the gap is:

$$\Gamma = \frac{Z_1 - Z_{in}}{Z_{in} + Z_1} \qquad (2.6)$$

The transmission coefficient at that boundary is:

$$\mathrm{T} = \frac{2Z_1}{Z_{in} + Z_1} \qquad (2.7)$$

To calculate the reflection and transmission coefficients as a function of the gap thickness, we choose Z_1=4.6×10^7 kg/m^2·s for the steel, Z_2=4.27×10^2 kg/m^2·s for the air and Z_3=2.4×10^6 kg/m^2·s for lucite in case of polymer injection molding and Z_3=1.7×10^7 kg/m^2·s for Al in case of die casting of Al, respectively. Figure 2.4(a) shows the result for the steel-air-lucite case and Figure 2.4(b) for the steel-air-Al case. The operating frequency is f = 5 MHz. From these two figures, a gap over 0.1 μm prevents most of the ultrasound energy transmitting through the gap for both cases. The Al case, the reflection coefficient changes even more dramatically.

Meanwhile, if a polyethylene part is 2 mm thick and the shrinkage is 3% of the volume, there exists a gap of 10 μm formed at both sides of the part at the end of the process. Thus the ultrasonic detection of the gap formation is a very sensitive and reliable approach.

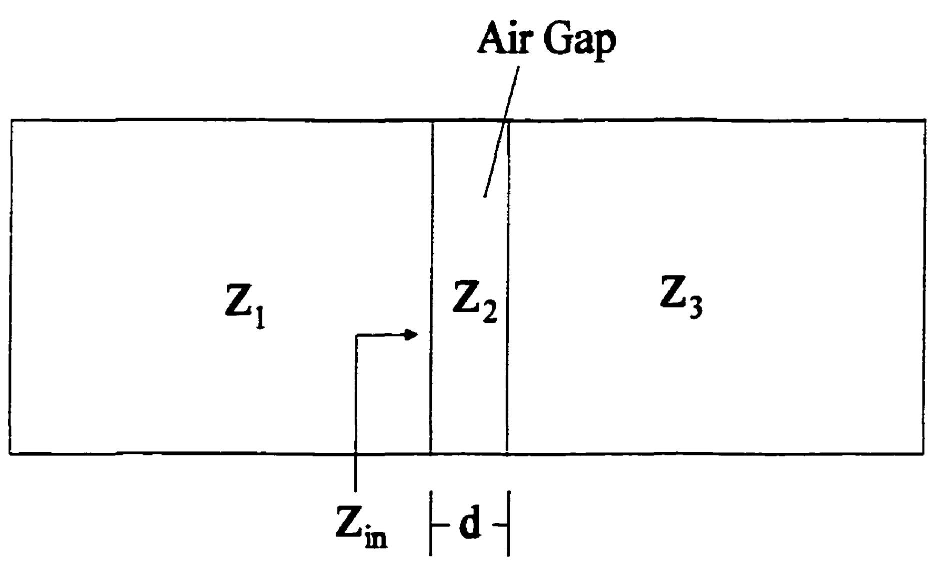

Fig.2.3: A three layer-model for reflection coefficient calculations.

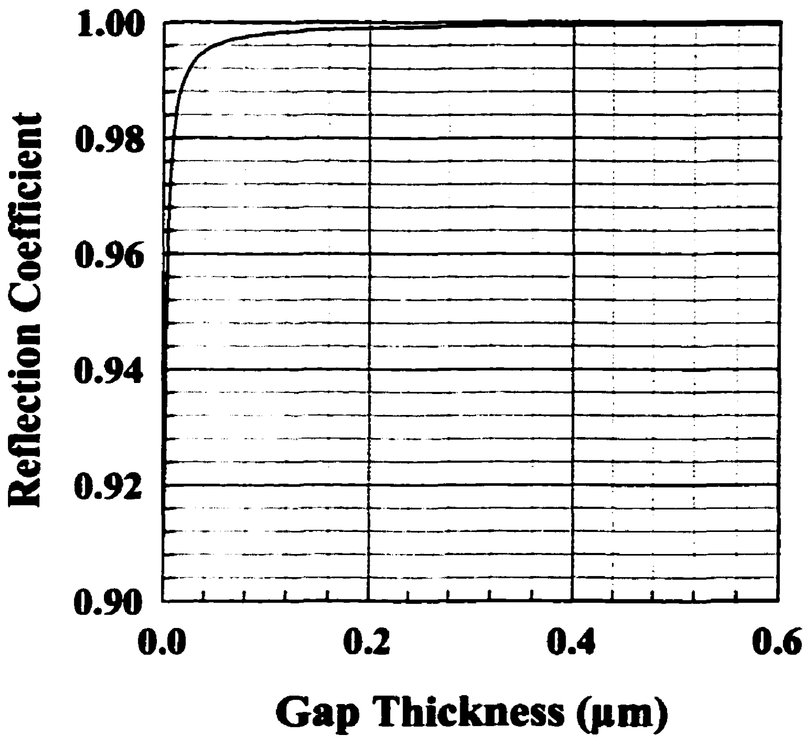

(a)

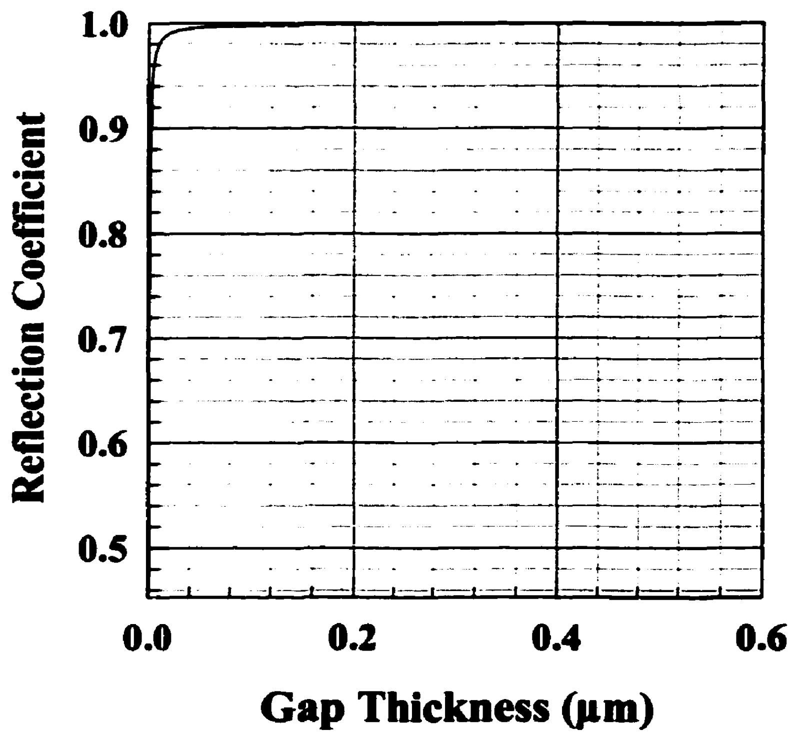

(b)

Fig.2.4: Reflection coefficient vs thickness of air gap for the three layer structure of (a) steel-air-lucite and (b) steel-air-aluminum.

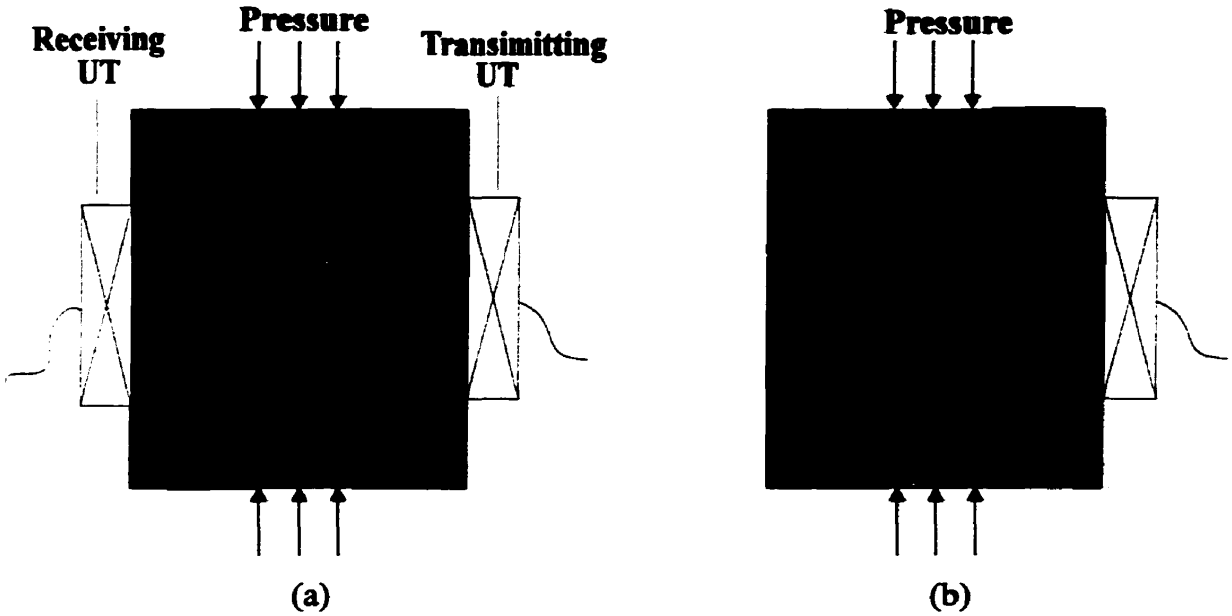

Fig.2.5: Schematic of solidification monitoring in (a) transmission and (b) reflection mode.

2.2.3 Solidification monitoring

As soon as the molten material is injected into the cavity, it comes into contact with the mold or die which is cold, solidification starts. During solidification, part properties such as density and moduli together with temperature and pressure change continuously. The ultrasonic signals that travel inside the part thus carry the information related to these properties and their variations.

Figure 2.5(a) shows a schematic of the solidification monitoring in transmission mode. After the filling stage and before the gap formation, the ultrasonic waves can be transmitted into the material and received by the receiving UT. The amplitude and the transit time of the received signal may reveal the velocities of the ultrasonic waves in the part. The velocity and attenuation of the part during material process may reveal some significant information. Since in transmission mode the ultrasonic wave also travels through the steel mold or die wall, the influences such as temperature variation of steel wall during the process should be considered.

The transmission method is often limited for practical use because it is not feasible to install the two UTs at desired locations which demand two-side access in a real industrial material processing machine, i.e., injection mold or die. The reflection mode is preferred because only one side access is required. Figure 2.5(b) shows a schematic of the solidification monitoring in reflection mode. The reflected signal from the further part-mold interface can be used for the evaluation of the part solidification because it travels through the entire part in the thickness direction. However, this method suffers a high loss leading to a poor signal to noise ratio (SNR). Because the wave travels a round trip inside the part, it has twice the signal loss than that experienced in transmission mode. Proper signal processing algorithm, UT and coupling, etc., may overcome the difficulties.

2.3 Summary

The principles of ultrasonic monitoring of the flow front advancement, gap development and solidification of the injection molding and die casting processes are introduced. The reflection and transmission coefficients of the longitudinal wave at the interface between mold or die and part can be used to monitor the flow front arrival time and the gap formation. Effects of air gap on the reflection or transmission coefficient are theoretically investigated and results show that the gap of 0.1 μm can be detected. Both reflection and transmission configurations may be used to obtain the ultrasonic signals that propagate inside the part. Reflection mode is preferred over the transmission mode but signal enhancement may be required due to the low SNR.

Chapter 3:

Data Acquisition System and Signal Processing

The advantages that ultrasonic waves have the capability to probe interior part of the material have been mentioned several decades ago. However, the application of ultrasound for process control could not be achieved due to the limitation to acquire, store and analyze the ultrasonic signal continuously and efficiently. With the significant development of the digital technology and the improvement of computers, even very complex signals may be acquired, recorded and processed in a short time duration to achieve on-line monitoring. In this chapter an on-line ultrasonic system for the monitoring of injection molding and die casting processes will be presented and several signal processing procedures will be introduced.

3.1 Data acquisition system

For our studies, 5 MHz and 10 MHz ultrasonic longitudinal transducers were chosen because of their efficiency, compact size and acceptable loss in the probed parts. In order to meet the Nyquist sampling theory to process the digital signal without aliasing high sampling rates were used. In some cases, a very high acquisition repetition rate (e.g. 1000 Hz) was required in order to monitor very short duration processes. For example, during the filling stage in die casting of aluminum (Al), the molten Al may be filled into the die in a duration less than 40 ms and the acquired data interval should cover 1 ms in which enough information may be obtained. A PC based plug-in acquisition system was chosen in our study.

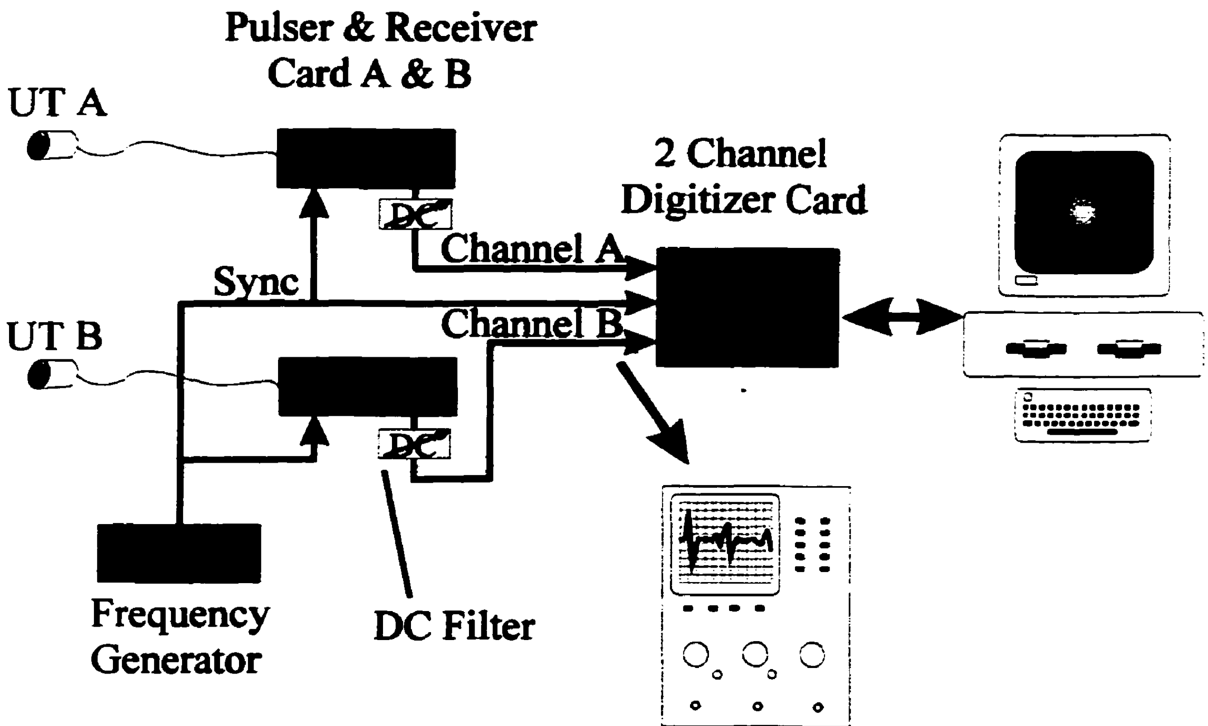

Fig.3.1: Schematic of a two-channel on-line ultrasonic monitoring system.

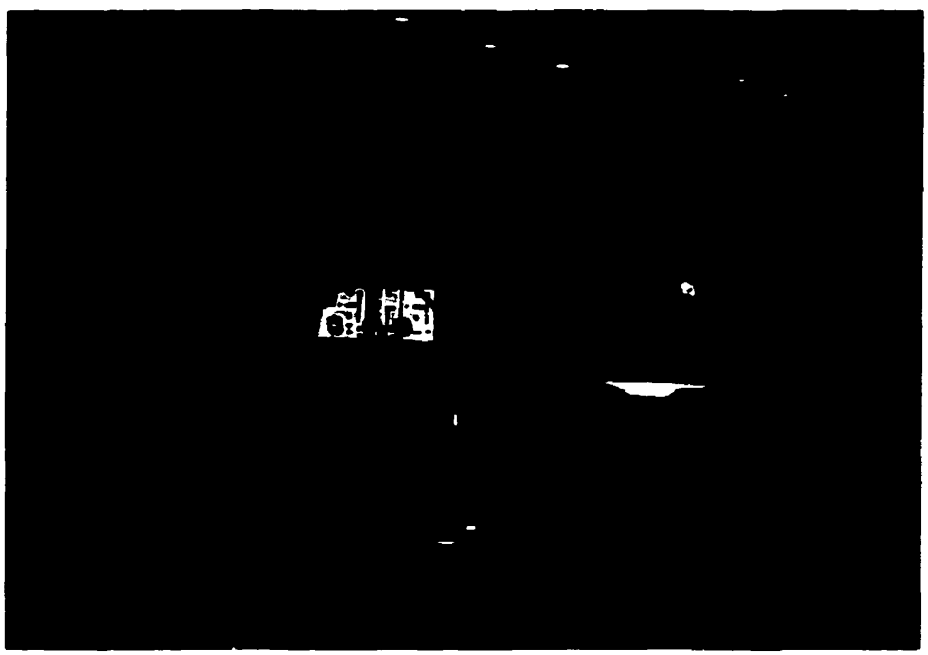

Fig.3.2: A two-channel on-line ultrasonic monitoring system setup.

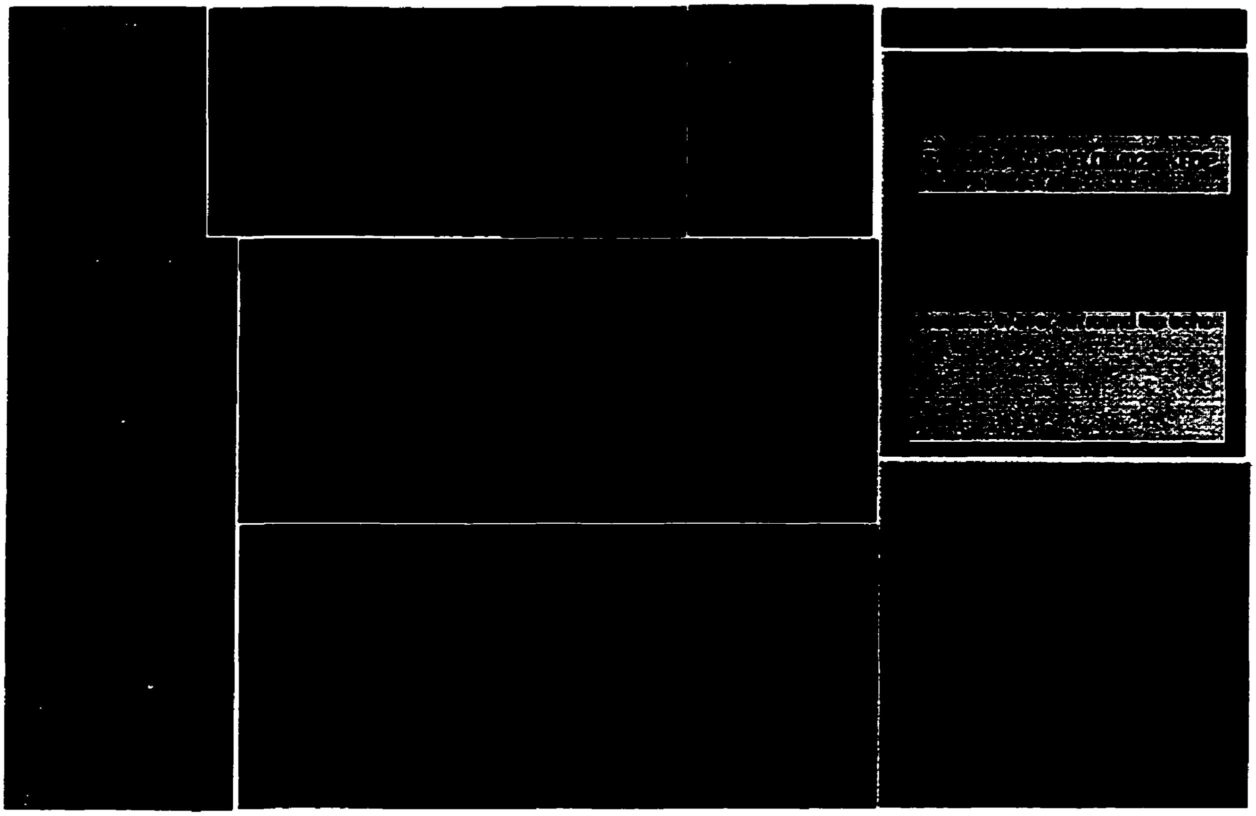

Fig.3.3: Panel of the virtual scope of the two channel system.

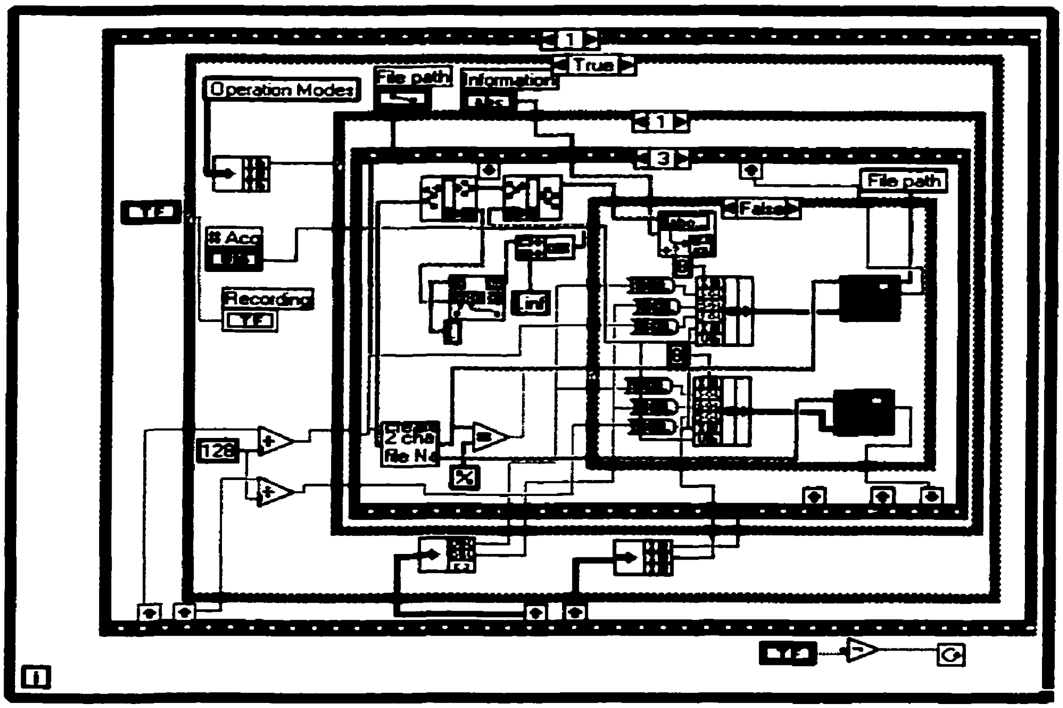

Fig.3.4: Block diagram programming in Labview.

3.1.1 Hardware specifications

- Digitizer:CompuScope 250, from Gage Applied Science, Inc.
  Sampling rate: up to 100 MPS for one-channel mode and 50 MPS for two-channel mode.
  On-board memory depth: 32K upgradable to 8M
  A/D resolution: 8 bits
- Pulser and receiver: MP 203 Pulser and MR 101 Receiver from MetroTek, Inc.
  Frequency range from 0.5 MHz to 20 MHz.
- Frequency Generator: HP 811A
- Oscilloscope: Tektronix 7854
- Computer: Pentium 90

Figures 3.1 and 3.2 show the data acquisition system setup. A frequency generator is used to generate a synchronization signal with the desired frequency to synchronize all the devices including the two pulsers and digitizer cards, thus to control the acquisition rate. A detailed description will be given in **3.1.3** *acquisition rate control.* The pulser and receiver can be operated at different configurations; namely reflection and transmission. An oscilloscope is used to monitor the signal in real time. The digitizer CS250 can be used in one-channel or two-channel mode, and has a direct access to the computer RAM address for performing the acquisition and transferring the data. Two high pass filters are also used here to eliminate DC components of the signals from the outputs of the receivers before the signals are fed to the digitizer, thus full range D/A conversion may be achieved without the interference of the DC component.

3.1.2 Virtual instrument

The entire acquisition system was designed as a virtual instrument on Window environment using Labview software. Labview, introduced ten years ago by National Instruments Inc., allows the user to build the instrumentation systems with standard computers and cost-effective hardware. These software-centered systems leverage off the computation, display, and connectivity capabilities of computers to provide the strength and flexibility for building up the instrumentation functions.

Figures 3.3 and 3.4 show the panel and block diagram of the virtual scope of the two-channel acquisition system used for the experiments. Acquisition configurations, such as operation mode, triggering and data recording requests can be easily set up as a conventional instrument with user friendly interfaces. Integrating with the CS250 Compuscope card at the maximum 100 MPS sampling rate, the system works well as a wide bandwidth oscilloscope up to 50 MHz. With the high throughput from the acquisition card to the computer, burst signal can be recorded, and then post signal processing software are performed under the Labview programming with its powerful analysis function library. The functions of the system can be modified easily to meet different situations with the graphical programming method. Such a flexibility reduces the programming time and enhances the performance of the system especially for research under different requirements.

3.1.3 Acquisition rate control

At present, Labview only has the time resolution of 55 msec under Windows 3.1. It means that the acquisition rate can be only controlled by the software no more than 20 times/sec. In our case, especially for die casting of Al, the flow front monitoring requires a much higher time resolution which is better than 2 ms. The solution to this problem is the hardware, either to choose an acquisition card that is program controllable or to use a signal generator to trigger the whole system with the needed acquisition time interval.

In our system, we chose the latter method which uses a function generator with a desired operating frequency range to realize the acquisition rate control. The same trigger source from the frequency generator triggered the whole system. The two ultrasonic signal generators and the acquisition card were operated in the external trigger mode and to achieve the synchronization. The function generator could produce a high frequency signal up to 20 MHz and the maximum repetition rate could be 100K for the MP 203 pulser. Usually the limitation for acquisition repetition rate comes from the digitizer card throughput to the computer that depends on the card, computer bus as well as the acquired signal size.

3.2 Design of a PC based plug-in high speed acquisition system

3.2.1 High speed acquisition rate design

PC-based plug in card can access the computer bus directly during the acquisition. During an acquisition, firstly, the computer sends an initial message to the card and the card initiates the parameters such as trigger setup, sampling rate, voltage range, memory depth, etc. Then the computer sends a signal to tell the card that the computer is ready to capture the data. As soon as it detects the trigger signal, the card samples the analog signal at the given sampling rate for a given time depth and saves it to the card memory. Finally, the computer can retrieve the data from the card memory to display, record or process.

In addition, during the acquisition, there are many I/O interrupts, data transfers and system operation tasks that may limit the card acquisition data throughput. Below are several important factors which may affect the acquisition system performance:

1. Performance of the data acquisition card: That is the most important issue. If it needs to transfer the acquired data to the computer during a continuous acquisition, the throughputs of the card to the computer memory determine the system acquisition rate. If the card saves the data directly into its memory, the card memory size and the acquisition throughput will affect the acquisition rate.

2. Performance of the computer: The type of the CPU chip, bus speed, cache and RAM sizes are all of concerns. A high speed CPU, bus, large cache and RAM size will improve the throughputs of the system.

3. The operation environment of the card driver software: The card driver needs an efficient operation system to operate the card driver and optimize the I/O operation to improve the card performance. For a complex operation system such as multitask operation system, there are lots of unexpected events during the acquisition and they may affect the card operation.

Below are the additional considerations for our system to achieve a high speed acquisition rate:

1. Use the block transfer routine in which the card transfers the data in blocks (up to 4k bytes) to the computer instead of transferring one data point each time. It decreases the I/O operation and increases the throughputs.

2. Transfer the data from the card memory to the computer memory buffer instead of saving to a disk file during the acquisition. It always takes time to save the data

directly to the file and the throughputs are limited by the disk operation. The computer memory is usually big enough to handle the data temporarily except the data occupy too much RAM size and slow down the whole computer operation.

3. Simplify the card driver software function during the acquisition in order to give more CPU time to the card operation. Some functions such as the display of the count number during the acquisition can occupy the CPU operation time and decrease the throughput significantly.

3.2.2 High acquisition rate simulation

In order to evaluate the performance of the system under high speed acquisition, simulations were performed at different acquisition rates to evaluate the stability and the maximum acquisition rate of the system.

Two signal generators were used in the simulation. One generates a signal with the an expected repetition rate as the card trigger signal. Another generates a square signal with a known low frequency as the card input signal. After the acquisition, we can retrieve the square signal by plotting the maximum value of each acquired frame. We know precisely the input square signal frequency thus the time interval between two signals. So we can count the number of the acquired square signals thus derive the acquisition rate for the system. For example, the input square signal is 1 Hz and the triggering signal is 500 Hz. All the trigger signal should be detected by the system if the maximum repetition rate of the system is over 500 Hz. Therefore, we could obtain 500 acquisitions data between two rising edges of the obtained square signal. If the maximum acquisition rate is less than the trigger signal, only part of the trigger signals can be detected and the acquired data between the two rising edges will be less than 500. In Figure 3.5, the counted points between two rising edges of the obtained square signal is around 500 and follows the trigger signal of 500 Hz. It indicates that the maximum acquisition rate is higher than 500 Hz.

Below are the computer and acquisition card conditions:

- Computer: Pentium 90, RAM 16 Mbytes, Cache enable
- Card: Gage CS250, Card memory 32 Kbytes, Multiple Record unable
- Card drivers : Labview for Windows

Table 3.1 shows the simulation results in the case of a two-channel mode. The frame sizes are 64 byte and 128 bytes, respectively. It shows that the system acquisition rate follows the trigger frequency up to 800 times /sec. Below this rate, the acquired square signal has an evenly distributed shape (see Fig.3.5). When we increased the repetition rate of the trigger signal further more, it was observed that the trigger rate is in excess of the capacity of the card and some trigger signals were ignored as the card was still busy at the moment of the trigger arrival. A maximum acquisition rate can be achieved if we increase the trigger frequency to a very high level, i.e., 100 KHz, thus the card keeps working nearly without any free time between acquisitions because there is always a trigger signal arrived as soon as the card finishes one acquisition. From our simulation, the maximum acquisition rate is 1100 times/sec for 64 bytes frame case and 920 times/sec for 128 bytes frame case. For monitoring the die casting of Al process 64 bytes frame size will be used because of the speed requirement.

Similar simulations were also performed in single channel mode. The results are given in Table 3.2. The maximum acquisition rate is around 1300 times/sec.

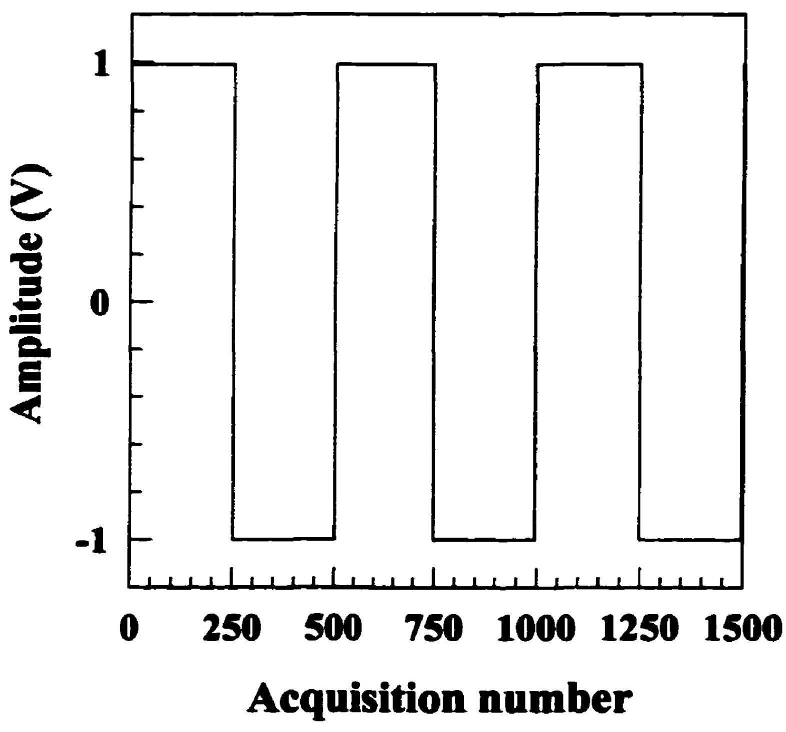

Fig.3.5: Simulated 1 Hz square signal (Trigger signal frequency 500 Hz and frame size 128 bytes).

Table.3.1: Simulated acquisition results for 64 bytes and 128 bytes frames in the two channel mode

Trigger Signal Frequency (Hz)	400	500	600	700	800	900	10k	100k
Acquired Acquisition Rate (Hz) (Frame size 64 bytes)	393	502	597	691	773	864	1021	1099
Acquired Acquisition Rate (Hz) (Frame size 128 bytes)	408	502	597	691	785	838	890	916

Table.3.2: Simulated acquisition results for 64 bytes and 128 bytes frames in the single channel mode

Trigger Signal Frequency (Hz)	700	800	900	1000	1100	1200	10k	100k
Acquired Acquisition Rate (Hz) (Frame size 64 bytes)	691	811	890	995	1099	1178	1309	1387
Acquired Acquisition Rate (Hz) (Frame size 128 bytes)	707	796	890	995	1073	n.a.	1204	1230

3.2.3 Future improvement

Two aspects will be improved to the current system in the future. One is the multiple channels capacity and another is the further improvement of the acquisition rate thus the sub-millisecond time resolution can be achieved.

A multiplexer card is suggested here to increase the acquisition channel numbers, e.g., 48. efficient multiplexier can offer the system with reasonable acquisition rates. Under such situation only one pulser and receiver card is necessary.

In case of die casting, sub-millisecond resolution is preferred. The CS250 card has a solution called multiple recording mode. In this operation mode, the card can acquire the data as long as there is a trigger signal and saves it to the card memory instead of transferring to the computer memory or disk. But the card memory size needs to be upgraded to, e.g., 4 Mbytes in order to have a sufficient recording length.

3.3 Signal processing algorithms

3.3.1 Digital signal interpolation

It is known that a digital signal obtained from sampling a continuous signal above the Nyquist rate can be reconstructed back exactly to its original form by an ideal low pass filter. The value of the signal between two samples is interpolated by a lower pass filter. In practice, the analog signal is recovered by a D/A converter to achieve such interpolation. In some applications, a signal is digitized, processed and some information can be derived directly from the digitized signal without going through the reconstructing. In such cases, the interpolation between samples may require the digital processing methods.

One approach is the classical polynomial interpolation method [80]. Linear interpolation involves only two consecutive samples and it equals to a low pass filter which is appropriate only if the original sampling rate is many times of the Nyquist rate. The inadequacies of linear interpolation lead to the use of higher order polynomials which mean that several samples are needed to obtain one value. In addition, other numerical methods such as cubic spline interpolation may be used.

Finite duration impulse responses (FIR) and infinite duration impulse response (IIR) digital filters as interpolation filters were also introduced. It was indicated that FIR filters were generally preferred because of its linear phase response [80]. Improved interpolation can be achieved by inserting the zeros between two samples and then filter the sequence with an ideal digital low-pass filter, and it is equivalent to increase the sampling rate [80-81]. In practice, first, the original digital signal is converted to frequency domain using the digital Fast Fourier Transform (FFT), then zeros were padded with the number according to the desired interpolation resolution and finally, the interpolated signal can be obtained by the inverse FFT.

3.3.2 Envelop of the analytic signal

Traditional ultrasonic signal processing often neglects the phase information and rectifies the signal as the approximation to the envelope of the signal. Such approximation may be satisfactory for the cases involving narrow band signals. In order to increase the resolution of the amplitude and time delay measurements, wide band signal is applied and the above rectification may affect the measurement accuracy especially for the evaluation of closely spaced interfaces and accurate samples of small velocity variations. These shortcomings of conventional ultrasonic signal processing are particularly severe for automated decision-making process [82].

The true analytic signal envelope deduced by both the real and imaginary parts of the ultrasonic signal can improve the measurement. Usually, the real part of the signal is recorded and the imaginary part is the Hilbert transform of the real part [81]. Digital implementation was introduced in [82] to obtain the analytic signal and it is appropriate for sampled data system.

In our program, the envelope of the analytic signal z(n) is defined as the inverse Fourier transform of Z(k) given by:

$$Z(k) = \begin{Bmatrix} S(k)\ for\ k=0 \\ 2S(k)\ for\ k=1\ to\ N/2 \\ 0\ for\ k=N/2\ to\ N-1 \end{Bmatrix} \tag{3.1}$$

where S(k) is the Fourier transform of the recorded signal s(n).

3.3.3 Several process routines

In our study, the amplitude of the signal and the transit time inside the material will be used for studies. Digitized ultrasonic signals were recorded as a finite length arrays. Various windows and digital filters are applied to the digitized signals in order to reduce the leakage and filter the noise. The smoothing windows can minimize the transition edges of truncated waveforms in order to overcome the spectral information leakage produced by the discontinuities of the finite length waveform [81]. Two process routines were developed to find the maximum amplitude value of a signal and to calculate the time delay between two waveforms.

(a) Routine for finding maximum amplitude

Firstly, window and filter are applied to the digital sequence. The window can be varied according to the recorded signal. In our program, cosine tapered window is used which will not affect the maximum amplitude because we always record the minimum length of the waveform in order to achieve the maximum higher acquisition rate. The filter can be IIR as the linear phase response is not demanded. Butterworth bandpass filters are used with the cutoff frequency selected according to the transducer main operation frequency. Secondly, we obtain the analytical signal envelope using Hilbert transform. FFT and inverse FFT are also used in the program. Finally, the maximum magnitude on the analytical signal envelope is derived using interpolation which can be either numerical or frequency zero padding as we introduced before. Schematic of this routine is shown in Fig.3.6.

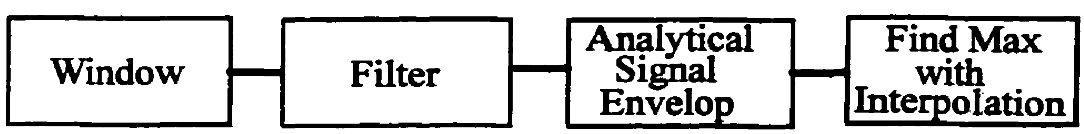

Fig.3.6: Schematic of the routine to find the maximum amplitude of each acquired signal frame.

(b) Time delay calculation routine

Time delay between two waveforms can be calculated by cross correlation. Correlation detection probably provides one of the most reliable ways that disregard the random noise and increase the precision of the measurement. It becomes a standard method for ultrasonic signal processing. In our program, windows and filters are applied to the waveforms first, and the calculation of the envelope of the analytical signal can be an option depending on the needs. Cross correlation between two waveforms is carried out together with an interpolation scheme thus the time delay measurement can be quite accuracy. It is noted that some process program examples are presented in the Appendix.

3.4 Summary

On-line ultrasonic monitoring data acquisition system was developed. The PC based plug-in acquisition system has the advantage of the portable PC system and also achieved the high speed acquisition rate by optimizing the data acquisition operation. Acquisition speed of 1000 frames/sec was achieved from our simulation for a two channel system with the frame size of 64 bytes. A higher speed was also obtained for a single channel mode. The virtual instrument concept was applied here using the graphic programming language Labview which offers flexible development method and user friendly interface. The sampling rate has been up to 100 MHz for single-channel mode and 50 MHz for two-channel mode.

Several ultrasonic digital signal methods including the digital interpolation between sampled values and the envelope of the analytical signal deduced by Hilbert transform were also introduced. Two process routines to obtain the signal amplitude and signal transit time were explained as well.

Chapter 4:

Ultrasonic monitoring of the injection molding process

4.1 Introduction

The principles for on-line ultrasonic monitoring of polymer injection molding have been introduced in Chapter 2. Although some aspects such as mold filling, flash, shrinkage and solidification in the mold have been investigated [54-56,58,59], in this chapter, the flow front advancement, the gap development and the solidification monitoring during injection molding will be investigated. Measurements of the reflection or transmission coefficients at the steel mold-polymer interface and wave velocity inside the polymer during the process will be performed to accomplish above monitoring tasks. Along this chapter the improvements or different techniques adopted in our approach over the reported methods will be given in due places.

The monitoring will be carried out on an Eagel injection molding machine. Practical considerations involving the use of a box mold will be demonstrated in order to optimize the ultrasonic signal and improve the precision. The box mold is chosen because it is simple and satisfactory for the ultrasonic studies. The two-channel acquisition system introduced in Chapter 3 will be used to acquire the flow front arrival time at two different locations and with different injection speeds. Gap detection using both pressure and ultrasonic sensors will be evaluated and compared. The time during which the part is in contact with the mold wall will be measured by the ultrasonic sensor at different packing pressures. Effects of the gap on cooling could be obtained by relating the ultrasonic experimental results to those obtained by an infrared technique. Velocity measurements of the part will be carried out in transmission as well as reflection mode using the cross correlation method.

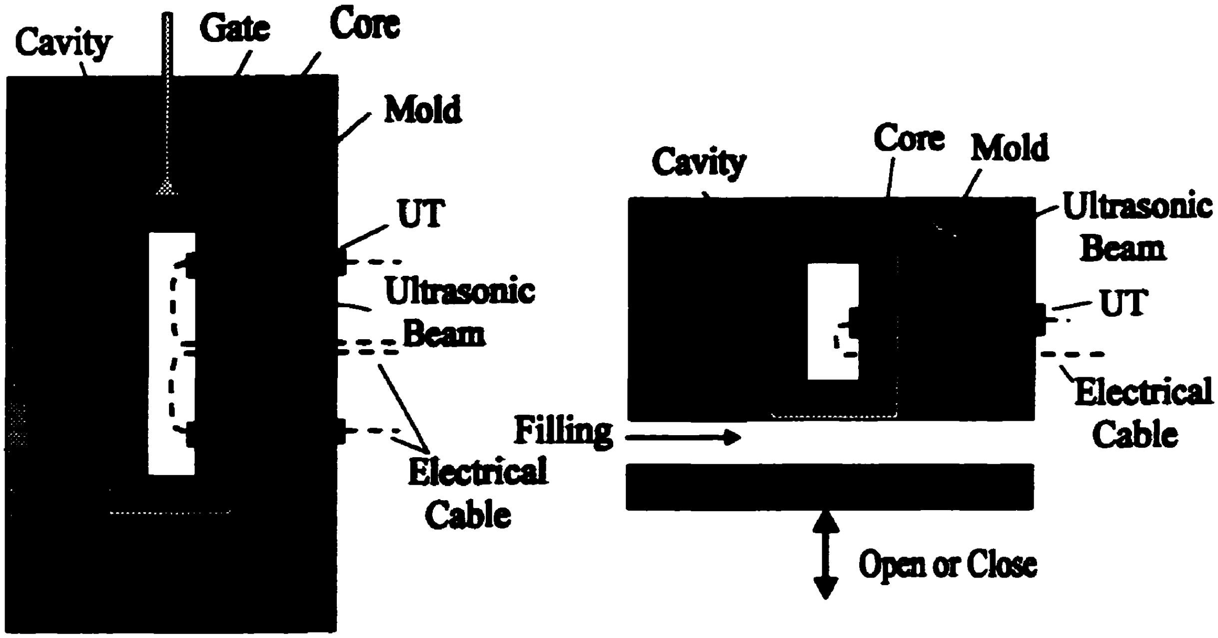

Fig.4.1: Cut view and top view of the mold.

4.2 Experimental setup

4.2.1 Mold and sensor installation

Small boxes, 122 × 50 × 27 mm, were molded on a 70 ton Engel injection machine. The mold consists of a cavity and a replaceable insert core, as shown in Fig.4.1. The insert core used in the present study has a 3° draft angle in the direction of the demolding; and it produces boxes having a bottom of 4.76 mm thick and four side walls of 3.85 mm thick. In addition, the core is deliberately made hollow to permit the installation of ultrasonic transducers (UTs) for detecting the steel core-part interface condition in reflection mode from the core side and performing the transmission mode measurements as well.

A transparent plastic plate was used on the outside of the mold as a fixture to hold the UTs at desired locations with proper pressure provided by screws. The UTs inside the insert core were fixed by springs installed within the hollow space. Viscous ultrasonic couplant was used between the UT and the mold in order to extend the working time of the couplant. It was observed that such a couplant can work well at least for one month.

4.2.2 Injection machine operation conditions

For this study, the polymer boxes were molded with the following conditions:

- Injection speed: 1 inch/sec ~ 3 inch/sec
- Packing time: 30 sec
- Cooling time: 5 sec
- Melt temperature: 190°C and 230°C
- Mold temperature: 22°C
- Hydraulic packing pressure: 0~8000 psi

To study the flow front the injection speed was varied; different packing pressures were applied in order to study the effects on gap formation and part cooling. The main polymer used in the test is a high density Polyethylene, HDPE 6706, manufactured by Exxon. The boxes were molded with an addition of 4% by weight of the master batch material (CE-80695) which makes the boxes black in color to facilitate the thermal study using an infrared method.

4.3 Operation considerations

The detailed geometry inside the mold is very complex because of the cooling lines, insert runners and ejector pins. These elements cause undesired multiple ultrasonic reflections and interfere with the desired signals. In addition, during the process, the mold temperature can vary and affect the performance of the UT and couplant. All these factors should be considered for the optimization of the operation.

4.3.1 Echo selection

As shown in Fig.4.2, ultrasonic signals traverse back and forth inside the mold wall. Properly choosing the echo may enhance the monitoring result such as time resolution related to the amplitude variation rate of the reflection coefficient and noise caused by the wave diffraction with the mold wall.

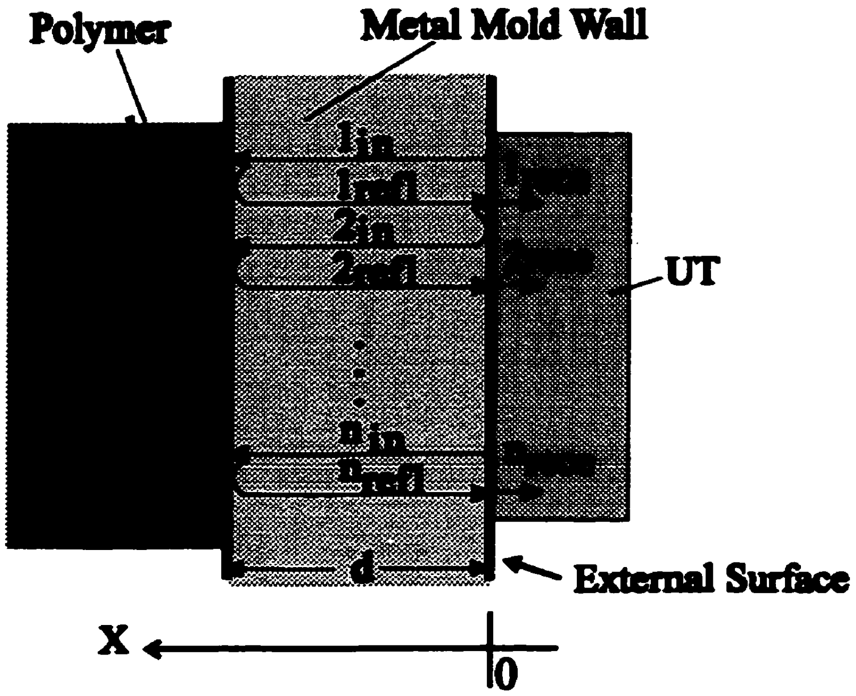

Fig.4.2: Different echoes traversing inside the mold wall.

(a) Echo Sensitivity

First of all, let us analyze the sensitivity of the amplitude of different echoes to the change of reflection coefficient.

The emitted signal, reflected signals, transmitted signals and received signals are shown in Fig.4.2. Let's define:

Γ : reflection coefficient at polymer-steel boundary

η : reflection coefficient at the steel-UT boundary

α : coefficient of attenuation inside the steel wall (for unit thickness)

and the amplitude of $A1_{in|x=0}=a$,

then, $A1_{refl|x=d}=\Gamma(1-\alpha d)a$,

$A1_{rece}=\Gamma(1-\eta)(1-\alpha d)^2a$,

$A2_{in|x=0}=\Gamma\eta(1-\alpha d)^2a$,

$A2_{refl|x=d}=\Gamma^2\eta(1-\alpha d)^3a$,

$A2_{rece}=\Gamma^2\eta(1-\eta)(1-\alpha d)^4a$,

....,

$An_{rece}=\Gamma^n\eta^{n-1}(1-\eta)(1-\alpha d)^{2n}a$

Because $An_{rece} \propto \Gamma^n$, the sensitivity of the received signal amplitude to the change of the reflection coefficient Γ is thus $dAn_{rece}/d\Gamma \propto n\Gamma^{n-1}$. It shows that further round trip echoes are more sensitive to the interface condition change.

Figures 4.3 (a)-(f), respectively, are the amplitude plots of the 1st, 2nd, 4th, 7th, 9th and 10th echoes recorded from the UTs installed external to the mold wall during the process. One can see that the rate of the amplitude reduction increases for further round trip echoes (i.e., larger n).

For the detection of the polymer flow front inside the cavity, the reflection coefficient reduces about 10% from a steel-air interface before filling to a steel-polymer interface after the filling. Since the reduction rate is sharp, the time resolution of the flow front detection is good. When the steel-polymer interface changes to a steel-gap due to the shrinkage, this process usually takes time and the interface conditions are complex thus it is difficult to determine the gap formation time in high precision.

(b) Diffraction and multiple reflection noises

Figures 4.4 (a)-(d) show that more noises originated from diffraction and multiple reflections for further round trip signals. For instance, in Fig.4.4.(d), the 11th echo is even larger than the 10th echo because the signal is super-imposed with the noise. We also notice that in Fig.4.3 the smoothness of the curves for the 9th and 10th echoes is not much better than that of the 4th echo, but a round curve appears for the 9th and 10th echo after the reflection coefficient returning to ~1. Such phenomenon indicates the interference of noises coming from diffraction and multiple reflections..

With the consideration of both amplitude sensitivity to the interface condition and the noise factor, the fourth echo was chosen for the monitoring of flow front and gap development using the UTs installed at the external mold wall. In previous works [54-56,58,59] such consideration was not taken and the 1st echo was used for monitoring, therefore poor sensitivity was observed (e.g. see Fig.3.3-3 and 4 in [55]).

As mentioned before, the insert core used in the present study has a 3° draft angle (i.e., non-parallel surface) in the direction of the demolding and the signal will not receive after several round trips. Thus using the similar criteria, we choose the second echo for the detection of flow front and gap development from the internal core. For different molds, the echo selection will be varied depending on the SNR of the signal.

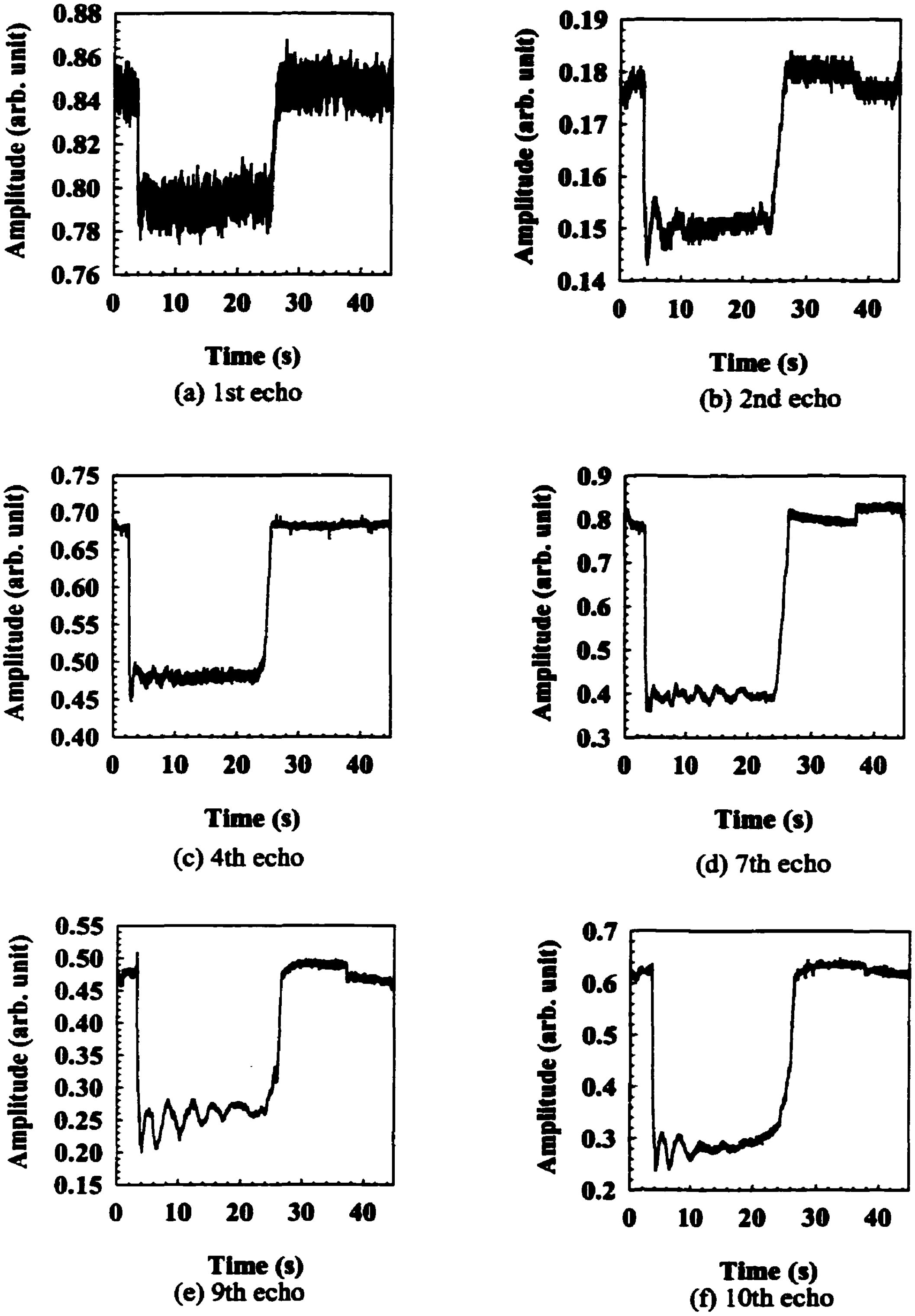

Fig.4.3: Amplitude vs time for different echoes (a)1st (b)2nd (c)4th (d)7th (e)9th (f)10th.

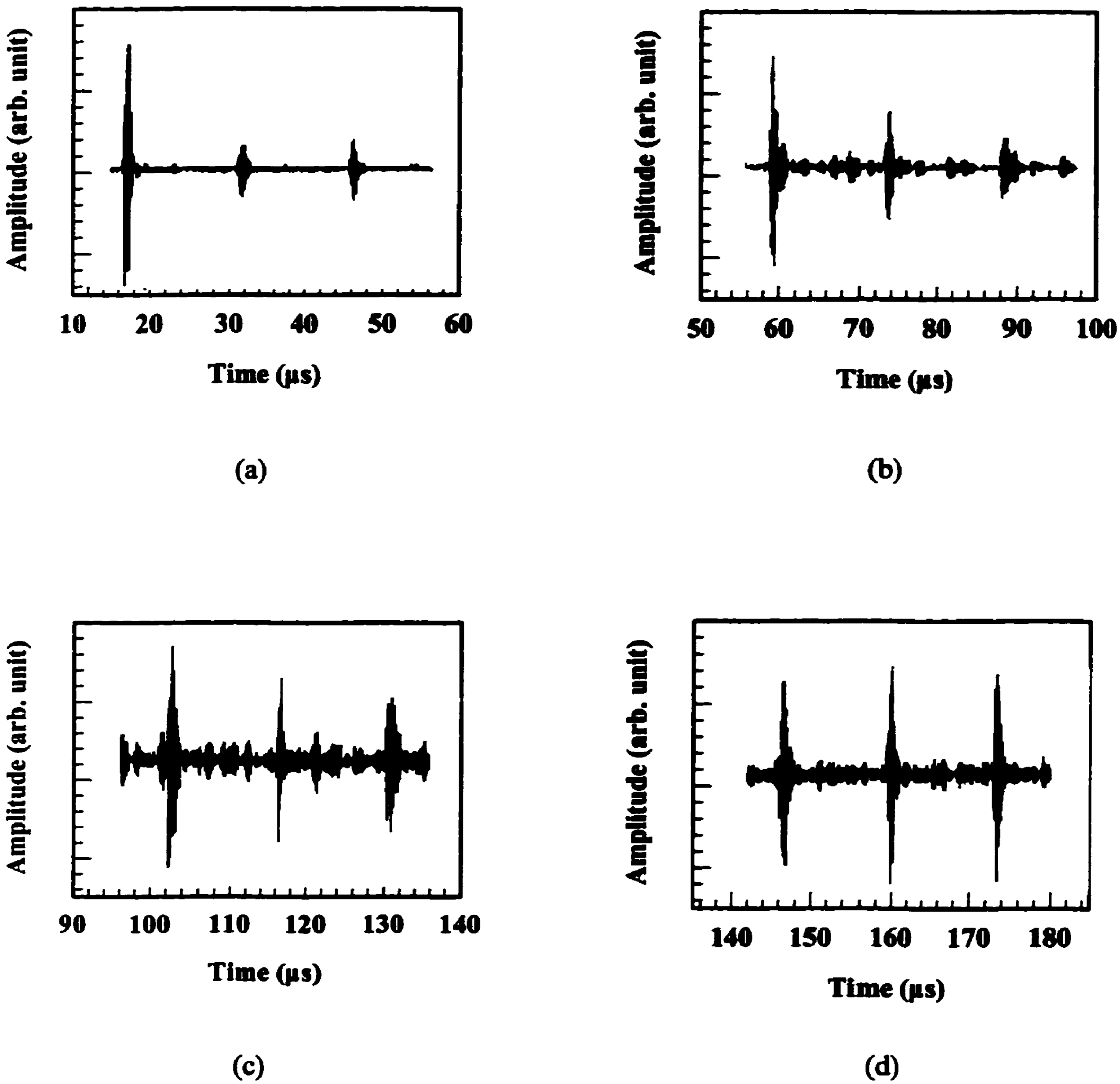

Fig.4.4: Recorded signals consisting of echoes (a)1st-3rd (b)4th-6th (c)7th-9th (d)10th-12th.

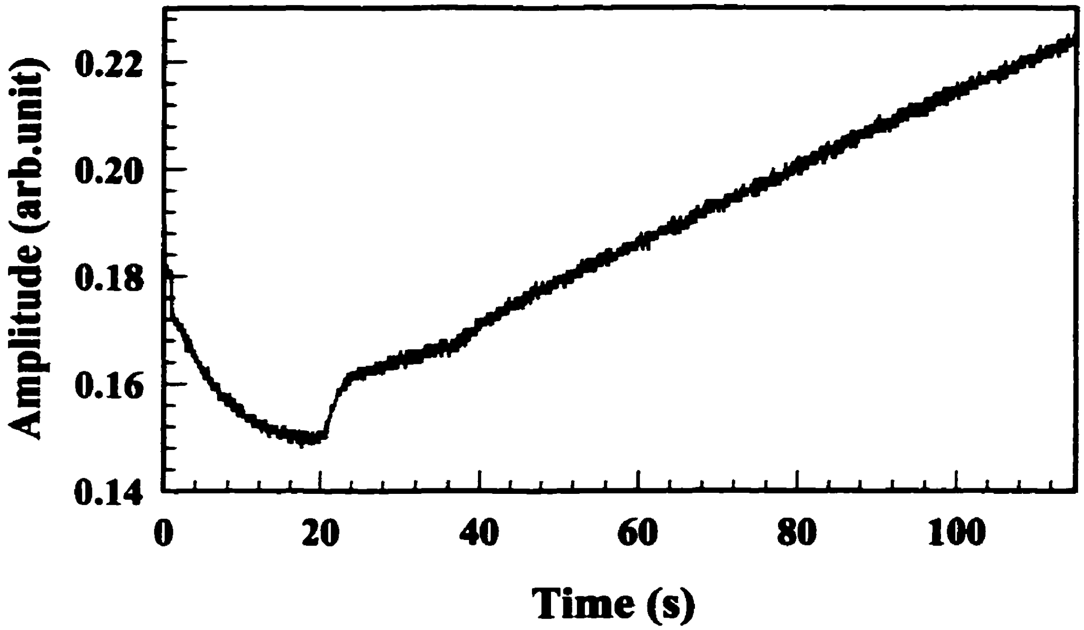

(a)

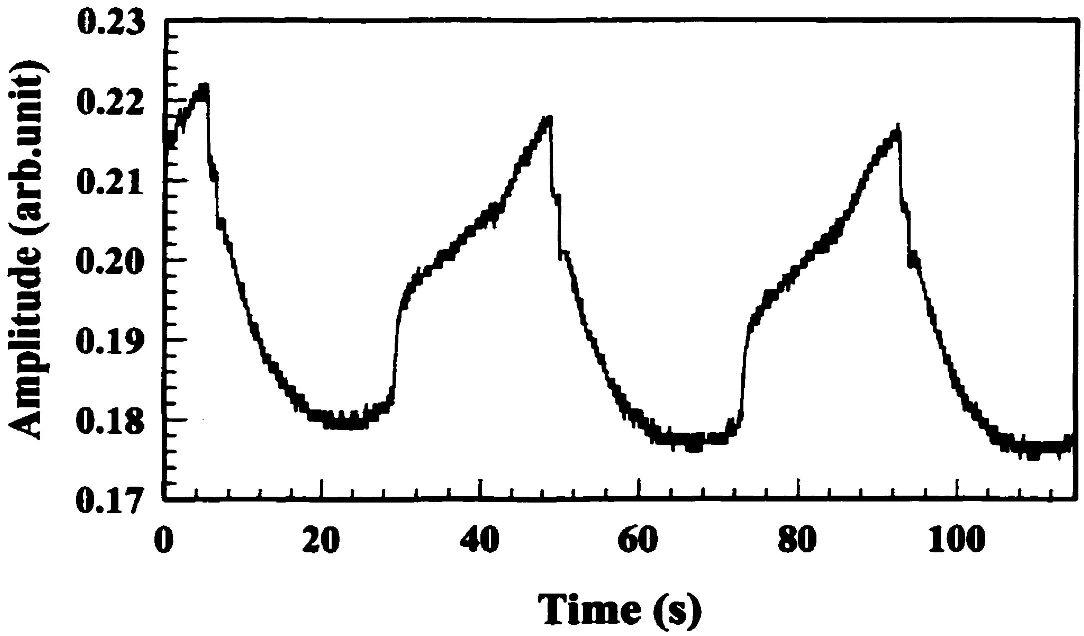

(b)

Fig.4.5: Temperature effects on the transducer and couplant from core side. (a) Mold was kept open after part ejection and (b) Record of three consecutive cycles.

4.3.2 Temperature effects

Since the temperature varies over a large range during injection molding, its effects on the performance of UT and couplant and thus signal can not be ignored. Figure 4.5 (a) is the amplitude plot curve obtained from the UT installed inside the insert core when the mold is kept open after the part ejection. As the mold is kept open, the core temperature decreases as it is exposed to the cool air. In this situation the amplitude of the reflected signal increased. It is noted that this particular insert core is not efficiently cooled because of the lack of cooling lines within the core. In addition, Fig.4.5 (b) was the measurement record for three consecutive runs and it clearly shows the temperature effects again. The smooth slope of the changing amplitude after the increase of the amplitude of the reflection coefficient results in high uncertainty in determining the gap development time to be explained below. However, temperature effects do not affect the flow front monitoring because the signal amplitude decreases significantly as the interface condition change suddenly in comparison with that induced by the temperature effects.

Since the external mold wall is thick and also cooled efficiently by the cooling lines, the change of the temperature at the external mold surface is very small. Thus temperature effects on the UT and couplant were negligible. This is another major reason why we prefer to install UTs externally to the mold in addition to the simplicity for installation and non-invasive nature. However, the temperature may still have minor effects on the velocity thus the time delay of the signal traveling inside the mold wall. This time delay variation of the signal could provide information on temperature change during the process.

For solidification monitoring, as the ultrasonic wave travels through both the polymer part and the mold wall, the variations of the amplitude and time delay combine factors from both media thus the temperature effect is an important issue. However, it is observed that the temperature effects on the transit time inside the steel mold wall is small compared to that in the polymer part.

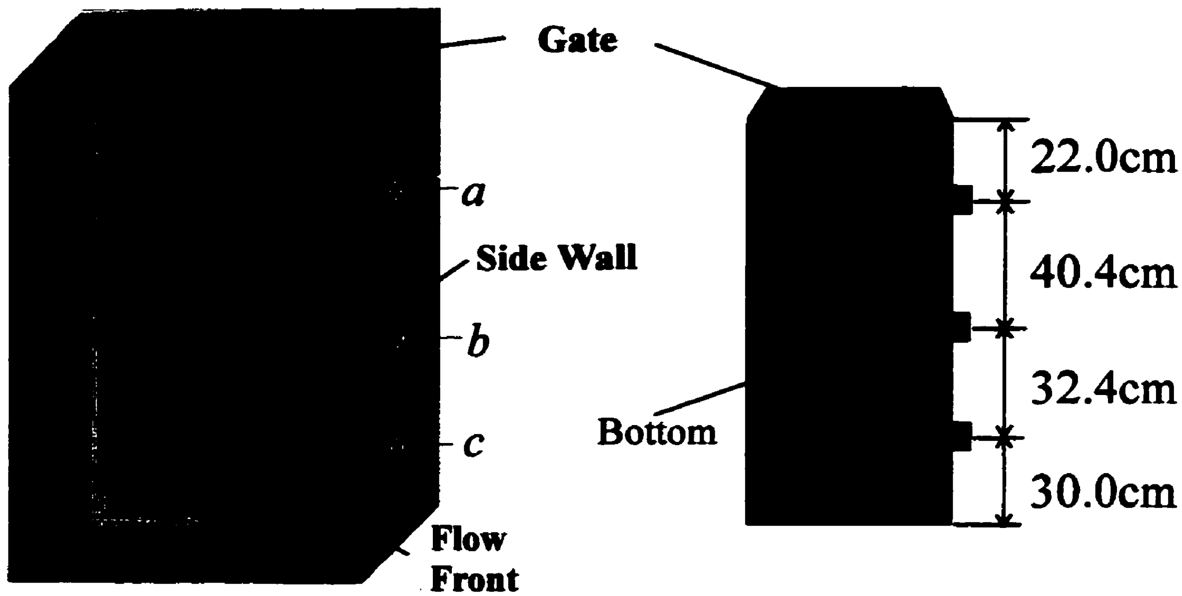

Fig.4.6: Transducers locations and corresponding positions at the part of a box shape.

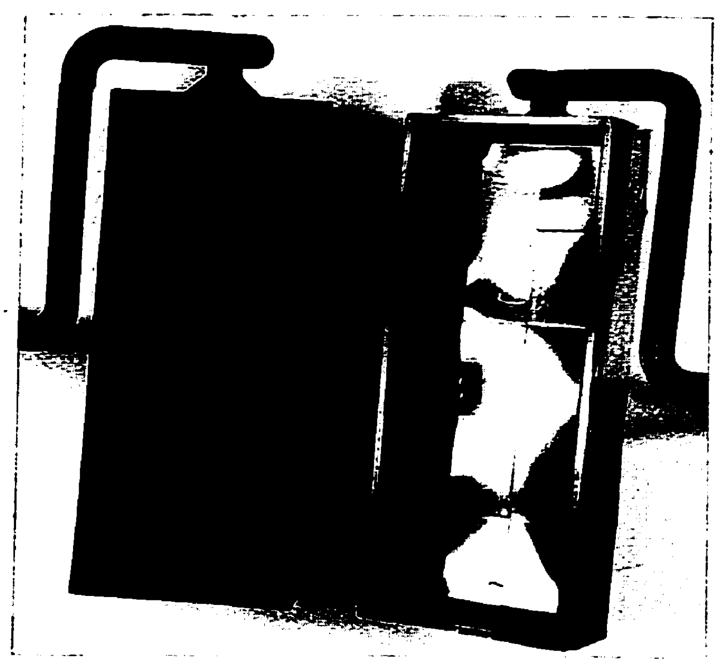

Fig.4.7: A molded box.

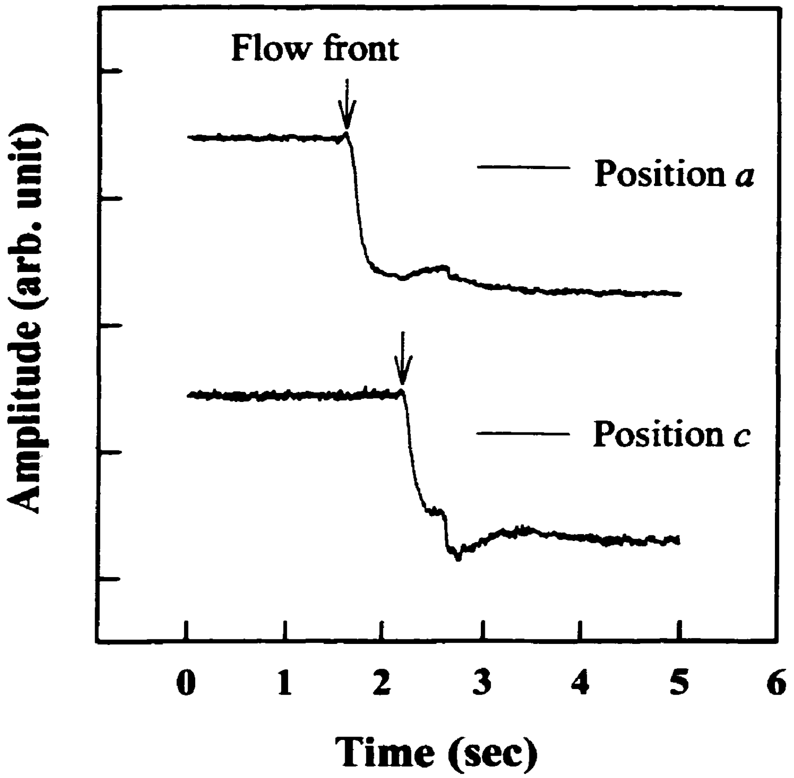

Fig.4.8: Amplitude plot of flow front monitoring using a two-channel system.

4.4 Flow front monitoring

As mentioned in **2.2.1**, the sudden decrease of the reflection coefficient indicates the arrival of the flow front. Using a multiple-channel acquisition system, one can monitor the arrival times at different locations simultaneously and obtain the flow front advancement inside the cavity. In this study, a two-channel system was used to detect the difference of the arrival times at two different locations for each molding cycle. From different combinations of the monitoring locations, the advancement of the molten polymer flow front path could be sampled. Different injection speeds were applied in order to see the variation of the flow front advancement inside the cavity. This two channel system is appreciated because it is much more effective to monitor the flow front advancement than a single channel system used in [55].

In these experiments, three UTs were installed external to the steel mold and two UTs inside the core facing the bottom part of the box. Figure 4.6 shows the UTs' locations and the corresponding positions in the part. The internal two UTs *a'* and *c'* were at the same position levels as those of *a* and *c*. One actual molded box is given in Fig.4.7.

The acquisition rate was set to 500 Hz, which means that the time resolution was 2 ms. That was precise enough comparing to the filling time of several seconds. For the data processing, "Find maximum value routine" was used to find the peak value of each acquired signal and the peak amplitude change along the process time was plotted. Then the flow front arrival times and the arrival time difference at two locations were determined. Figure 4.8 represents a typical result of the flow front monitoring using the two-channel acquisition system. In this case the injection speed was 2 inch per second. The location at which the amplitude suddenly decreases indicates the arrival time of the flow front.

4.4.1 Flow front speed

By using the given distance d between two UTs and by measuring the arrival time delay t, the flow front speed v is derived as $v=d/t$. Figure 4.9 shows the flow front speeds measured at different injection speeds. It is obvious that flow front advances faster inside the cavity when the injection speed is higher.

As shown in Fig.4.6 position *a*, *b* and *c* correspond to the top, middle and bottom positions at the side wall, respectively. The average flow front speed is slightly higher from *a* to *b* than that from *b* to *c*. It indicates that the flow front speed slows down as it advances along the side wall. Furthermore, for the box part in which the bottom is thicker than that the side wall, the flow front advances slower along the bottom than that along the side wall.

4.4.2 Flow front advancement

In order to obtain the profile of the flow front advancement inside the mold, arrays of transducers with a multiple-channel acquisition system are needed. In our study, using a two-channel system, the flow front arrival time differences at different combinations of two positions were measured. Thus relative arrival time differences at any two positions in the mold cavities could be deduced provided that the ultrasonic transducers can be installed.

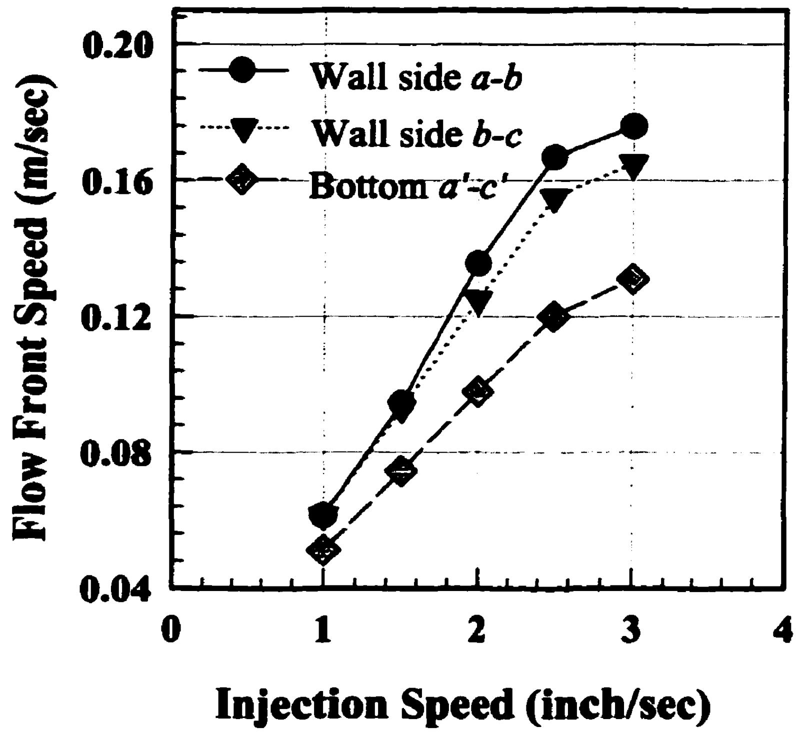

Fig.4.9: Flow front speed vs injection speed.

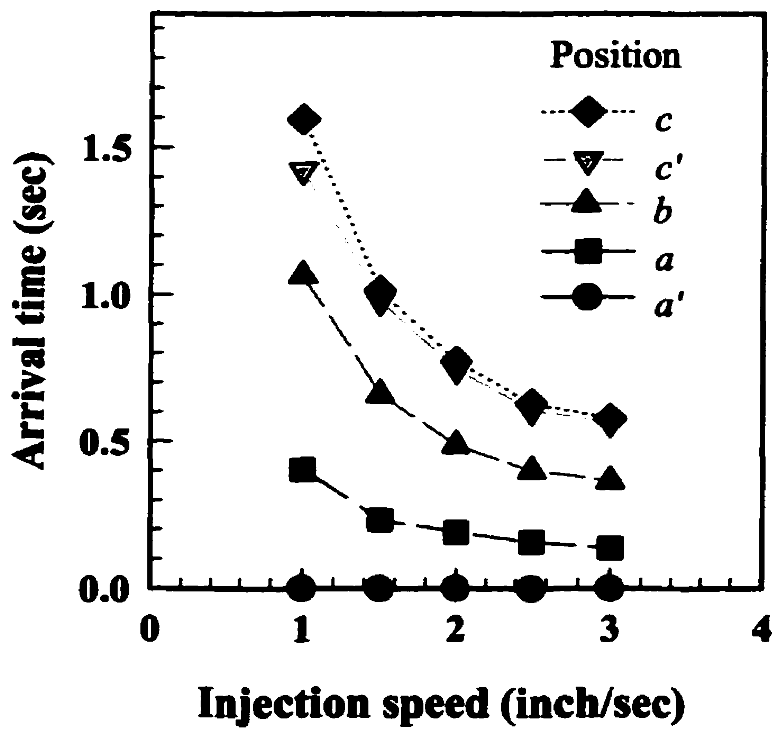

Fig.4.10: Arrival times at different positions.

Figure 4.10 shows the arrival times at different locations at the bottom and side of the box. Since the gate is located at the top of the box bottom wall as shown in Fig.4.6, the flow front paths to the locations at the bottom wall are shorter than the locations at the side wall with the same height, i.e., the flow paths to a' and c' are shorter than those to a and c, respectively. Here, the flow front arrival time to a' is chosen as the reference. It shows that the flow front arrives at a' first and then at a and there is about 0.4 sec difference in the case of injection speed at 1 inch/sec. The similar difference has also been observed between positions c' and c. In addition, the arrival time difference between c' and c is shorter than that between a' and a. For example, at injection speed 1 inch/sec again, the arrival time difference between c' and c is about 0.17 sec which is shorter than 0.4 sec between a' and a. It is understood as the flow front advances along the thicker bottom wall with a lower advancing speed as shown in Fig.4.9.

4.5 Gap development monitoring and contact time measurements

As mentioned before, gap can be detected because it prevents the ultrasonic energy from penetrating into the polymer and changes the reflection and transmission coefficients at the steel-polymer interface. During the gap development the amplitude of the reflection coefficient will rise. As one can detect both the flow front arrival time and the gap time, the part contact time can be deduced.

Usually, pressure sensors are used to detect the cavity conditions [55,58]. In our experiments both pressure and ultrasonic sensors were used and their performances were compared. Different packing pressures were applied in order to study the relationship between the packing pressure and the contact time. Results were further compared to the related IR temperature experiments to evaluate the packing pressure effects on part cooling. The majority of the experiments was performed by monitoring at the external surface of the mold in reflection mode. Monitorings from the internal core side in reflection mode as well as transmission mode were also carried out to obtain additional process information. In transmission mode, one UT was installed at the external surface of the mold and another at the internal core side. These two UTs should be aligned.

4.5.1 Pressure and ultrasonic amplitude profiles

The cavity pressure profile measured under the condition of 190 °C melt temperature and 7525 psi packing pressure is shown in Fig.4.11. The pressure sensor Hunkar-91017 was installed behind the ejector pin. It is seen that the load cell has a sharp response to the arrival of flow front, but the portion concerning the gap formation during which the pressure dropped to zero is not well defined. This prevents a precise detection of the gap development at the interface. It is also noted that the pressure gives no reading before the end of 30 sec packing phase because the gate had become frozen.

Figure 4.12 represents a typical measured ultrasound amplitude variation at the mold-part interface (external side) for the same experiment carried out in Fig.4.11. Point *A* corresponds to the start of the injection and the arrival of the flow front. Then the signal stays at the reduced level but having minor variations. From point *B*, the signal starts to increase rapidly indicating the gap formation. A ~1 μm gap is formed between the mold wall and the polymer at point *C*. By monitoring these three changing points, we may probe the development of the gap. Let us define the time from *A* to *B* as the good-contact time because the part always has a good contact with the mold from the applied packing pressure. The time from *B* to *C* is the partial-contact duration in which the part has partial contact with the mold as the polymer shrinks due to the solidification. After the point *C*, the signal level returns to that prior to injection and we believe that there exists a gap of more than 1 μm thickness. We also define the time from *A* to *C* as the total contact time.

A comparison between the signals detected by the pressure sensor and by the UT can be made from Fig.4.11 and Fig.4.12. Although the pressure sensor can detect the injection or the flow front, it may not be practical to insert many load cells inside the mold. The UTs can be installed external to the mold and thus do not disturb the injection molding process. In Fig.4.12, although the point *B* at which the partial contact starts is not so sharply defined, it is still observable in the reflected ultrasonic signal. But this point is not clear at all in the measured pressure profile. Thus the ultrasonic probing is superior to that carried out by the pressure sensors.

4.5.2 Gap detection at different locations

Different ultrasonic monitoring locations were chosen to see whether the variation of gap development exists. The results recorded by the two-channel acquisition system indicate that there is no significant difference along the wall side of the box as shown in Fig.4.13. Although a slight difference of the flow front arrival time (the flow front arrival time is small comparing to the whole contact time) can be observed, a gap was developed nearly at the same time. For this case, the point *C* defined in Fig.4.13 is not so distinct and will be studied in the future.

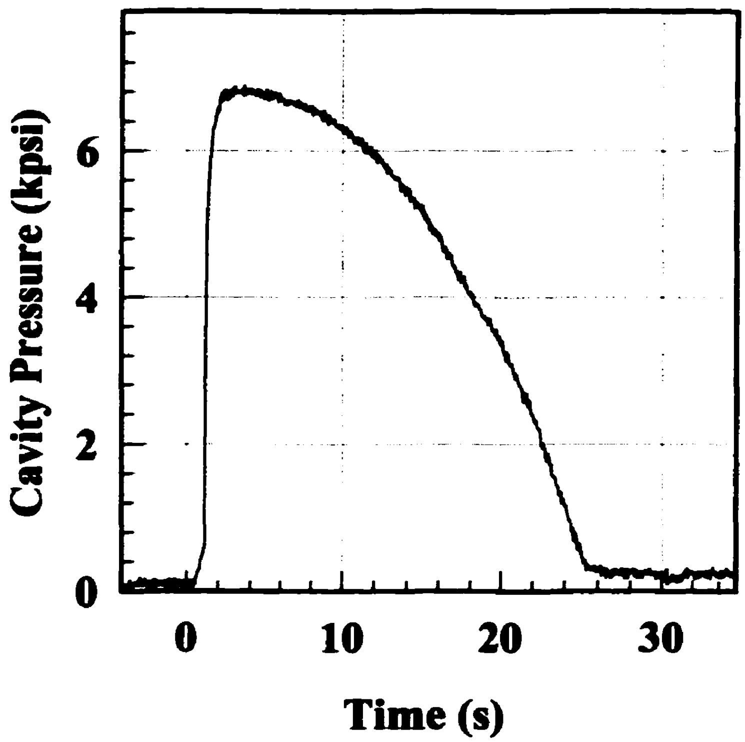

Fig.4.11: Cavity pressure profile measured by a pressure probe.

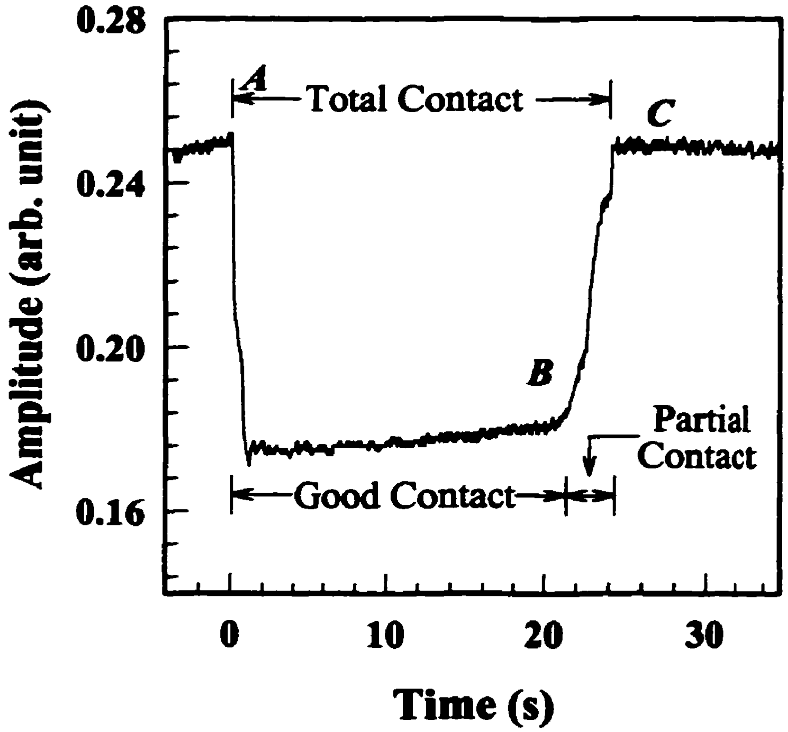

Fig.4.12: Definition of good, partial and total contact time.

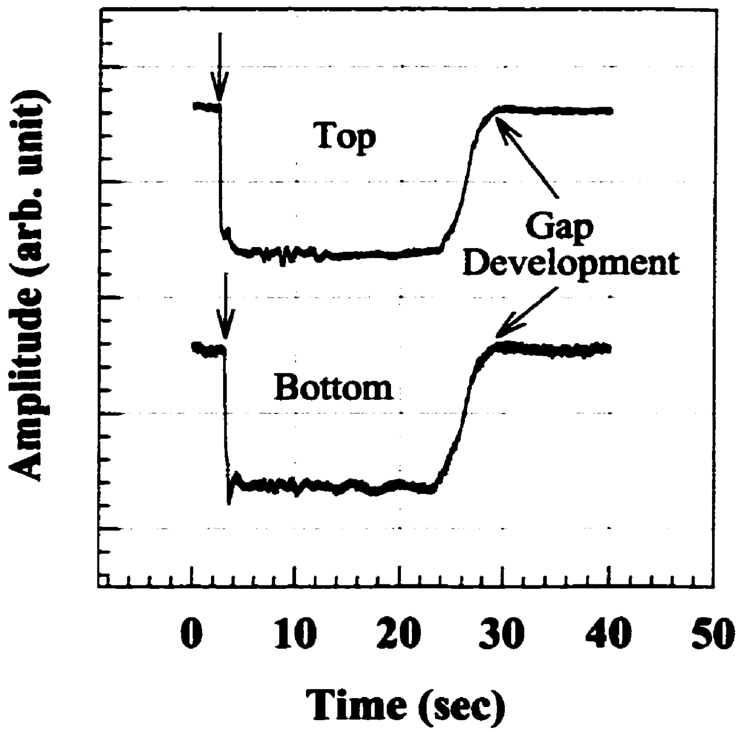

Fig 4.13: Gap development monitoring using two transducers installed at the top (upper curve) and bottom (lower curve) of the side wall from the external mold.

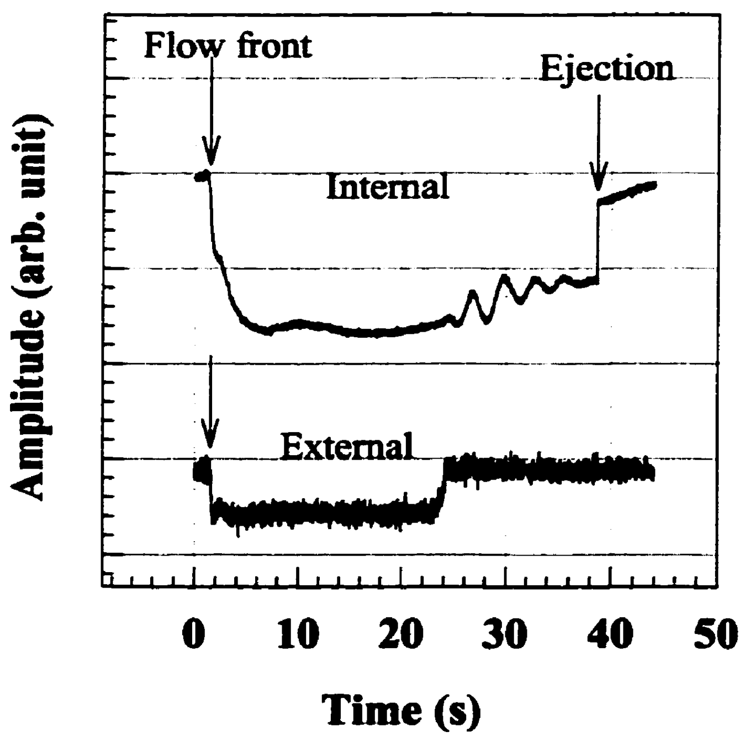

Fig.4.14: Gap development monitoring at the bottom of the box (upper curve) and side wall of the box (lower curve).

Figure 4.14 shows the amplitude plots for both developed and undeveloped gap cases. The upper curve was probed by a UT inside the core which monitored the bottom of the box at the location *a'* in Fig.4.6. The lower curve was obtained by the UT installed at the position *a* at the outside of the mold. The lower curve is noisy because of the limitations of our current two-channel system, thus the first echo from the steel-polymer interface had to be used for monitoring in order to achieve simultaneously monitoring at two different locations in the same cycle. The detailed explanation was given in section **4.3.1**.

A gap is formed at the side wall. The difference may be because of the larger thickness of the bottom which requires a longer time to be solidified. Another reason could be that the residual stress in the box structure during the injection molding may force the bottom to contact the mold, thus the gap is not developed. From the observation, there is an amplitude oscillation at the bottom wall curve right after the gap is formed at the side wall. This is caused by an oscillation induced by the detaching of the side wall, the structure force from the wall side detaching from the mold after the gap developed. From our calculation shown in Fig.2.4(a), this oscillation displacement along the thickness direction may be within a few tenths of one micron.

4.5.3 Packing pressure effects on the contact time

Figure 4.15 shows the results obtained again at the position *a* by the UT mounted at the external mold wall and operated in reflection mode. The melt temperature was 190°C. The good, partial and total contact times are defined in Fig.4.11. The partial-contact time is almost constant, but the good-contact time has a strong dependence on the packing pressure. As one increases the pressure from very low pressure, 1075 psi, the good-contact time increases very sharply at the beginning and then with a slower rate as the packing pressure is continuously increased. The results indicate that increasing the pressure improves the duration of good-contact, while the partial-contact time remains approximately unchanged.

Figure 4.16 shows the good-contact time curves obtained at different positions along the box side wall again by the UTs mounted at the external wall and operated in reflection mode. The melt temperature was 190°C. The monitoring results obtained from the UT installed inside the insert core using reflection mode and those obtained from the transmission mode are also presented in Fig.4.17 with a same melt temperature of 190°C. In Fig.4.18, the results were obtained using the same experimental arrangements in Fig.4.16 except the polymer melt temperature was 230°C. It is seen that all these results obtained at different positions, using different methods and at different melt temperature conditions show the same trend of the part contact time dependence on the packing pressure.

4.5.4 Gap effects on the cooling

Effects of the gap on part cooling were evaluated using the infrared radiometry technique. Fig.4.19 shows an infrared image of a box right after ejection (within 4 seconds). The average temperature of a 2 cm by 2 cm region, which corresponds to the area probed by the ultrasonic waves in Fig.4.15 for melt temperature of 190°C, is plotted in Fig.4.20 versus the packing pressure. It is seen that, for the packing pressures less than 3225 psi the part surface temperature was constant at about 82°C; but as the pressure was increased to 7525 psi the recorded temperature dropped by 15% to about 70°C. This decreased temperature may be due to the enhanced contact time and the shorter gap duration.

It is thought that a larger contact time will lead to a lower part temperature right after ejection. However, in Fig.4.15 the shapes of the part-mold contact time curve measured by ultrasound and part surface temperature curve in Fig.4.20 measured by thermograph do not follow this trend. The differences may be explained as follows. From 1075 to 3225 psi the contact time changes from 7 to 19 sec but the part was not ejected until it remained in the mold for a total of 35 sec. During this time diffusion of heat reduced thermal gradients in the part and warmed the part surface. Between 3225 and 7525 psi the contact time increased gradually to a maximum of 25 sec and as expected under these conditions there is a large reduction in the observed surface temperature. The small increment in the contact time is significant in that after the part pulls away from the wall there is less time for heat at the center of the part to diffuse to the surface and warm it before ejection. Therefore, trends in the part temperature depend on where it is measured in the molding cycle.

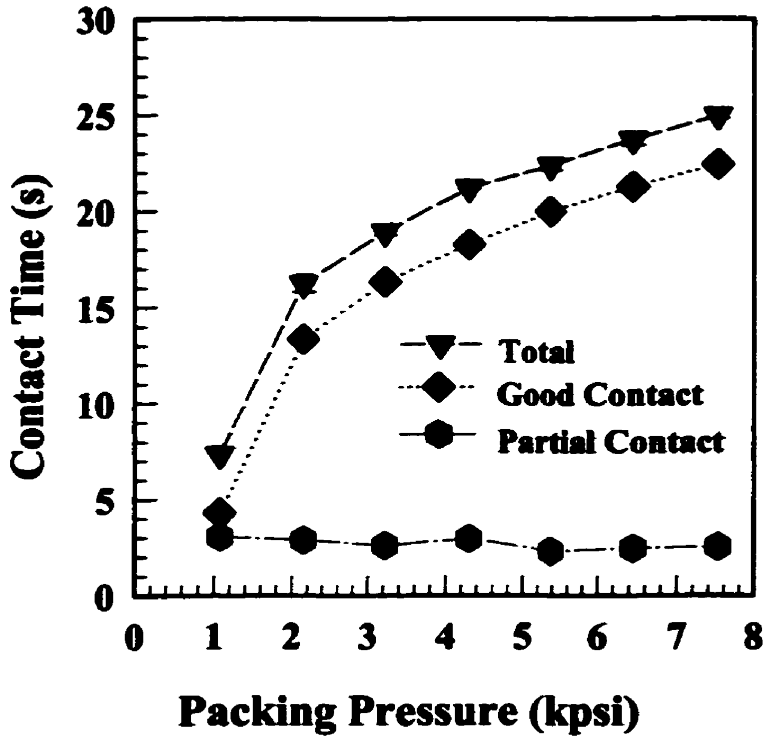

Fig.4.15: Different stages of contact as a function of packing pressure. Transducer locations: bottom & external; melt temperature:190°C.

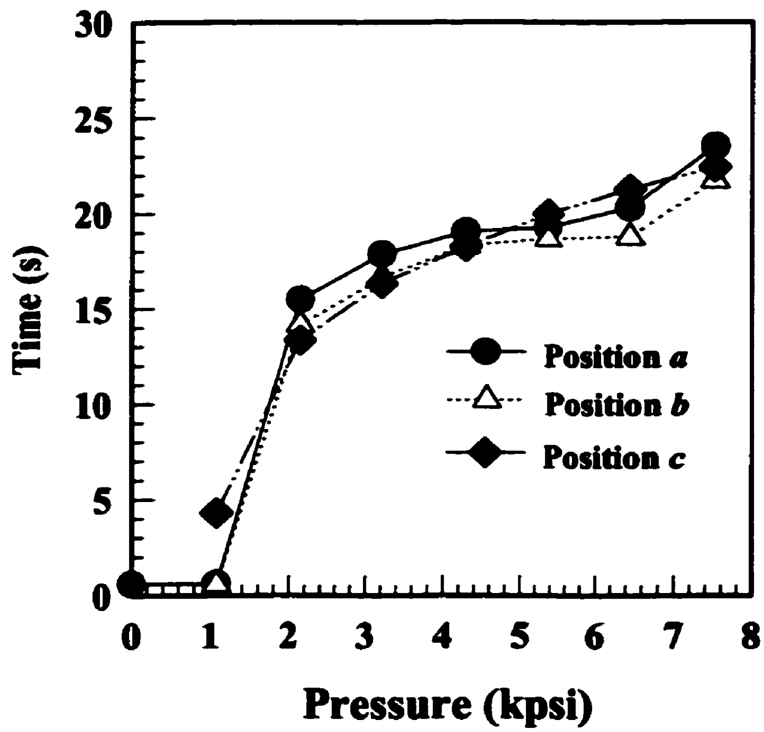

Fig.4.16: Good-contact time at different positions. Transducer locations: external; Melt temperature: 190°C.

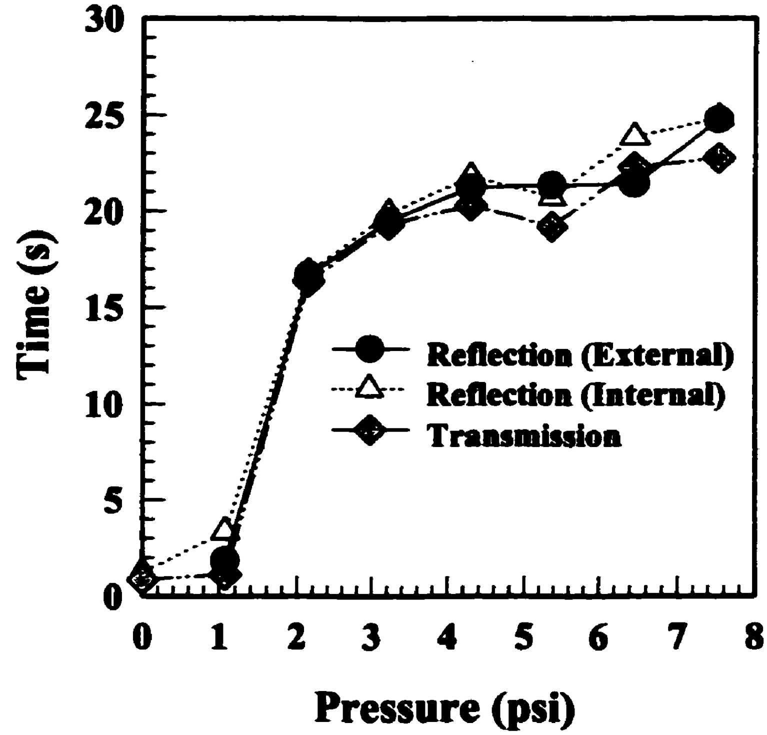

Fig.4.17: Total-contact time obtained by different methods (Melt temperature:190°C).

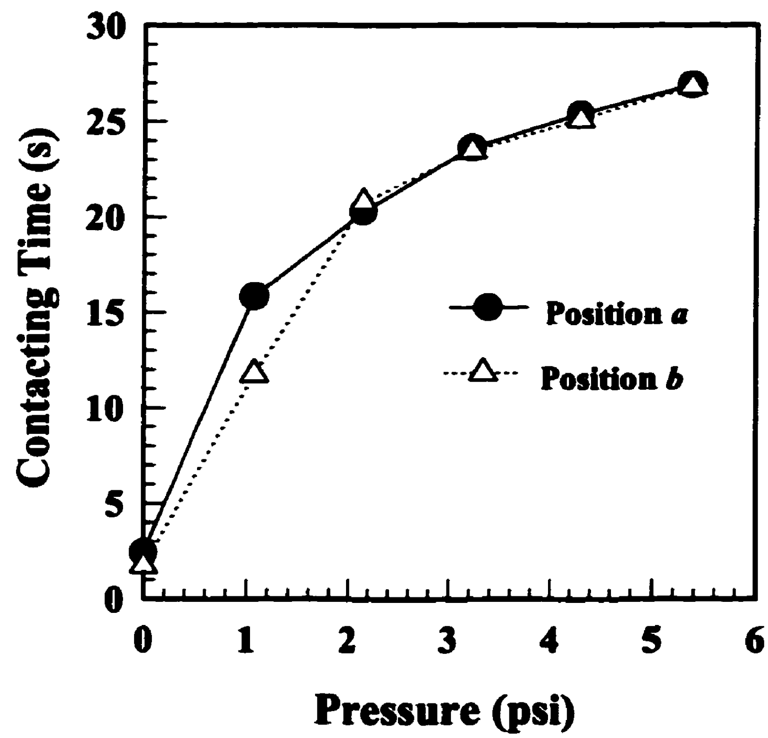

Fig.4.18: Total contact time obtained at different positions. Transducer locations:external; Melting temperature: 230°C.

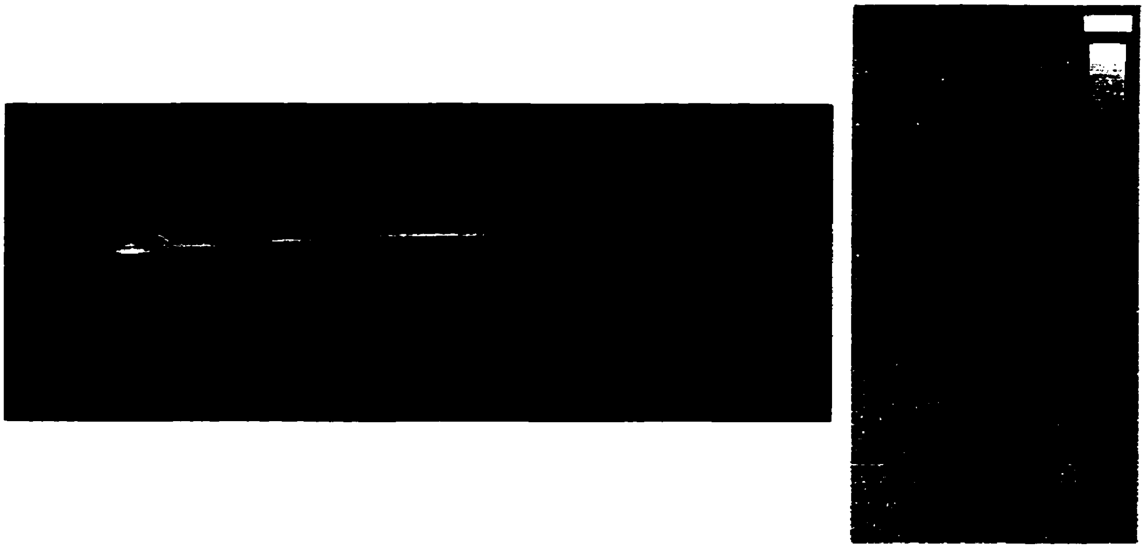

Fig.4.19: Infrared image taken right after ejection of a box. Temperature is in °C.

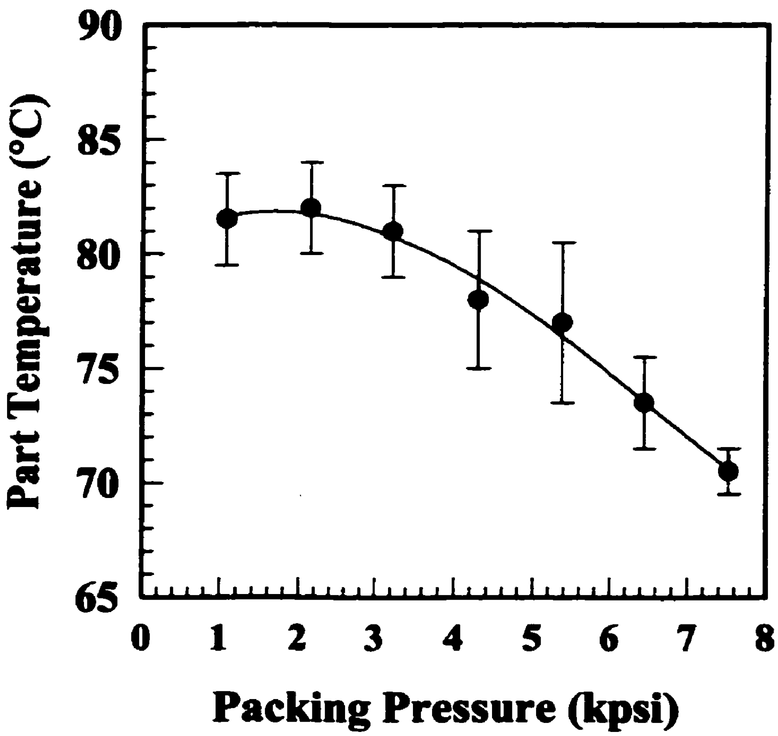

Fig.4.20: Part surface temperature vs packing pressure.

Another difference between the ultrasonic and thermal curves can be attributed to the differences between ultrasonic and thermal waves. As illustrated in Fig.2.4(a), ultrasound at 5 MHz is an effective probe for detecting gaps of 1μm size or below. By decreasing the ultrasonic frequency the range of probing may be increased slightly, but nevertheless, linear ultrasound can resolve only gap variations less than 1μm. In contrast, air gaps of less than 0.5μm provide little resistance to heat transfer and the effect of the TCR becomes important when the gap reaches a thickness of microns. To this end ultrasound will detect the onset of gap formation, but the TCR value can not be directly inferred.

4.6 Solidification monitoring

Gap development is caused by the shrinkage of the part that provides some information of the part solidification. However, ultrasonic velocity and attenuation inside the part are also strongly related to physical properties of the molded part. Thus the ultrasonic wave velocity and attenuation measurements can be related to more part solidification parameters. But injection molding is not ideal for accurate attenuation measurements which require at least two echoes with high SNR (e.g. > 30 dB) because the complicated components of the mold such as cooling line, ejector pin and non-parallel mold surface may generate noises which interfere with the desired signals. However, velocity measurements can still be carried out with a considerable accuracy using two echoes with low SNR (e.g. 10 dB).

For solidification monitoring, ultrasonic measurements using both transmission and reflection modes were performed.

4.6.1 Transmission mode

In the measurements of solidification, the schematic of the UTs setup is shown in Fig.4.21(a). The UT A installed on the outside of the mold served as the signal transmitter and the UT B installed inside the insert core as the receiver. Using the two-channel acquisition system, the transmitted signal from A to B and the reflected signal from UT A →mold-part interface→UT A were recorded simultaneously. In reflection mode, UT A also acts as a receiver.

The ultrasonic signal in transmission mode travels through the external mold wall, the part and the core mold wall and then is detected by the UT B. The reflected signals at the external mold-part interface are received by the UT A. The total ultrasound travel time inside the external mold, polymer part and internal core mold can be given as t_1+t+t_2, where t_1, t and t_2 represent the ultrasound travel time inside the external mold wall, the part and the internal core wall, respectively as shown in Fig.4.21(a). In this case because the thickness of the mold internal core wall is thinner than that of the external mold wall, t_2 is smaller than t_1 as shown in Fig.4.21(b). In Figure 4.21(b), the upper signal is the recorded round trip signals inside the external mold wall and the lower one is the signals received by the UT B. One can measure t_1 and t_2 directly by correlating the echoes S_{a1}, S_{a2} and S_{b1}, S_{b2}. Using the cross correlation between the echoes S_{a1} and S_{b1}, t_3 as shown in Fig.4.20(b) can also be obtained. Since $t_3=2t_1-t_1-t-t_2=t_1-t-t_2$, the ultrasound transit time inside the part t can be obtained as $t=t_1-t_2-t_3$.

The reason we choose the above method which uses the high precision cross correlation method to deduce the travel time inside the polymer instead of determining the total travel time t_1+t+t_2 directly from the transmitted ultrasonic signal is that the wave form of the signal is not well defined and it is difficult to extract the precise arrival time. Our approach takes the advantage of the two-channel acquisition system and can dynamically measure the t_1 and t_2. Since the temperature effects on the travel times, t_1 and t_2, inside the external and internal steel mold were very small comparing to the change of the travel time, t, inside the polymer, t_1 and t_2 were treated as the constant during the injection molding cycle.

Since the insert core has a 3° draft angle, the average thickness of the part was used for the calculation at the location of the UT. Figure 4.22 show the velocity and the amplitude of the transmitted ultrasonic wave inside the polymer. Although this amplitude curve also includes the attenuation factor of the mold, it may still be used to show the attenuation inside the part qualitatively. The packing pressure in the experiment was 5375 psi and the melt temperature was 190°C. It is seen that the ultrasonic velocity inside the polymer varies from 1000 m/s to 1900 m/s and this indicates a transformation from the molten state to solid state. The velocity increases sharply just after the injection and has a decrease at the end of the solidification. Such variations are related to crystallization and will be studied in the future. From the amplitude curve, it is noticed that the amplitude decreases to zero when the gap is formed. Since the gap prevents the ultrasonic energy from going through and reaching the polymer part, this is a disadvantage of the ultrasonic monitoring method. It means that the solidification can only be monitored when the part has a good contact with the mold.

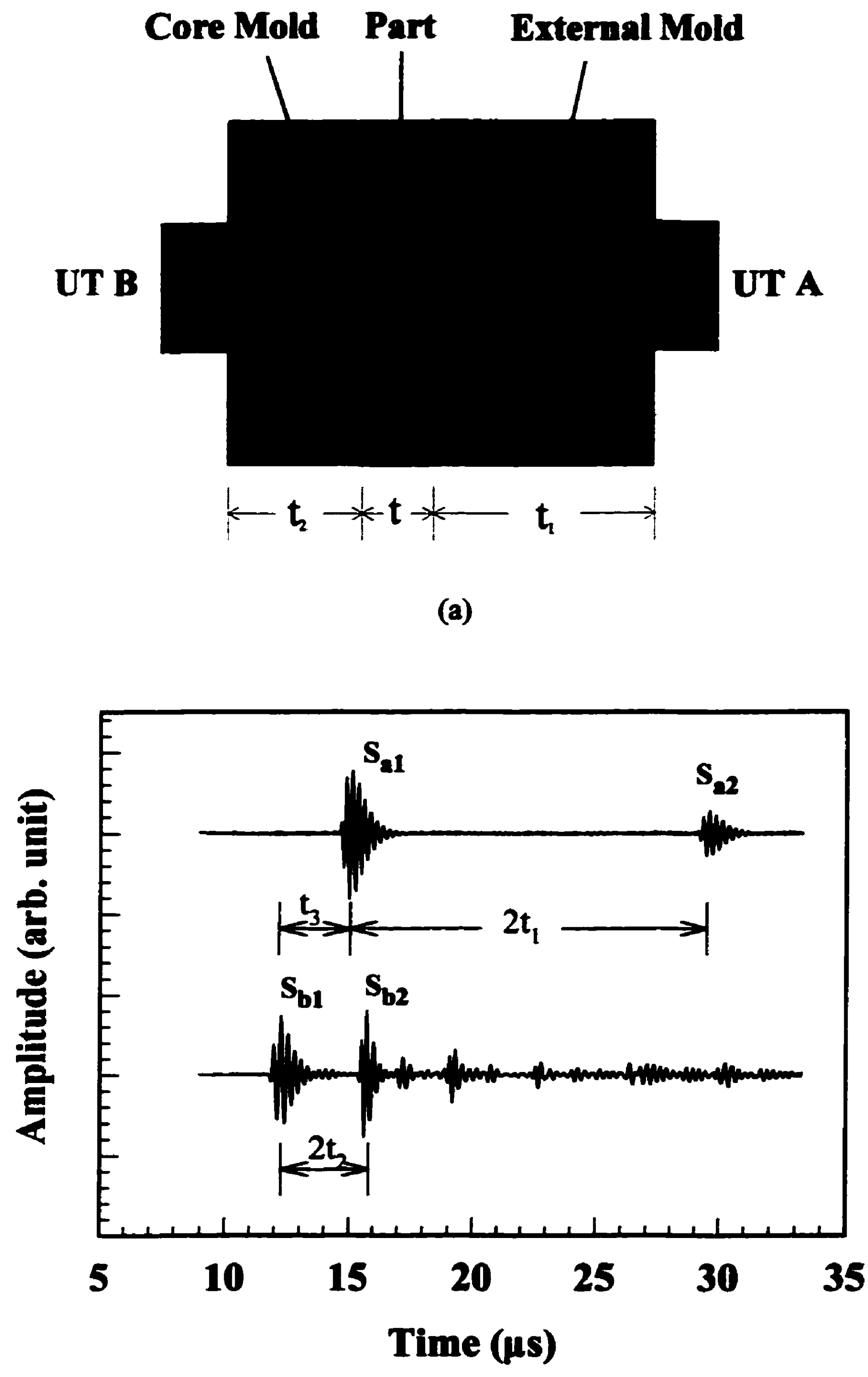

(b)

Fig.4.21: Schematic of the travel time measurement in transmission mode. (a) Measurement setup and (b) Acquired signals using the two-channel acquisition system.

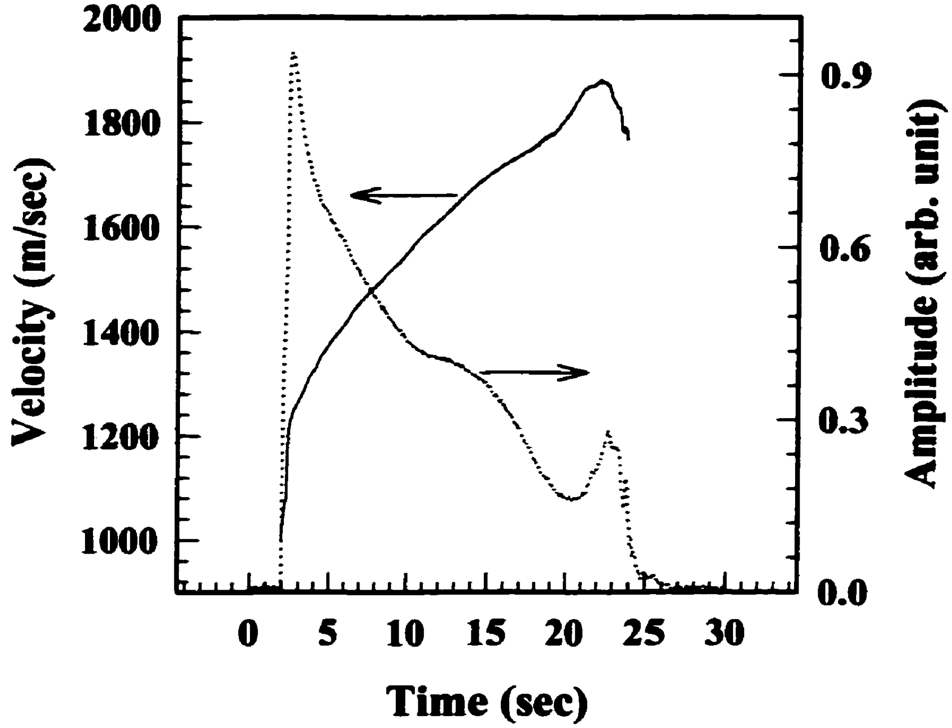

Fig.4.22: Velocity and amplitude change inside the part.

4.6.2 Reflection mode using the transducers installed at the external mold wall

The schematic for monitoring the solidification in reflection mode is shown in Fig.2.5(b). This approach is attractive since the configuration in which the UTs are installed at the external mold wall is simple and non-invasive, but a large ultrasonic loss after the round trip inside the part may impose some difficulties.

Preliminary results are shown in Fig.4.23(a). It is seen that the desired echo containing elastic information of the polymer part is 20 dB smaller comparing to the large noise caused by mainly the grain structures of the steel mold wall and multiple reflections from mold components such as cooling lines and ejector pins.

In order to enhance the SNR of the desired signal that was moving because of velocity changes during the solidification, signal processing techniques are used. The principle of one processing technique is to use the subtraction method to reduce the noise. We first recorded the base signal when the machine was warm and no polymer was inside the cavity. This base signal is then subtracted from each acquired signal. In addition to this subtraction, frequency domain zero padding was applied to increase the sampling rate and interpret the value inside the sampled data in order to minimize the digitizer error. Furthermore, a cross correlation between the base signal and the acquired signal was used to find the maximum similarity and then properly adjust the time sequence of these two signals before the subtraction.

Figures 4.23(a) and (b) show the moving echo before and after the signal processing. It is seen that the SNR of the moving echo is significantly enhanced and the variation of the travel time inside the polymer is clearly demonstrated.

4.6.3 Reflection mode using the transducer installed at the internal mold wall

The solidification monitoring performed by the UTs installed inside the insert core in the reflection mode was also carried out because the core geometry which does not have the cooling lines and ejector pins, was much simpler and its thickness is much thinner than that of the external mold wall. This results in a better SNR of the desired signal. Since the side wall has a 3° draft angle, we perform the monitoring facing the flat bottom side inside the core. Figures 4.24 (a)-(d) show the acquired signals. The round trip echoes traversing back and forth inside the polymer part enable us to directly deduce the travel time inside the polymer using correlation method and thus obtain the wave propagation velocity. Although the echoes from the mold-polymer interface may overlap with the desired signal, it can be overcome by signal processing. The results presented here are not to suggest the future monitoring to be carried out from the insert core because it has the same inconvenience as the transmission mode as the UTs must be installed inside the core. The purpose here is to show that on-line monitoring of material solidification in reflection mode is feasible but demands high SNR.

In previous works [55] velocity of the polymer during solidification has been monitored at difference pressures, melt temperatures and hold times but only in transmission mode. Here we have demonstrated that the more practical and convenient reflection mode may be used to perform the similar monitoring.

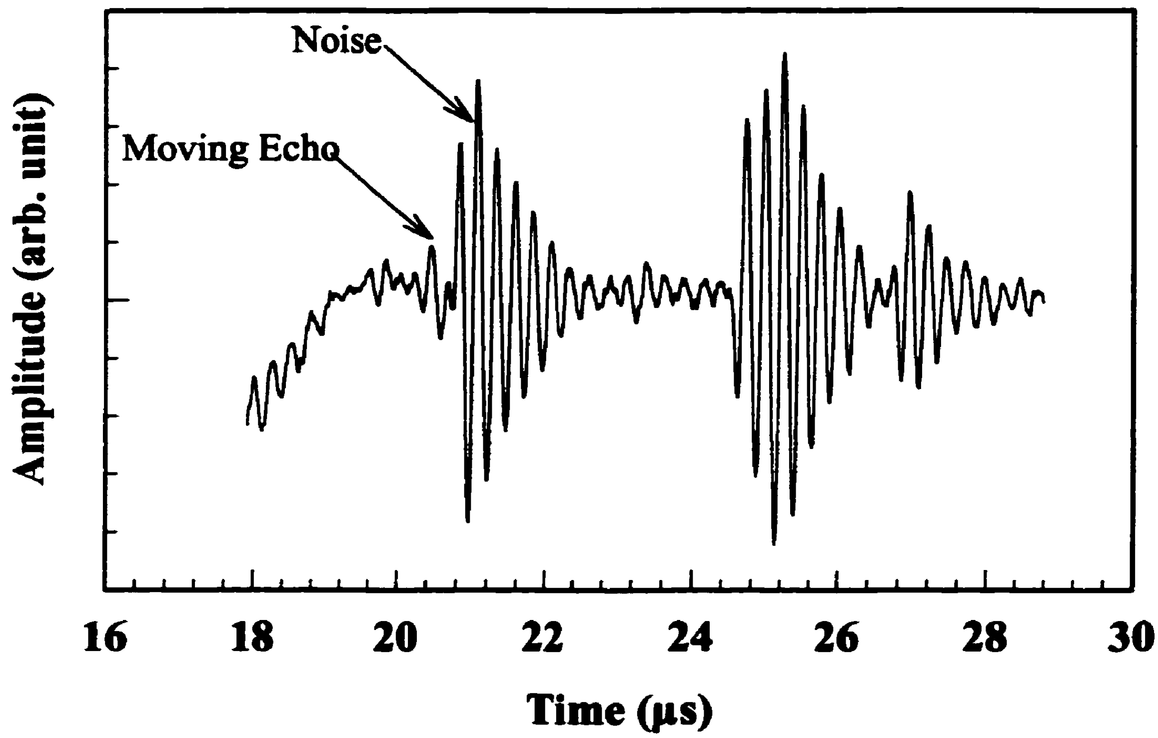

(a)

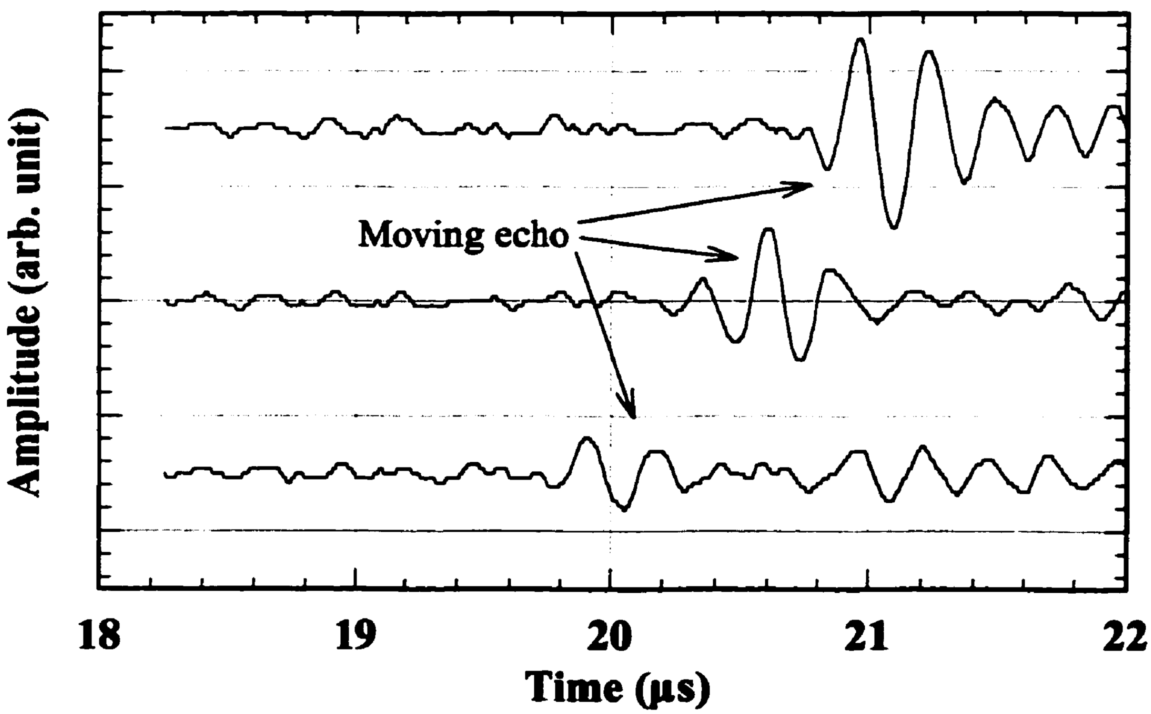

(b)

Fig.4.23: Solidification monitoring by the transducers installed at the external mold in reflection mode. (a) Moving echo before processing and (b) Moving echo after processing.

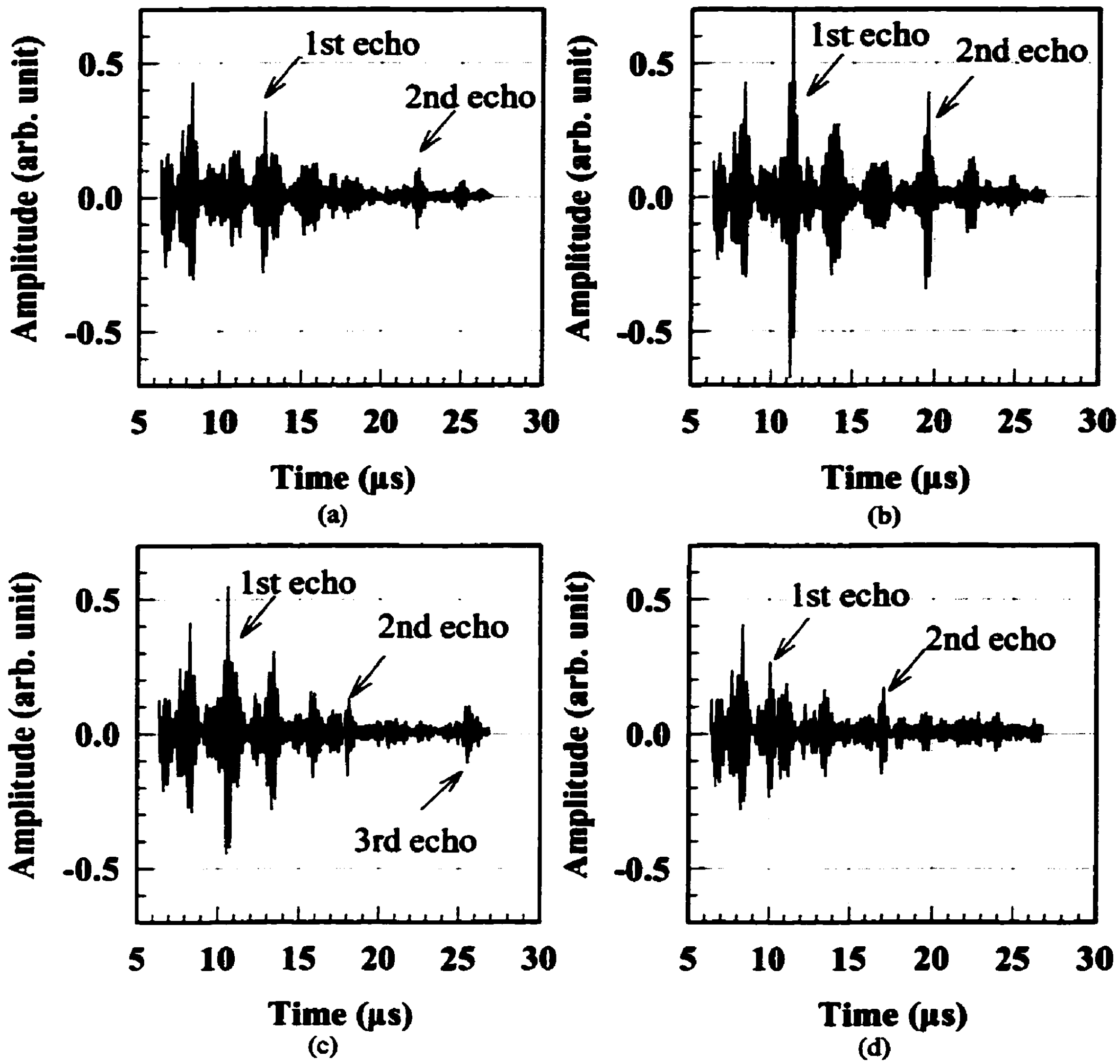

Fig.4.24: Acquired signal of solidification monitoring from the internal mold wall in reflection mode. Time sequence:(a)-(d).

4.7 Summary

On-line ultrasonic monitoring of injection molding was intensively investigated on a small box mold. The material employed was polyethylene. The molten polymer flow front arrival during the filling stage was detected by monitoring the change of the ultrasonic wave reflection coefficient at the steel mold-polymer interface. Using a two-channel acquisition system, the flow front speed and the advancement inside the cavity were obtained. The onset of the gap between the mold and the polymer caused by the shrinkage through the part thickness during the post-filling stage was also successfully detected by the change of the ultrasonic reflection and transmission coefficients at the mold-polymer interface. Meanwhile, the contact time between the part and the mold wall was measured. The contact was defined as good-contact and partial-contact stage according to the amplitude of the signal level. The comparison between the traditional pressure and the ultrasonic sensors detecting the gap development was investigated. It was found that ultrasonic sensor had a superior performance. Furthermore, the contact time dependency on the packing pressure was studied and the gap formation effect on the part cooling was analyzed by relating the experiment results to those obtained by infrared temperature measurements.

Solidification monitoring of the part during the packing stage was carried out using ultrasonic velocity measurement which may be related to the part elastic properties. Cross correlation method was applied to precisely obtain the ultrasonic velocity inside the polymer with the help of the two-channel acquisition system. In transmission mode the emitter was mounted on the external mold and the receiver was installed inside the insert core. The ultrasonic velocity variation inside the part during the process was obtained. Feasible study of the velocity measurement in reflection mode in which the UTs are only mounted on one side of the mold surface was investigated. The monitoring from the external mold wall was carried out and the signal having a poor SNR was extracted by signal processing methods. Meanwhile, the monitoring from the internal mold wall obtained a relatively higher SNR for the desired signal. Thus, on-line monitoring of the solidification in reflection mode was feasible provided that a signal of high SNR could be obtained.

Chapter 5:

Ultrasonic monitoring of the die casting process

5.1 Introduction

The process of die casting is very similar to that of injection molding. However, since the cast materials are molten metals such as aluminum (Al) in our case, process temperature in die casting is higher than that in injection molding. On-line ultrasonic monitoring measurements may be performed at elevated temperature around 300°C, which is the external surface temperature of the die (mold) under cooling. One intuitive approach is to employ broad band piezoelectric contact ultrasonic transducers (UTs) together with a couplant, both should work well at such temperature. Because there is no reliable broad band and high performance commercial UTs which can operate at the above temperature, new probing methods or sensors with high SNR performance are needed.

Another difference between the Al die casting and polymer injection molding is that the molten Al must be fed into the cavity at high speed. Furthermore, the solidification rate of Al is also much faster than that of the polymer. In general the filling stage is completed within a short time, e.g., less than 40 ms and the solidification takes less than 5 seconds. Therefore, high speed acquisition system is required to fulfill the monitoring task, in particular, for the flow front advancement inside the cavity.

In our study, an experimental die is designed and fabricated for the on-line ultrasonic monitoring. A clad buffer rod with high SNR will be inserted in the die wall for the probing. Again by using the two-channel high speed acquisition system described before, the flow front of the molten Al and gap development will be monitored simultaneously.

5.2 Buffer rod

Due to the unavailability of high performance high temperature UTs and couplants, one classic approach for the process monitoring at high temperature is to insert a metallic ultrasonic waveguide (buffer rod) between the UT and the materials to be monitored. One end of the buffer rod is water cooled down to 60°C or below thus the commercial high performance UTs and couplants can be used. The ultrasonic waves are generated by the UT, transmitted through the buffer rod and then into the processing material. The reflected wave is back to the UT through the reversing path [48]. The application of buffer rods for ultrasonic monitoring in polymer extrusion was reported in [52]. Usually for on-line material process monitoring, certain signal to noise ratio is required to achieve the monitoring task. Due to wave diffraction effects and the finite diameter of the buffer rod, spurious ultrasonic echoes, also termed trailing echoes, may be present in the midst of the signals containing the desired sample information. These trailing echoes will always arrive later than the directly transmitted or reflected longitudinal echoes and often interfere with the desired signals [48,74-78].

In order to reduce the trailing echoes thus increase the SNR, threading at the periphery of the buffer rod is the most commonly used technique for buffer rods to disturb the rod-air boundaries. But often the result is not satisfactory, in particular, if the diameter for the buffer rod is required to be small [48,78]. A buffer rod of a smaller diameter requires less cooling to reach the desired low temperature than that of a larger diameter. In our study a novel and high performance clad buffer rod with a solid core and a solid cladding is used. The ultrasonic waves are guided in these clad buffer rods in a very similar way as that of the optical waves guided in a clad optical fiber. It means that the energy is concentrated and well guided in the core. In brief, these high performance clad metallic buffer rods have the following merits: (1) high signal to spurious ultrasonic noise ratio due to the significant reduction of the trailing echoes, (2) high signal amplitude due to proper wave guidance, (3) suitable for reflection and transmission measurement geometries, (4) suitable for both longitudinal and shear waves, (5) low loss, (6) machinable, (7) usable at elevated temperatures, (8) no cross talk between adjacent buffer rods since the ultrasonic energy is concentrated in the core, (9) no loss during immersion in molten metals and (10) simple and easy fabrication [74,78,79].

For monitoring the die casting of Al, three buffer rods with a zirconium (Zr) core and a stainless steel (SS) clad fabricated by a thermal spray technique were installed inside the die. Figure 5.1 is the cut view of the zirconium rods with and without the cladding. The detailed dimensions in which the core is of 6.35 mm diameter, the length of the buffer rod is 69.9 mm and the actual fabricated buffer rod are given in Figs.5.2 (a) and (b) respectively. The Zr core is a low ultrasonic loss material and the SS cladding steel is easy to be machined. A commercial available broadband and high performance UT is attached to the cooling end of each buffer rod with the use of a viscous couplant and under pressure. The UT end is cooled below 60°C by water during the casting. Again, as for injection molding, the viscous couplant is used in order to have a long and stable operation.

The entire buffer rod is inserted into the wall of the die and proper cooling is also provided as shown in Fig.5.3. The other end of the buffer rod directly contacts the die cavity. Figure 5.4(a) shows the reflected 5 MHz longitudinal wave signal from the end of the buffer rod after machining. Figure 5.4(b), shown here for comparison purposes, is the signal for a 6.35 mm diameter 70 mm long bare zirconium rod without cladding. Our measurement results indicated that the signal strength in Fig.5.4(a) is 15 dB stronger than the corresponding one in (b). From Fig.5.4 it is seen that the trailing echoes are reduced significantly. For this clad Zr rod, the signal to noise ratio is more than 45 dB except about 20 dB around the first trailing echo. It is noted that improved clad buffer rods having the similar dimensions and SNR above 45 dB for all time are also developed very recently [76].

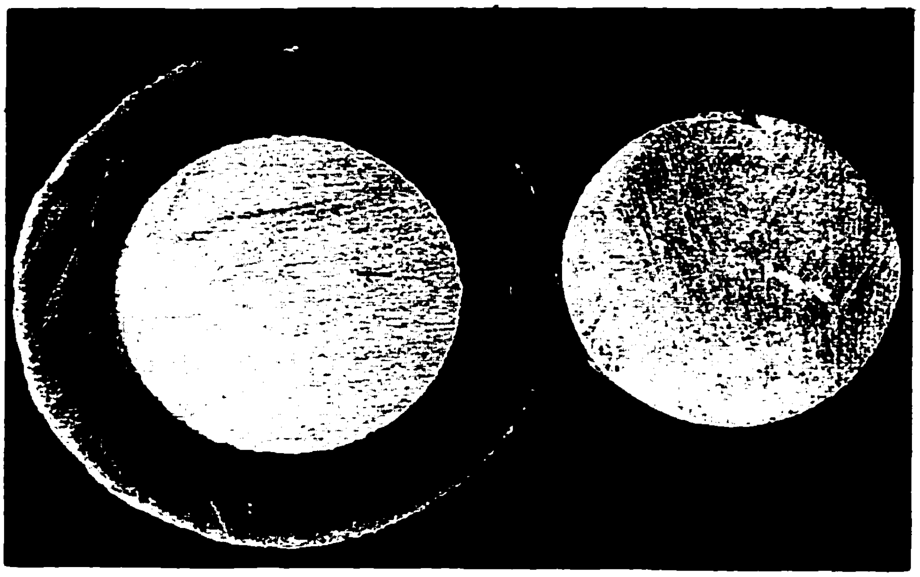

Fig.5.1: Cut view of the zirconium buffer rod with and without steel cladding.

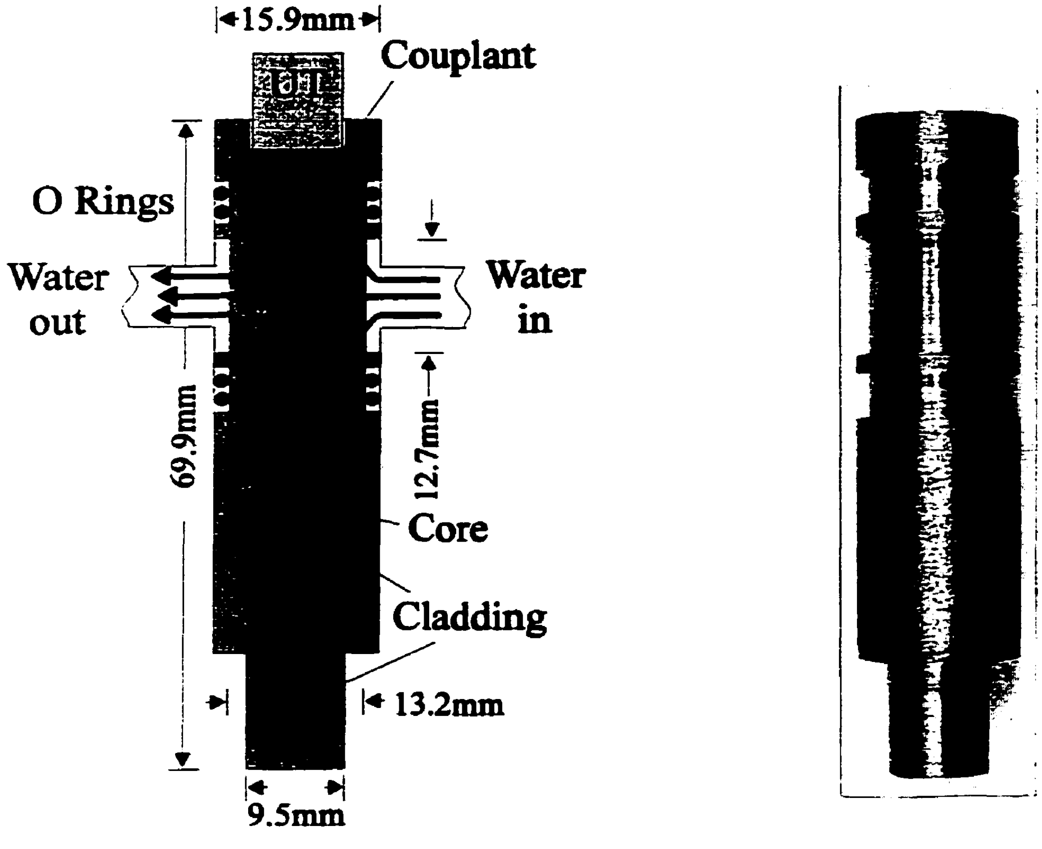

Fig.5.2: Schematic of the buffer rod design for die casting of aluminum; (a) Buffer rod design with cooling and (b) Picture of a buffer rod after the machining.

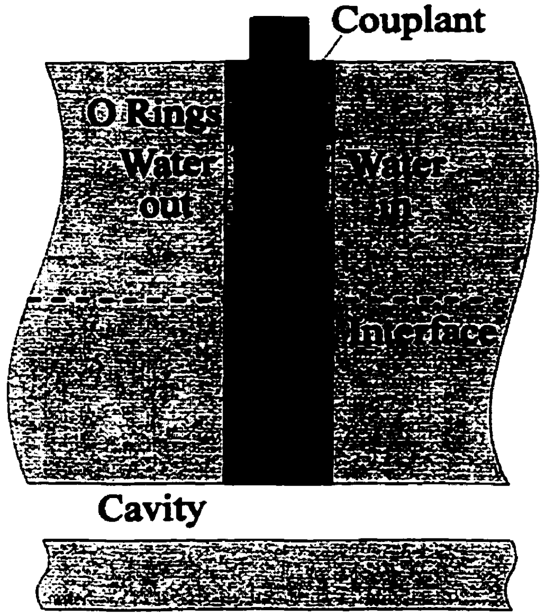

Fig.5.3: Schematic of the buffer rod with cooling inside the die.

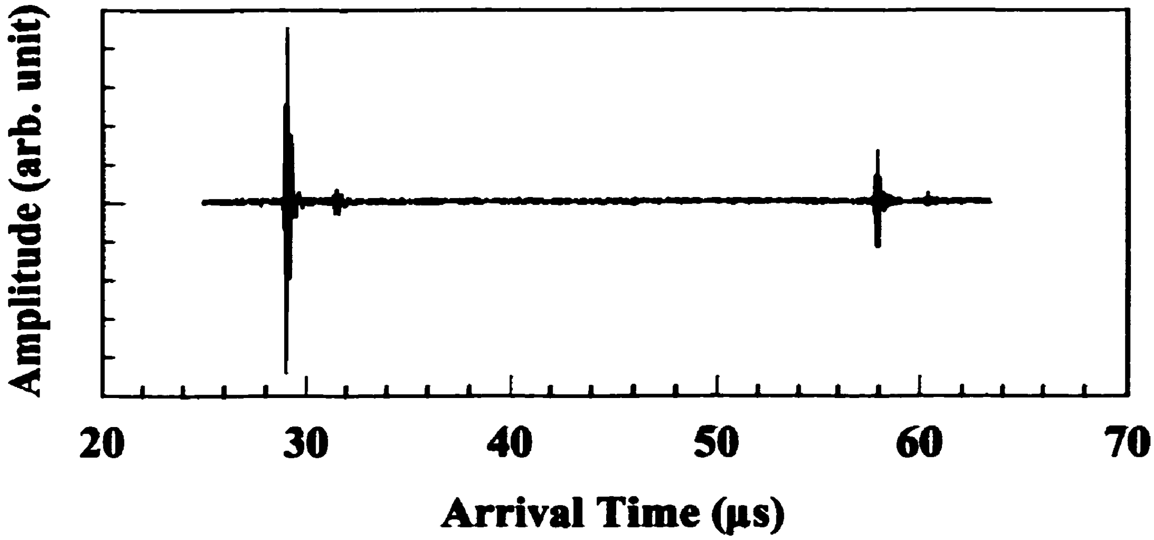

(a)

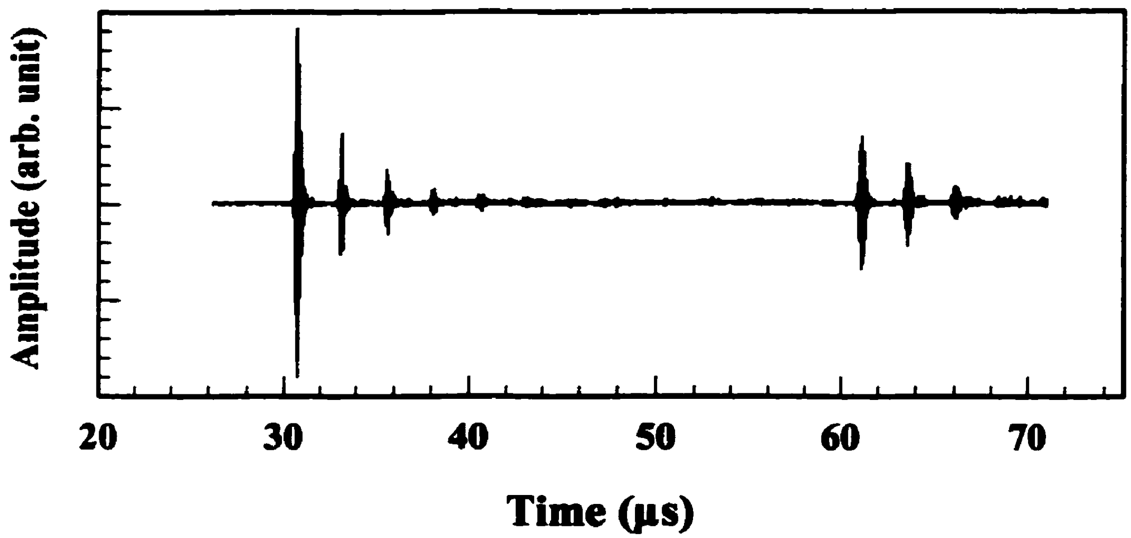

(b)

Fig.5.4: Reflected 5 MHz longitudinal wave signals for (a) the clad zirconium rod and (b) the non-clad zirconium rod.

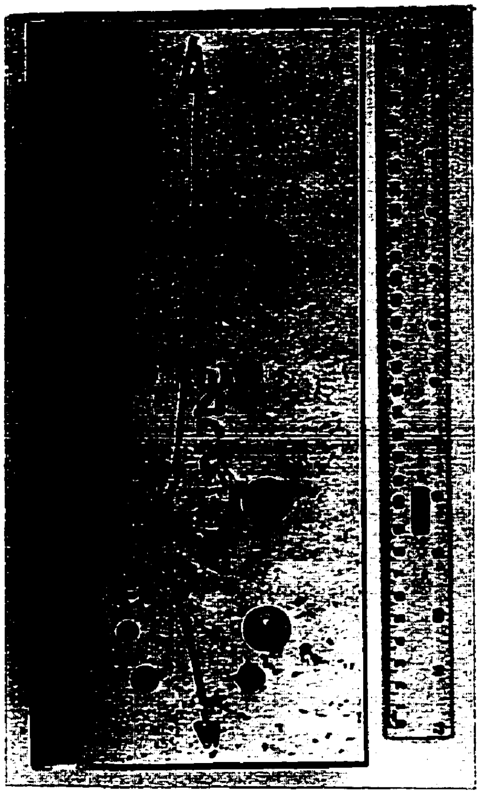

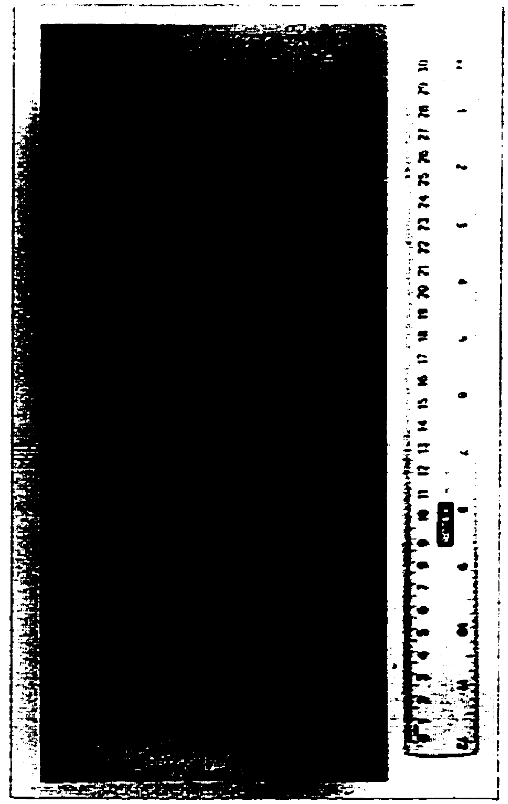

(a) (b)

Fig.5.5: The die with the installed buffer rods. (a) The external surface of the die and (b) The internal surface of the die.

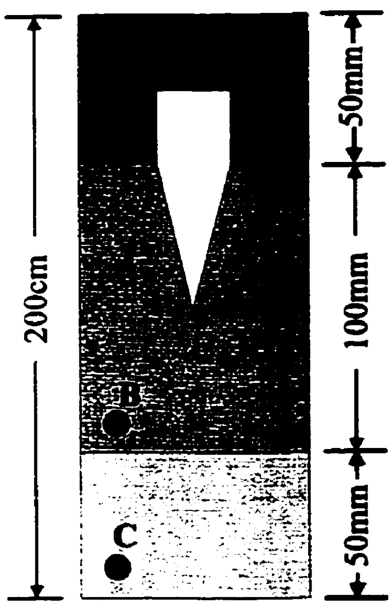

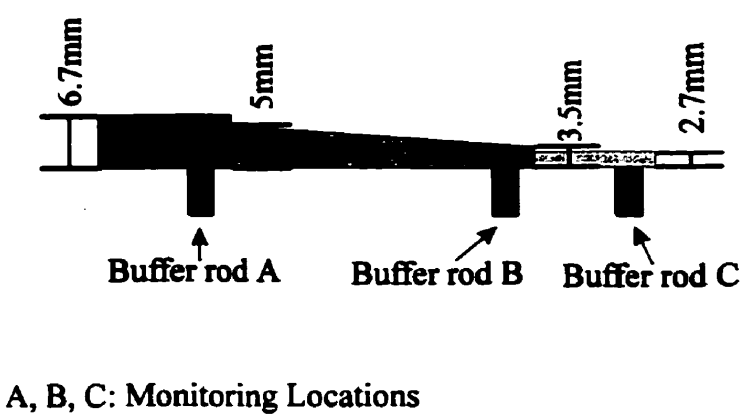

(a) (b)

Fig.5.6: (a) Top view and (b) side view of the cast aluminum part.

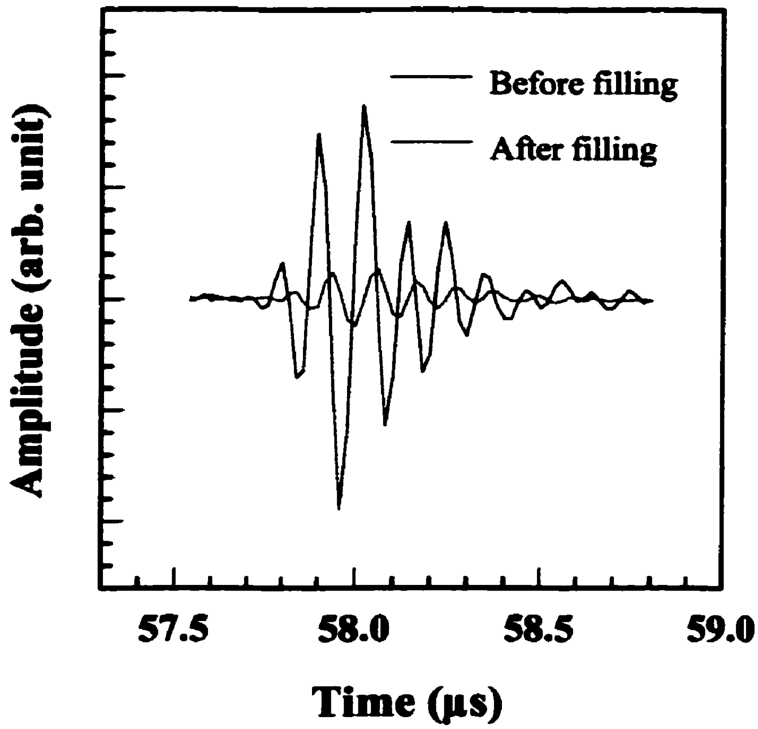

Fig.5.7: Reflected signal before and after filling.

5.3 Die design

Figure 5.5 shows the actual experimental die including the three inserted buffer rods. Both ends of the buffer rods can be seen from both sides of the die. The top and side views of the cast Al part and associated dimensions are given in Figs.5.6 (a) and (b) respectively. The ultrasonic monitoring locations *A*, *B* and *C* where the three buffer rod are inserted are also indicated. The locations are chosen for the convenience to monitor the flow front advancement and different gap development time at different thicknesses.

5.4 Results and discussion

Monitoring of the die casting of Al was performed at different plunger speeds. The two-channel acquisition system was used to perform the data acquisition at two locations simultaneously, i.e., *A* and *C*, or *A* and *B*. The acquisition rate was operated around 1000

Hz leading to an arrival time measurement resolution of around 1 ms. As mentioned in 2.2.2, since the molten Al impedance is close to that of the buffer rod, when the molten Al contacts the buffer rod and the die wall, a significant ultrasonic energy can be transmitted into the Al thus the reflection coefficient at the buffer rod end-Al part interface decreases significantly, ~70%. Therefore, even the first echo of the reflected signal would have a sufficient sensitivity to the change of the interface condition. It is noted that in polymer injection molding experiments the fourth echo was used to increase the sensitivity for monitoring.

Figure 5.7 shows the received echoes reflected from the internal die surface before and after the filling. The amplitude which decreases after the filling can be clearly observed. There exists a time delay after filling for the received signal because the temperature of the die thus the buffer rod increases after the molten Al is injected into the cavity. Like many other metals the ultrasonic velocity of Zr decreases as the temperature arises. Later we will use this phenomenon to investigate the die temperature during the process. The observed ultrasonic signal also indicated that the buffer rod together with the cooling system, UT and ultrasonic couplant worked well at such a high temperature condition. Other noises such as coming from the cooling lines and ejector pins have been eliminated because the desired ultrasonic signals were guided along the core of the buffer rod and the noises are significantly attenuated at the cladding-die interface and in the cladding region.

5.4.1 Flow front monitoring

Figure 5.8 shows the flow front monitoring using the buffer rods at locations *A* and *C*. The plunger speed was 0.37m/s and the estimated flow velocity at the gate was 3.5m/sec which is a very low speed. Each dot in the curve was the result of one acquisition and the time resolution was 1.06 ms. The flow front arrival time difference for this case is around 10 ms. Monitorings of die casting under faster plunge advance speeds were also performed. However, since the part length was 200 mm and the distance from location *A* to *C* was 150 mm, the time for a complete filling exceeded the time resolution of our current acquisition system.

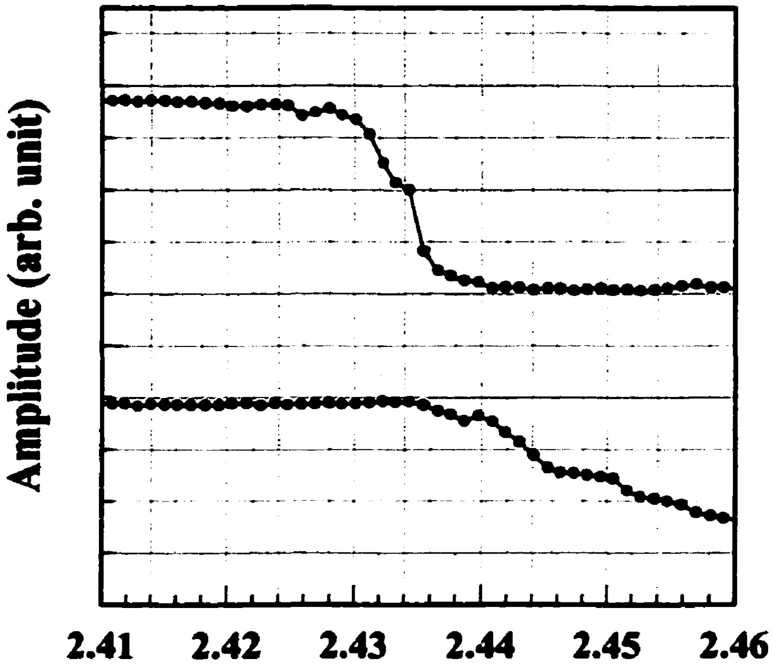

Fig.5.8: Molten aluminum flow front monitoring.

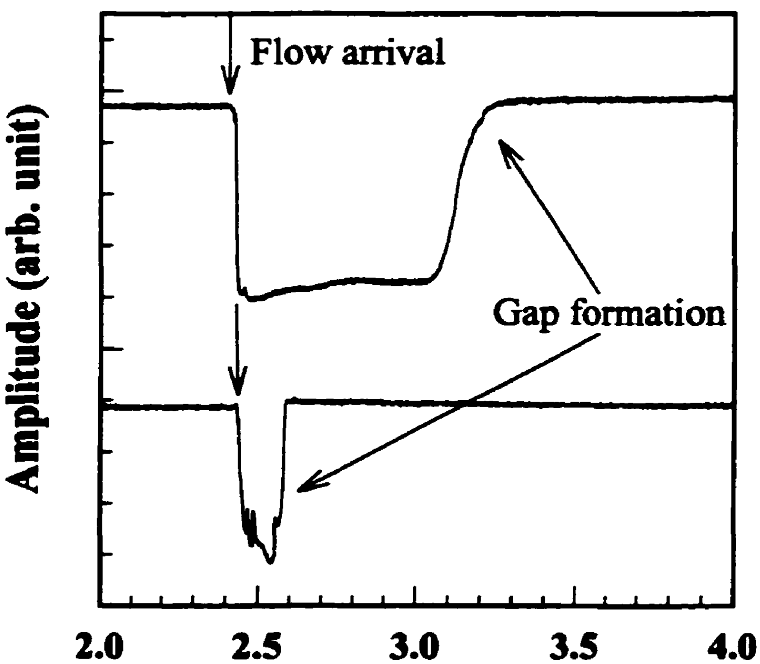

Fig.5.9: Amplitude plot for gap development in die casting of aluminum.

Due to the high filling rate of the molten Al flow could be in a state so-called jetting. It means that the molten Al may be filled in a form of a liquid jet which leads to an early complete filling at the rear end of the part rather than the front end. In addition, the wettability and wetting speed of the molten Al to the mold surface (in this case, to the zirconium core surface) is unknown. This may be a concern because the wetting speed must be faster than the time resolution of the flow front monitoring. Further studying on the reaction between the mold and the flow after the flow arrival is needed and an upgraded acquisition system with a sub-millisecond time resolution is required.

5.4.2 Gap development monitoring

A typical amplitude plot of the reflected signal from the clad Zr buffer rod-Al interface is shown in Fig.5.9. The decrease of the amplitude indicates the arrival of flow and the molten Al attached to the Zr. The increase of the amplitude shows that the gap caused by the part shrinkage is developing and prevents ultrasonic energy from penetrating into the Al part. The amplitude after the gap was slightly different from that before the filling since the temperature was high at that time and could affect the UT, couplant and thus signal.

Figure 5.9 indicates that the gap is developed earlier at location C than that at A. It is understandable because the part thickness at the location A is larger than that at C and a thicker part needs a longer time to be solidified. The contact time which is evaluated starting from the flow arrival until the formation of the gap can be also obtained. It is also observed that the part contact time varied with the part thickness and a thicker part had a longer contact time.

As mentioned in Chapter 4 on injection molding process, the ultrasonic gap is an indication of the onset of the thermal gap. For die casting, the gap detected by the ultrasound is in the order of 0.1 μm. The investigation of the die temperature near the monitoring location may be used to study the effects of the detected ultrasonic gap on the thermal contact resistance (TCR). Since the change in the average temperature inside the buffer rod will cause the variations of the guided ultrasonic wave velocity, the time shift of the received ultrasonic signals can be used for monitoring such temperature change. In fact, a higher temperature in clad Zr rods leads to a lower ultrasonic propagation velocity thus a longer time delay.

Figures 5.10 and 5.11 show the monitoring results of the amplitude and time delay shift variation of the reflected echo at the clad Zr buffer rod-Al interface during die casting of Al at two different filling speeds. In Fig.5.10 measurements at locations *A* and *C* were recorded simultaneously and presented in (a) and (b) respectively. Figures 5.10 illustrates the results of a run with a plunger speed of 0.37m/s and an estimated flow velocity of 3.57m/s at the gate. Monitoring with the plunger speed at 2.29m/s was also carried out and the results are given in Fig.5.11. In Figs.5.11 (a) and (b) measurements were performed at locations *A* and *B* respectively. The estimated flow velocity at the gate was 25m/s for this case.

The signal time shifts in Figs.5.10 and 5.11 were measured by the cross correlation method and error bar was around 0.02 μs. In the figures the average values obtained by the "median filter" in which the values of twenty nearby points are averaged are also plotted. From the above two figures, the time shifts at locations *A*, *B* and *C* were around 0.17μs, 0.13μs and 0.09μs which were about 0.3%, 0.23% and 0.16% change, respectively, of the velocity of clad Zr buffer rod. These results indicate that the die temperature around a thicker part increases more since more heat would transfer to the die wall and buffer rod. It is understood that along the buffer rod direction a temperature gradient, thus a velocity gradient, would exist during the part solidification.

It is also observed that the change in the time shift which indicates the change in the average die wall temperature at the monitoring locations are consistent with the amplitude plots indicating the Al flow arrival and gap development. The sudden rise of the time delay hence the temperature corresponds to the flow front arrival which means the heat starts to conduct and warm the die wall and clad Zr buffer rod when the molten Al wets the die wall. When the molten Al contacts well with the die wall, the temperature increases sharply. This indicates that the heat transfer is efficient due to the good heat conduction. After an ultrasonic gap is detected and the amplitude recovers to the high level, the rate of increase for the temperature of the buffer rod drops significantly. This may reveal that a severe TCR exists and the part is no longer cooled efficiently inside the cavity.

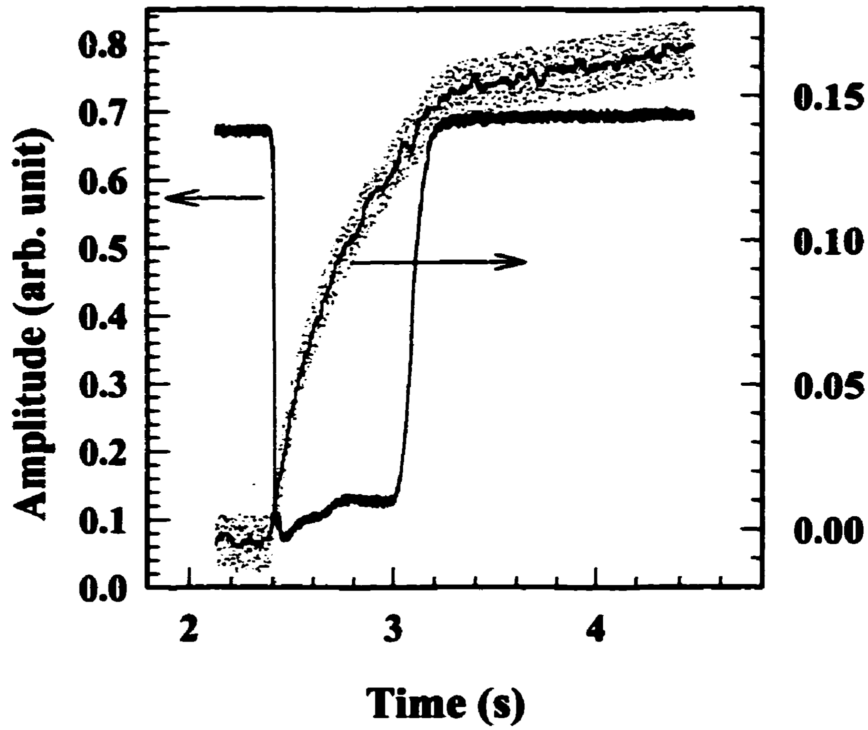

(a)

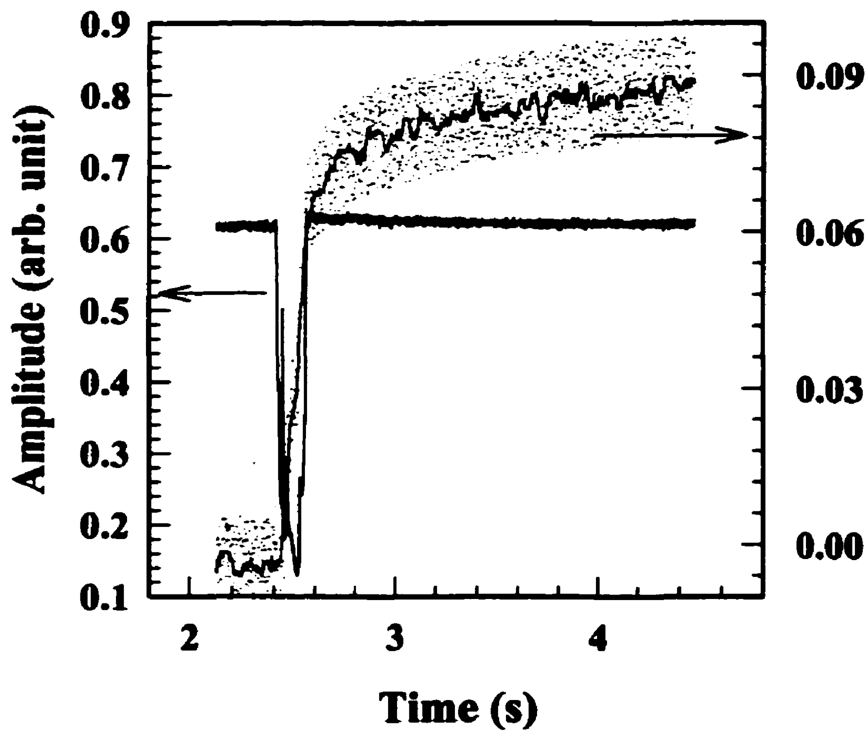

(b)

Fig.5.10: Amplitude plot and signal time shift plot (Plunge speed 0.37m/s). (a) Monitoring at location *A* and (b) Monitoring at location *C*.

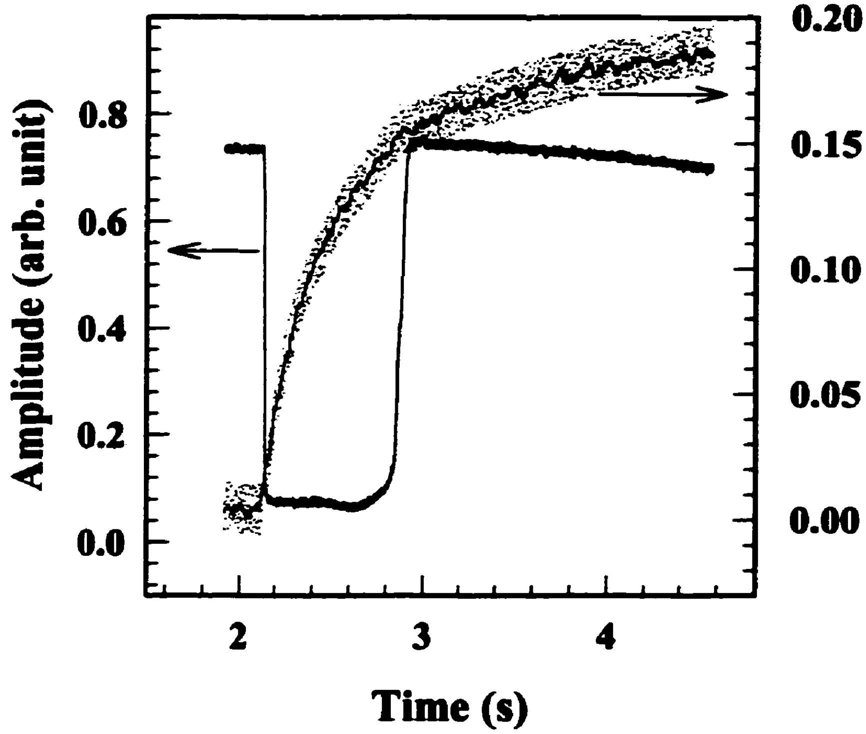

(a)

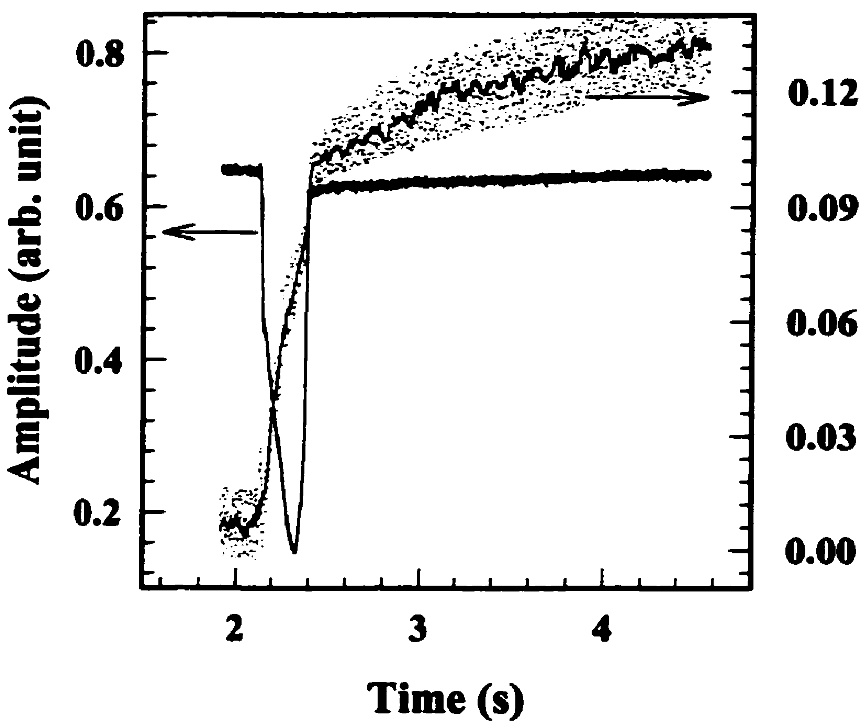

(b)

Fig.5.11: Amplitude plot and signal time shift plot (Plunge speed 2.29m/s). (a) Monitoring at location *A* and (b) Monitoring at location *B*.

5.4 Summary

The ultrasonic monitoring of the flow front during filling and the gap development during the part solidification in die casting of Al part was carried out. Three buffer rods with a zirconium core and a stainless steel cladding fabricated by a thermal spray technique were integrated into the die. The transducer end of each buffer rod was water cooled down to 60°C or below during the monitoring. Commercial high performance 5 MHz UTs and couplants were then used for the measurements. Signals with good SNR were achieved under such high temperature operation conditions, i.e., around 300°C at the external surface of the die.

The flow front was detected at a low plunger speed of around 0.37m/s. Gap formation due to the part shrinkage was monitored and the Al part contact time with the die wall was also measured. It was found that a thicker part had a longer contact time. By measuring the signal time delay shift along the buffer rod caused by the die temperature increase, the die temperature changing trend during the process was measured. A temperature gradient along the die surface where the temperature is higher at the location of thicker part was observed. The observed die wall temperature variation derived from the signal time shift measurements also indicated that there existed a significant thermal contact resistance right after the detection of the ultrasonic gap which was detected by the monitoring of the amplitude variation.

Chapter 6:

Conclusion

6.1 Thesis summary

On-line ultrasonic monitoring of polymer injection molding and die casting of aluminum (Al) was carried out. Pulse-echo method using 5 MHz longitudinal wave was employed in our study. The molten material flow front arrival and the gap development change the interface condition between the mold and part thus cause the changes of the ultrasonic signal reflection and transmission coefficient at this interface. Thereby, the flow front and the gap formation were monitored from the amplitude variations of the acquired ultrasonic signal. It is noted that before the polymer injection the reflection coefficient is 1 due to the large ultrasonic impedance mismatch between the steel mold wall and air in the cavity. After the filling the steel (mold)-air interface changes to the steel-polymer interface, the reflection coefficient decreases because a part of the ultrasonic energy is transmitted into the part inside the cavity. The transit time and the amplitude of the ultrasound inside the part during the process were also measured, thus the ultrasonic velocity and attenuation which are related to the part solidification could be obtained. After about ~1 μm gap is developed between the mold and the part, the interface changes back to steel-air case, the reflection coefficient returns to 1 and the monitoring for the above three tasks ceases.

In order to perform the monitoring tasks, a PC-based plug-in data acquisition system was developed. A two-channel acquisition card with the maximum sampling rate up to 100 MHz was plugged into a Pentium PC computer and can directly access the computer bus. The acquisition control was written in Labview software with user friendly interface. High acquisition repetition rate up to 1000 frames/sec per channel was achieved for a two-channel acquisition and the time resolution can be up to 1 ms. This two channel system was appreciated because the flow front monitoring would not be effective if a single channel system reported in [55] was used, in particular, for a very short time duration as existed in die casting of aluminum. Post signal processing softwares were also performed under the Labview programming in this study.

Several essential monitoring tasks such as flow front, gap development and solidification were performed on polymer injection molding. A simple box mold was studied. The material was a high density polyethylene. In most cases, ultrasonic transducers (UTs) were installed at external mold wall and at desired locations to perform monitoring in reflection mode. Meanwhile, an insert hollow core was designed for the preliminary laboratory investigation purposes. Using this type of core UTs could be installed inside the core, then both transmission mode and reflection mode inside the core were carried out. A viscous ultrasonic couplant was used and it worked well without refreshing for weeks. Several practical considerations such as signal echo selection and temperature effects were also discussed. Proper echo selection can enhance the sensitivity for monitoring the flow front arrival and the gap development. Such selection was not used in [55] for the monitoring of the polymer injection molding, thus poor sensitivity was observed.

With the two-channel acquisition system, the flow arrival times at two locations were recorded simultaneously thus the time delay of the arrival times between two locations was measured. Then the flow front speed inside the cavity between these two locations was obtained. By using the different combinations of two positions, we may know the advancement of the flow front inside the whole cavity. Different injection speeds were applied, and the monitoring results showed that the flow front speed increased with the increase of the injection speed, the polymer flow front speed slowed down slightly along the flow path and the flow front at a thicker part had a lower advancement speed.

Gap development was successfully monitored at the box side walls. A total contact time was defined from the reflected signal amplitude plot. It starts from the time when the front flow arrived until the a ~1 μm gap is developed. After the filling, the amplitude of the reflected signal stayed at the low level for a while because part of the ultrasonic energy is transmitted into the filled part then it starts to rise due to the gap formation. We defined the time from the filling to that when the amplitude starts to rise as the good-contact time which means that the part had a good contact during this time period. Partial-contact time was defined from the time when the amplitude starts to rise until a ~1 μm gap is developed. During this time period the part partially contacted the mold. After the ~1 μm gap is formed, the amplitude of the reflection coefficient is recovered to 1 which is the same as that before the polymer injection. The advantages of ultrasonic monitoring of the cavity conditions over the pressure sensors were the high sensitivity to the gap formation, fast response, simple installation and the clear identification of the above mentioned contact stages.

Different packing pressures were applied in the injection molding. The experimental results obtained from the monitoring of reflected signals which were received by the UTs installed at the external mold showed that a higher pressure led to a longer contact time, a shorter gap time thus a better part cooling. This result was also confirmed by the part surface temperature after ejection measured by an infrared technique [83]. Similar results were also obtained from the measurements at different locations, those performed in transmission mode and at different melt temperatures. No gap was detected at the bottom of the box while a gap was monitored at the side wall. The bottom was thicker than the side wall indicating that the thicker part needed more cooling time. An oscillation of the reflected signal amplitude from the monitoring of the bottom wall was observed after the gap formed at the side wall and could be caused by the structure force induced by the transient detaching of the part at the side wall.

Measurements of the ultrasonic velocity of the part during injection molding were carried out using the transmission mode in which the signal was emitted from the transmitting UT mounted at the external mold wall and received by the UT installed inside the hollow core. The two-channel acquisition system recorded both the reflected signal obtained by the UT at the external mold wall and the transmitted signal. These two signals enable us to achieve a high precision measurement which uses the cross correlation method to obtain the time delay between the echoes and then the ultrasonic velocity of the part. Further studies could relate the measured velocity to the part properties during the solidification.

In general, the solidification monitoring in reflection mode is preferred. Process monitoring using UT mounted at the external mold wall was firstly performed. A small signal which had a round trip inside the part was obtained. Its signal strength was around 50 dB less than that directly reflected at the mold-part surface. The SNR of this echo was small because noises coming from the multiple ultrasonic reflections at the cooling lines, ejector pins and large grain size of the steel mold appeared. Using the digital signal processing method, the desired signal was extracted though still with a low SNR. Nevertheless the results showed that monitoring of the solidification in reflection mode was feasible. In [55] the solidification of the polymer was monitored in the transmission mode which is not practical and convenient.

Secondly, the monitoring using the UT installed inside the core facing the box bottom wall was also operated in reflection mode. Multiple round trip signals inside part wall were obtained with reasonable SNR because the core mold wall was thin and no disturbance came from the cooling lines and ejector pins existed in the above case. Such reflected signals could be used to measure the velocity with an improved precision. Although installation of the UTs in the insert core may not be practical, the results indicate that by careful selection of the monitoring locations high precision measurements of the ultrasonic velocity of the part related to its solidification could be carried out in the reflection mode.

Since the die casting of Al was performed under high temperature conditions and there is no high performance high temperature UTs and couplant available, novel clad metallic buffer rods were employed. These buffer rods were used as ultrasonic waveguide between the UT and cast Al part with high temperature during the process. Three clad buffer rods consisting of a zirconium core and a stainless steel cladding fabricated by a thermal spray technique were integrated into the die wall. Each UT end of the buffer rod was water cooled down to 60°C or below. Then the commercial high performance ambient temperature UTs and couplants were applied. Ultrasonic monitoring of die casting of Al was successfully carried out under such measurement configuration.

Flow front monitoring of die casting of Al using a experimental die was performed using the same two-channel acquisition system but operated around 1000 frames/sec with the time resolution around 1 ms. The arrival time difference of molten aluminum flow at three different positions was observed under very low plunger speed. The arrival time differences at high plunger filling speed were not identified because the filling speed is very fast and the part in the generic die was very short, the required time resolution should be sub-milliseconds which is beyond of our hardware capacity. The wettability of the molten aluminum to the die wall surface was also a concern because the wetting speed should be faster than the time resolution of the monitoring.

Gap development monitoring of the Al part during the solidification was also performed. The results showed that a thicker part needed more time to be solidified, had a longer contact time with the die wall thus the gap was developed later. The amplitude plot shift inside the buffer rod due to increasing temperature during the process. The comparison clearly showed that detected ultrasonic gap indicated the onset of the significant thermal contact resistance (TCR) which was the barrier to the part cooling. The comparisons also showed that the die wall surface temperature was non-uniform during part solidification, i.e., the die wall surface near the thicker part had much higher temperature. It is noted that the largest gap which can cause total reflection in the case of die cast of Al is only ~0.1μm which is different from ~1μm in the polymer injection case.

The performed on-line ultrasonic monitoring of the injection molding and die casting process showed that the ultrasonic sensor is an excellent candidate to perform many on-line monitoring tasks. Molten material flow during the filling, the cavity condition including the gap development and temperature information both for the part and the mold surface, and the part solidification could be monitored using ultrasound. Multiple monitoring tasks may be carried out using the same setup, thus convenient, economic, fast response and multiple function can be achieved. As an example, Buhler (Uzwil, Switzerland) has used an electrical device to monitor the flow front in their die casting machines and claim much improved operation and products [84]. Our purposed ultrasonic method is believed to be able to perform multi-task monitoring and more robust.

6.2 Future work

For the monitoring of polymer injection molding, different materials and different operation conditions can be tested. A multiple-channel up to tens of channel acquisition system can be setup and more detail investigation can be implemented. Clad buffer rods may be installed inside the mold wall thus solidification monitoring using reflection mode could be carried out with a much enhanced SNR. The part surface temperature and the temperature profile along the mold wall could also be measured using the well-designed clad buffer rod fabricated with the thermal spray technique [76]. Combining the temperature measurements with the ultrasonic velocity measurement of the part which is related to the part average temperature, the investigation of the temperature profile inside the part along the thickness direction could be obtained using an inverse method.

The acquisition system can be further improved and sub-millisecond time resolution should be achieved to monitor the die casting of aluminum operated at high plunger filling speed. The casting process may be monitored at different operation conditions and phenomena such as the behavior of the molten aluminum flow and dynamic plunger speed control by the monitoring of the flow could be investigated. The temperature of the part surface along with the ultrasonic velocity measurement of the part may also be evaluated with the use of clad buffer rods thus solidification monitoring of the aluminum could be achieved even in reflection mode.

The ultrasonic techniques that were developed in this study could be applied to other industrial material processes, i.e., gas assisted injection molding, co-injection molding and co-extruded polymer blow molding. For example, co-injection molding, in which one part could be composed of different layered materials with different thicknesses, the advancement and direction of the flow front as well as the thicknesses of different material layers could be monitored on-line by ultrasound.

Appendix: Processing Programs

All the ultrasonic signal processing programs are written in Labview software, a graphic programming language. Below are the two main programs used in our study to obtain the amplitude profile and time delay between echoes.

(a) 2-channel amplitude plot

This program is used to obtain the maximum value of the acquired ultrasonic signal which is the reflection or transmission coefficient in each frame and plot the amplitude profile. The main subprogram is the routine for finding the maximum amplitude introduced in 3.3.3. Window, bandpass filter and signal interpolation are introduced in this program. The flow front arrival time difference between two locations and the contact time at each location can be derived from the plots. The panel of this program is shown in Fig.A.1. Figures A.2(a) and (b) show respectively the panel and diagram of the routine for finding the maximum amplitude.

(b) Time delay processor

This program is to calculate the time delay between ultrasonic echoes. The time delay between two echoes inside same graph or different graphs can be derived using the cross correlation method. Window and filters are introduced in the program. The method to calculate the travel time inside the part which was introduced in 4.6.1 can be implemented by this program. The panel is shown in Fig.A.3.

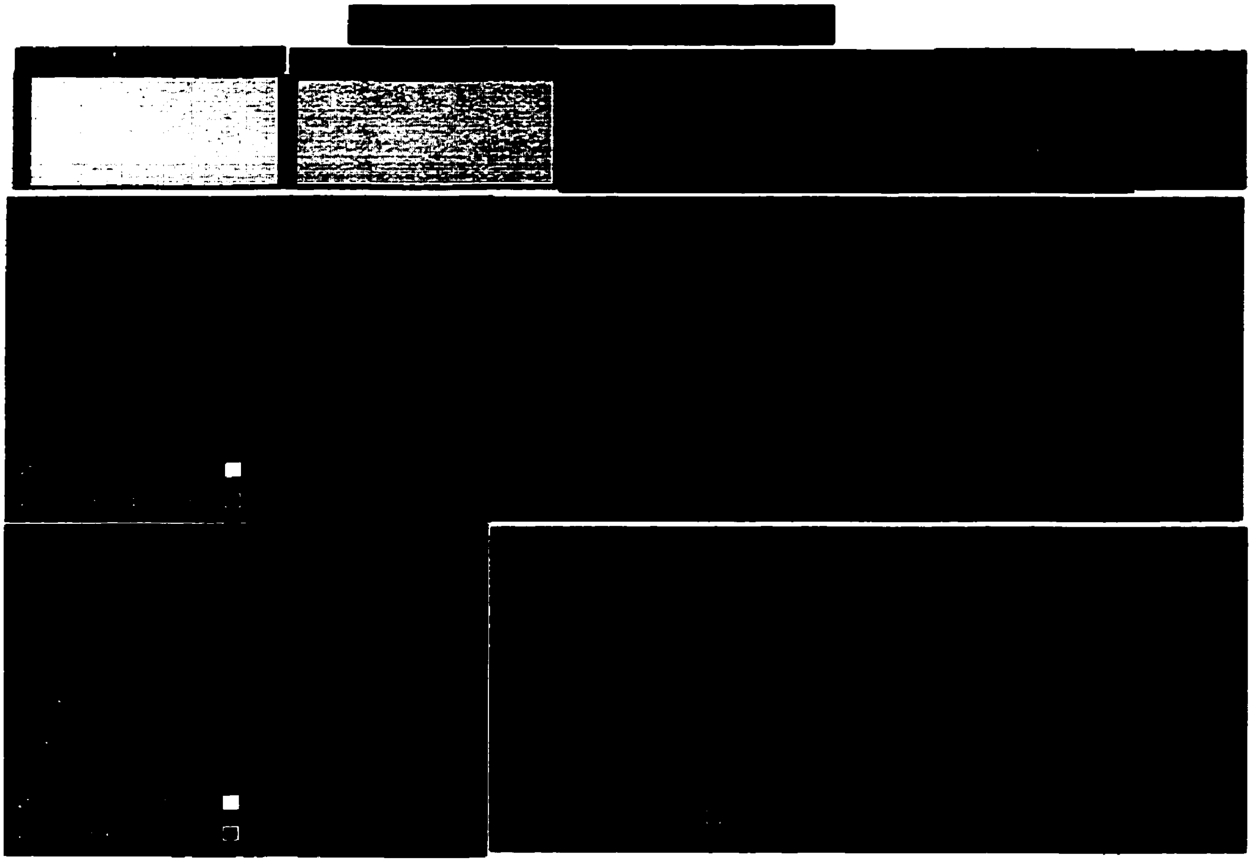

Fig.A.1: Panel of the 2-channel amplitude plot program.

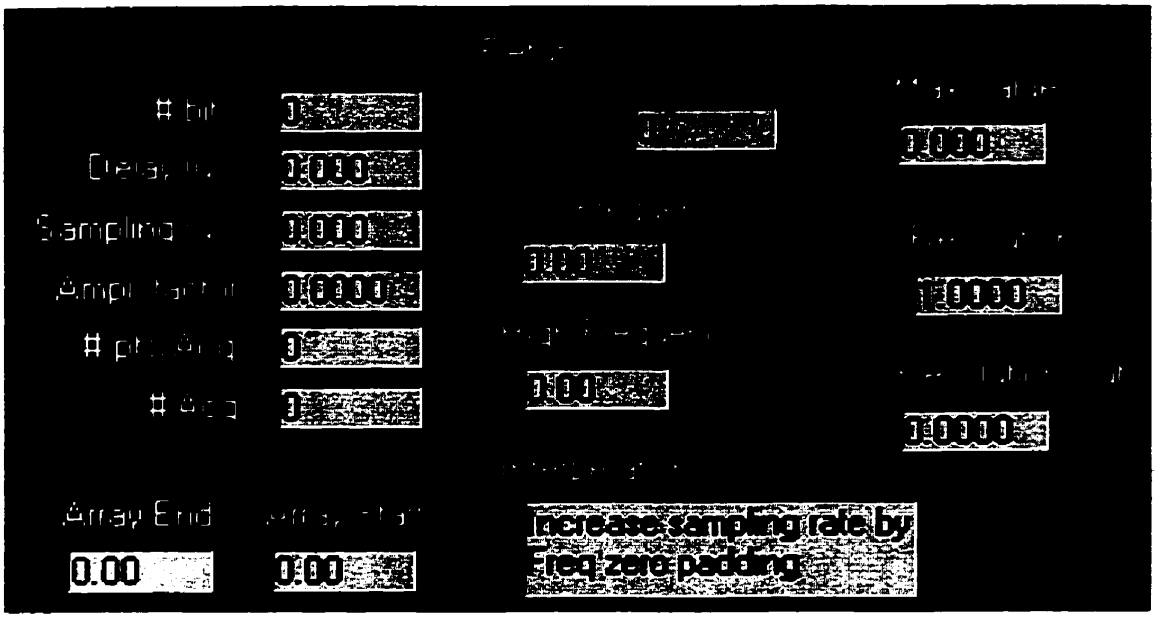

(a)

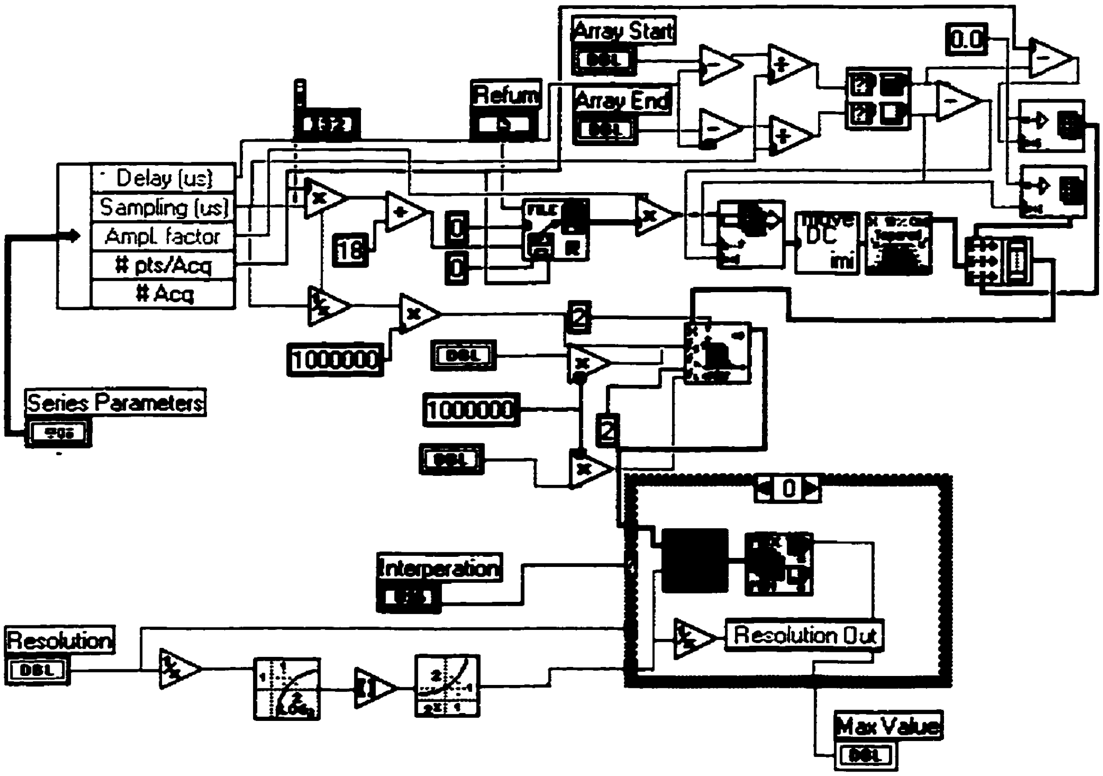

(b)

Fig.A.2: Routine for finding the maximum amplitude. (a) Panel of the program and (b) Diagram of the program.

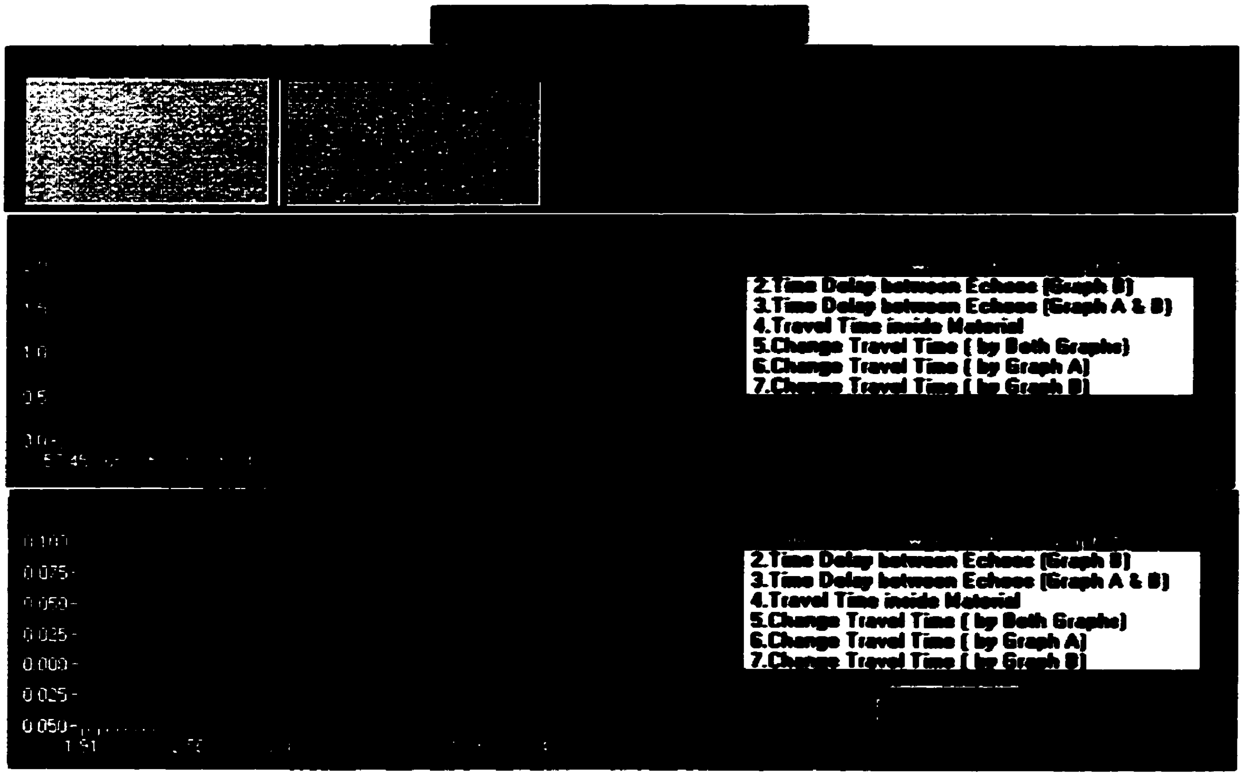

Fig.A.3: Panel of the time delay processor program.

References:

[1]R. Fendron and L. A. Utracki, "Material characteristics oriented computer control of extrusion-part 1", Proc. SPE ANTEC, pp.958-963, 1991.

[2]A.R. Agrawal, I.O. Pandelidis and M. Pechr, "Injection-molding process control-a review" Polymer Engineering and Science, vol 27, no.18, pp.1345-1357, 1987.

[3]R.E. Farrell and L. Dzeskiewiez, "Expert system for injection molding", Proc. SPE ANTEC, pp.692-695, 1994.

[4]J. Cann and Y. Shen, "Computer integrated information and control system for improved quality and profit", Transactions from the NADCA 15th International Die Dasting Congress and Exposition, G-T89-021, 1989.

[5]J.L. Wu, S.J. Chen and R. Malloy, "Development of an on-line cavity pressure-based expert system for injection molding process" Proc, SPE ANTEC, pp.444-449, 1991.

[6]B. Souder, S. Woll and D. Cooper, "Advanced method for monitoring injection molding processes" Proc, SPE ANTEC, pp.644-650, 1994.

[7]Y. Mochiku, Y. Hatamura and K. Shirahige, "Intelligent die casting and seven sensors", Transactions from the NADCA 15th International Die Dasting Congress and Exposition, G-T89-024, 1989.

[8]S.H. Patel, D.B. Todd and M. Xanthos, "Recent development in on-line analytical techniques applicable to the polymer industry", Proc. SPE ANTEC, pp.2214-2219, 1994.

[9]H.N.G. Wadley, S.J. Norton, F. Mauer and B. Droney, "Ultrasonic measurement of internal temperature distribution", Phil. Trans. R. Soc. London. A320, pp.341-361, 1986

[10]M. Haupt, "Computer-assisted optimization of working points in plastics processing", Proc. SPE ANTEC, pp.59-61, 1989.

[11]V. Miranda and F.S. Lai, "A study of the effect of gate design on holding time by theoretical calculations, computer flow simulation and experimentation", Proc, SPE ANTEC, pp.411-416, 1995.

[12]C.P. Chiu and K.A. Liu, "A method for measuring PVT relationships of thermoplastics using an injection molding machine", Polymer Engineering and Science, vol 35, no.19, pp.1505-1510, 1995.

[13]W.C. Bushko and V.K. Stokes, "Solidification of thermoviscoelastic melts, Part 3: Effects of mold surface temperature difference on warpage and residual stresss", Polymer Engineering and Science, vol. 36, no. 3, pp.322-335, 1995.

[14]W.C. Bushko and V.K. Stokes, "Solidification of thermoviscoelastic melts, Part 4:Effects of boundary conditions on shrinkage and residual stresss", Polymer Engineering and Science, vol. 36, no. 5, pp.658-675, 1995.

[15]Y. Yamamoto, Y. Iwata, M. Nakamira and Y. Oukouchi, "Molten metal velocities and gas pressure in die cavity and defects in commercial aluminum pressure die castings", Transactions from the NADCA 15th International Die Dasting Congress and Exposition, G-T89-081, 1989.

[16]J.R. Brevick, M. Duran and Y. Karni, "Experimental determination of slow shot velocity-position profile to minimize air entrapment", Transactions from the NADCA 16th International Die Dasting Congress and Exposition, pp.399-404, 1991.

[17]Y. Karni, "Optimization of process variables for die casting", Transactions from the NADCA 17th International Die Dasting Congress and Exposition, pp.153-156, 1993.

[18]J.K. Brimacombe and A.W. Cramb "Steelmaking, casting and molding", Proc. of 10th PTD conference, pp.211-224, 1992.

[19]H. Murakami, M. Hasan, and R.I.L. Guthrie, "A mathematical model for a vertical twin-roll caster", Proc. of 10th PTD conference, pp.347-354, 1992.

[20]S. Chen, D.B. Johnson and P.E. Raad, "Simulated filling of dies with cores", Transactions from the NADCA 16th International Die Dasting Congress and Exposition, pp.275-279, 1991.

[21]L.S. Turng, H.H. Chiang, and J.F. Stevenson, "Optimization strategies for injection molding", Proc. SPE ANTEC, pp.668-672, 1995.

[22]S.J. Liu, K. San and J.X. Rietveld, "Modeling and simulation of thermally induced stress and warpage in injection molded thermoplastics", Proc. SPE ANTEC, pp.684-701, 1995.

[23]M. Buchmann, R. P. Theriault and T.A. Osswald, "Polymer flow length simulation during injection mold filling", Proc. SPE ANTEC, pp 546-550, 1995.

[24]D.M. Gao, K.T. Nguyen, P. Girard and G. Salloum, "Numerical simulation of the sequential filling in injection molding process", Proc. SPE ANTEC, pp.554-558, 1994.

[25]P. Ehret, A. Davidoff, F. Jacque and H. Bung, "Simulation of the complete injection cycle", Proc. SPE ANTEC, pp.542-546, 1994.

[26]D. C. Schmidt and L. E. Smiley, "Success stories using solidification simulation", Transactions from the NADCA 17th International Die Dasting Congress and Exposition, pp.71-75, 1993.

[27]C.A. Loong, G. Salloum and D. Frayc, "Computer simulation of die cavity filling in 3-D by the finite element method", Transactions from the NADCA 16th International Die Dasting Congress and Exposition, pp.299-304, 1991.

[28]L. Kallien and J.C. Sturm, "Simulation aided design for die casting tools",Transactions from the NADCA 16th International Die Dasting Congress and Exposition, pp.305-309, 1991.

[29]D. Frayce, J.F. Hetu and C.A. Loong, "Numerical modeling of filling and solidification in die casting", Transactions from the NADCA 17th International Die Dasting Congress and Exposition, pp.13-17, 1993.

[30]Y. Iwata, Y. Yamamoto, K. Yonekura and Y. Kagami, "Computer simulation of molten metal flow in thin plate die castings", Transactions from the NADCA 16th International Die Dasting Congress and Exposition, pp.311-320, 1991.

[31]G. Engelstein, "Virtual molding: a challenge to the analysis industry", Proc. SPE ANTEC, pp.768-771, 1995.

[32]M.P. Schwarz, A.R. Musgrove, L.D. Hooper and P. Dang, "Validation of numerical simulation of gas bath circulation by LDV measurement", Proc. of 10th PTD conference, pp.123-132, 1992.

[33]H. Wang, M. Prystay, J.-F. Hétu, B. Cao and C.K. Jen, "Gap between mold and part and its effects on cooling of injection-molded plastics", Proc. SPE ANTEC, pp.1049-1053, 1996.

[34]M. Konno, A. Cui, N. Nishiwaki and S. Hori, "Measurement of polymer melt temperature in injection molding machine by using ultrasonic techniques", Proc. SPE ANTEC, pp.2798-2803, 1993.

[35]D.V. Rosato and D.V. Rosato, "*Injection molding handbook*", Second Editioin, Chapman & Hall, 1995.

[36]P. D. Coates, A. J. Daswson, A. Key, C. Peters and R. Jagger, "Intelligent monitoring for 100% automatic inspection of quality in injection moulding", Proc. SPE ANTEC, pp.525-529, 1996.

[37]R.G. Speight, J.B. Hull and P.D. Coates, "Control of polymer melt flow front position during the injection molding process", Proc. SPE ANTEC, pp.588-592, 1996.

[38]H. Wang, M. Prystay, G. Chouinard, R. Connolly and P. Cielo,"A feasibility study of using infrared radiometry for measuring mould surface temperature between injection moulding cycles", Technical Report, IMI95RT-50201-62077-G, Jan. 1995.

[39]R. Bluhm and W. Michaeli "Infrared temperature measurements-measured and calculated temperature profiles in the cavity of a mold", Proc. SPE ANTEC, pp.630-636, 1995.

[40]N. Dontula, D. A. Campbell and J. J. Wenskus, "A novel approach to determine melt temperature profiles in injection molding", Proc. SPE ANTEC, pp.642-646, 1995.

[41]R.G. Speight, E.P. Yazbak and P.D. Coates, "In-line pressure and infrared temperature measurements for injection moulding process control", Proc. SPE ANTEC, pp.647-651, 1995.

[42]M.G. Hansen and A. Khettry, "In-line monitoring of molten polymers: near infrared spectroscopy, robust probes, and rapid data analysis", Polymer Engineering and Science, vol. 34, no.23, pp.1758-1766, 1994.

[43]A.J. Bur and C.L. Thomas, "Real-time optical monitoring of polymer injection molding", Proc. SPE ANTEC, pp.490-495, 1994.

[44]D.W. Yu, M. Esseghir and C.G. Gogos, "The use of on-line optical microscopy for monitoring compounding and other polymer processing operations", Proc. SPE ANTEC pp.136-144, 1995.

[45]A.J. Bur and C.L. Thomas, "A multi-functional optical sensor for monitoring polyner injection molding", Proc. SPE ANTEC pp.2798-2804, 1995.

[46]A.J. Bur, F.W. Wang, C.L. Thomas and J.L. Rose, "In-line optical monitoring of polymer injectiooon molding", Polymer Engineering and Science, vol. 34, no.8, pp.671-679, 1994.

[47]F. Brant, "Advanced defect analysis techniques using real-time radioscopy", Transactions from the NADCA 15th International Die Dasting Congress and Exposition, G-T89-132, 1989.

[48]L.C. Lynnworth "*Ultrasonic measurements for process control, Theory, Techniques, Applications*", Academic Press Inc.,San Diego, 1989.

[49]R. Gendron, M.M. Dumoulin, J. Tatibouet, L. Piche and A. Hamel, "Measuring on-line polymer properties using an ultrasonic technique", Proc. SPE ANTEC, pp.2256-2261, 1993.

[50]R. Gendron, L.E. Daigneault, J. Tatibouet and M.M. Dumoulin, "Residence time distribution in extruders determined by in-line ultrasonic measurements", Proc. SPE ANTEC, pp.167-171, 1994.

[51]L. Piche, D. Levesque, R. Gendron and J. Tatibouet, "Ultrasonic probe of polymer flows", Proc. SPE ANTEC, pp.2715-2719, 1995.

[52]L. Piche, A. Hamel, R. Gendron, M. Dumoulin and J. Tatibouet, "Ultrasonic characterization of polymer melts under processing conditions", US Patent 5433112, July 18,1995.

[53]L. Piche, F. Massines, A. Hamel and C. Neron, "Ultrasonic characterization of polymers under simulated processing conditions", US Patent no.4754645, July 5,1988.

[54]C.L. Thomas, M. Jiang, C.C. Chen and A.J. Bur, "An ultrasonic instrument for PVT characterization of polymer", Proc. SPE ANTEC pp.2707-2714,1995.

[55]C.L. Thomas, "Sensor sense of injection molding", Phd dissertation, Department of Mechanical Engineering, Druxel University, 1993.

[56]C. Thomas, J.L. Rose and Z.K. Li, "An ultrasonic sensor to monitor the mold cavity conditions during injection molding", Review of Progress in Quantitative Nondestructive Evaluation, vol. 12, pp.2333-2340, 1993 .

[57]J.J. Magda, M.L. Parrott, C.L. Thomas and D.R. Lawson, "An ultrasonic technique for monitoring the interface in multi-layer polymer flows", Proc. SPE ANTEC, pp.1182-1186, 1996.

[58]C.L. Thomas, A.A. Tseng, J.L. Rose and A.J. Bur, "Closed loop control of injection molding hold time", Proc. SPE ANTEC, pp.143-148, 1993.

[59]C.L. Thomas, A.O. Adebo and A. J. Bur, "Ultrasonic measurement of polymer material properies during injection molding", Proc. SPE ANTEC, pp.2236-2239, 1994.

[60]C.B. Scruby and L.E. Drain,"*Laser ultrasonics--Techniques and applications* ", Adam Hilger, Bristol, 1989.

[61]A.D.W. McKie, R.C. Addison, Jr., T.-L.T. Liao and H.-S. Ryang, "Laser-based ultrasonics--applications to NDE and process monitoring", Proceedings of IEEE Ultrasonics Symposium, pp.641-649, 1993.

[62]R.C. Addison, Jr., A.D.W. McKie, T.-L.T. Liao and H.-S. Ryang, "In situ process monitoring using laser-based ultrasound", Proceedings of IEEE Ultrasonics Symposium, pp.783-786, 1992.

[63]R.C. Addison, Jr., A.D.W. McKie, T.-L. T. Liao and H.-S. Ryang, "In situ process monitoring using laser-based ultrasound", Proc. of Review of Progress in Quantitatives Nondestructive Evaluation, pp.2237--2244, 1993.

[64]K.D. Tackitt, J.W. Gillespie, J.N. Caron and J.B. Mehl, "High temperature measurements of ultrasonic wave speed using a laser ultrasonic technique", Proc. SPE ANTEC, pp.1198-1202, 1996.

[65]B.A. Salamon and R.J. Donald, "Characterizing and controlling secondary flows in injection molds", Proc. SPE ANTEC, pp.680-684, 1996.

[66]J.G. Hedenhag, "Real time closed-loop control system for the shot end", Transactions from the NADCA 15th International Die Dasting Congress and Exposition, G-T89-022, 1989.

[67]J.R. Mickowski and C.E. Teufert, "The control of impact pressure in the high pressure die casting process", Transactions from the NADCA 17th International Die Dasting Congress and Exposition, pp.349-3354, 1993.

[68]J.R. Vann, "Real time, dynamic shot control foe improved quality and productivity", Transactions from the NADCA 17th International Die Dasting Congress and Exposition, pp.373-385, 1993.

[69]B.O. Rhee, C.A. Hieber and K.K. Wang, "Experimental investigation of thermal contact resistance in injection molding", Proc. SPE ANTEC, pp.496-500, 1994.

[70]C.J.Yu, J.E. Sunderland and C. Poli, "Thermal contact resistance in injection molding", Polymer Engineering & Science, vol.30, no.24, pp.1599-1606, 1990.

[71]M. Rezayat and B. Jantzen, "Effects of inserts on the injection molding process", Polymer Engineering & Science, vol.35, no.3, pp.247-251, 1995.

[72]C.J. Yu, "Thermal analysis for injection molding of thermoplastics", Phd dissertation from Department of Mechanical Engineering, University of Massachusetts, 1990.

[73]M. Bandreddi, R. Nunn and R. Malloy, "An investigation of time based holding pressure profiles", Proc. SPE ANTEC, pp.348-352, 1994.

[74]C.K. Jen, "Acoustics waveguides having a varying velocity distribution with reduced echoes", U.S. Patent no.5,241,287, August 31, 1993.

[75]C.K. Jen, A. Safaai-Jazi, J.F. Bussiere and G.W. Farenell,"Longitudinal mode fiber acoustic waveguide with solid core and solid cladding", U.S. Patent no.4,743,870, May 10, 1988.

[76]C.K. Jen and J.-G. Legoux,"Clad ultrasonic waveguides with reduced trailing echoes", U.S. Patent application, submitted in May, 1996

[77]C.K. Jen, L. Piche and J.F. Bussiere, "Long isotropic buffer rods", Journal of Acoustic Society of America, vol. 88, no.1, pp.23-25, 1990.

[78]C.K. Jen, C. Neron, A. Miri, H. Soda, A. Ohno and A. McLean, "Fabrication and characterization of continuously cast clad metallic buffer rods", Journal of Acoustic Society of America, vol. 91, pp.3565-3570, 1992.

[79]H. Soda, C.K. Jen, G. Motoyasu, S. Okumura, A. Ohno and A. McLean, "Fabrication and characterization of an aluminum clad, Al-Cu alloy cored rod", Material Science and Tech., vol.11, pp.1174-1179, 1995.

[80]R.W. Schafer and L.R. Rabiner, "A Digital signal processing approach to interpolation", Proc.IEEE, vol.61, pp.692-702, 1973.

[81]A.V. Oppenheim, and R.W. Schafer, *"Discrete-Time Signal Processing"*, Englewood Cliffs, New Jersey: Prentice Hall, 1989.

[82]P.M. Gammell, "Coherent processing of the full analytic signal information of ultrasonic waveforms", International Advances in Nondestructive Testing, vol. 10, pp.183-266, 1984.

[83]M. Prystay, H. Wang and A. Garcia-Rejon, "Application of thermographic temperature measurements in injection moulding and blow moulding of plastics", Proc. SPIE, vol. 2766, pp.5-11, 1996.

[84]M. Loher and L. Iten, "Digital real-time control of the die casting process", Buhler Ltd, Uzwil (Switzerland), Diagram, issue no.101, pp 3-6, April 1992.